THESIS – RC 18 5401

ESTIMATION OF COMMERCIAL AIRCRAFT EMISSIONS AT JUANDA INTERNATIONAL AIRPORT BASED ON FLIGHT PATH

FREDDY DAVID CHILONGOLA
NRP. 03111750067001

SUPERVISOR
Ir. ERVINA AHYUDANARI M.E., Ph.D

MASTER PROGRAM
TRANSPORTATION ENGINEERING AND MANAGEMENT
DEPARTMENT OF CIVIL ENGINEERING
FACULTY OF CIVIL, ENVIREMENT AND GEO ENGINEERING
INSTITUT TEKNOLOGI SEPULUH NOPEMBER
SURABAYA

THESIS- RC 185401

ESTIMATION OF COMMERCIAL AIRCRAFT EMISSIONS AT JUANDA INTERNATIONAL AIRPORT BASED ON FLIGHT PATH

FREDDY DAVID CHILONGOLA
03111750067001

SUPERVISOR:

Ir. ERVINA AHYUDANARI M.E., Ph.D

MASTER PROGRAM

TRANSPORTATION ENGINEERING AND MANAGEMENT

DEPARTMENT OF CIVIL ENGINEERING

FACULTY OF CIVIL, ENVIROMENT AND GEO ENGINEERING

INSTITUT TEKNOLOGI SEPULUH NOPEMBER

SURABAYA

2019

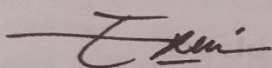**"This page is intentionally left blank"**
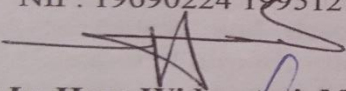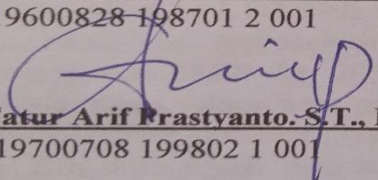
LEMBAR PENGESAHAN

LEMBAR PENGESAHAN

Tesis disusun untuk memenuhi salah satu syarat memperoleh gelar
Magister Teknik (M.T)
di
Institut Teknologi Sepuluh Nopember

Oleh:
Freddy David Chilongola
NRP 03111750067001

Tanggal Ujian   : 21 Januari 2019
Periode Wisuda   : Maret 2019

Disetujui oleh:

1. **Ir. Ervina Ahyudanari, M.E., Ph.D**   (Dosen Pembimbing)
   NIP: 19690224 199512 2 001

2. **Ir. Hera Widyastuti, M.T., Ph.D**   (Dosen Penguji I)
   NIP: 19600828 198701 2 001

3. **Dr. Catur Arif Prastyanto, S.T., M.Eng**   (Dosen Pemguji II)
   NIP: 19700708 199802 1 001

Fakultas Teknik Sipil Lingkungan Dan Kebumian
Dekan,

IDAA Warmadewanthi, S.T., M.T., Ph.D
NIP: 19750212 199903 2 001

iii

"This page is intentionally left blank"

ESTIMATION OF COMMERCIAL AIRCRAFT EMISSIONS AT JUANDA INTERNATIONAL AIRPORT BASED ON FLIGHT PATH

Student Name : Freddy David Chilongola
Student ID : 03111750067001
Supervisor : Ir. Ervina Ahyudanari M.E., Ph.D

ABSTRACT

Since Orville and Wilbur Wright made the first successful powered flight in 1903 air transport demand continues to increase. Indonesia as among ASEAN country the growth of aviation industry is due to various factors such as increasing of middle-income peoples and availability of low-cost carrier's flight. Juanda International airport not only known as one of the busiest airport in Indonesia in terms of aircraft movement and passenger numbers but also serves the fifth busiest route in the world that is Surabaya- Jakarta route. Similar to many major airports in the world, this airport also is the source of pollutant emission generated by aircraft engines exhaust combustion. The methods proposed are advanced approach ICAO landing and take-off (LTO) cycle and methodology for estimating emission from air traffic (MEET). Mapping of the emission of aircraft movements was done using ArcGIS. This work aims to estimates fuel consumptions on LTO cycle, non LTO cycle (climb and descent) phase operations by type of aircraft at Juanda International airport, estimates aircraft emissions concentration of HC, CO, CO_2, NO_x, SO_x, and to map the emissions of aircraft movement. The results showed that fuel consumptions on LTO cycle was 7307 kg, 5482 kg, 3338 kg and 2135 kg for taxi/idle, climb out, approach and take-off respectively. Non LTO cycle fuel consumption was 24396 kg, 2060 kg for climb and descent phase operations respectively, these values were generated based on the type of aircraft at Juanda International airport. Aircraft LTO cycle emissions concentration of HC, CO, NO_x, CO_2 and SO_x, during peak hour was 24 kg, 175 kg, 253 kg, 57530 kg and 18 kg respectively. The total amount of HC, CO, NO_x, CO_2 and SO_x emission during climb was 10 kg, 24 kg, 449 kg, 76887 kg, 24 kg respectively and during descent was 10 kg, 28 kg, 13 kg, 6490 kg and 2 kg respectively. The aircraft emissions affect the air quality around the vicinity of airport and climate change.

Key words: Aircraft Emissions, Airports, Air quality, Aviation, LTO Cycle.

"This page is intentionally left blank"

ESTIMASI EMISI KOMERSIALPESAWAT DENGAN JALUR PENERBANGAN DI BANDARA INTERNASIONAL JUANDA

Nama Mahasiswa   : Freddy David Chilongola
Mahasiswa ID   : 03111750067001
Dosen Pembimbing   : Ir. Ervina Ahyudanari M.E., Ph.D

ABSTRAK

Sejak Orville dan Wilbur Wright membuat penerbangan pertama yang sukses pada tahun 1903, permintaan transportasi air terus meningkat. Indonesia sebagai salah satu negara ASEAN pertumbuhan industri penerbangan meningkatkan harga pesawat dan penerbangan. Bandara Internasional Juanda tidak hanya dikenal sebagai salah satu bandara tersibuk di Indonesia dari segi pergerakan pesawat terbang dan jumlah penumpang tetapi juga melayani rute tersibuk kelima di dunia yaitu rute Surabaya-Jakarta. Sama halnya dengan banyak bandara besar di dunia, bandara ini juga merupakan sumber emisi polutan yang dihasilkan oleh mesin pesawat terbang yang membakar buangan. Metode yang diusulkan adalah ICAO mendarat dan lepas landas (LTO) *cycle* dan metodologi untuk memperkirakan emisi dari lalu lintas udara (MEET). Pemetaan emisi gerakan pesawat dilakukan menggunakan ArcGIS Peneletian ini bertujuan untuk memperkirakan konsumsi bahan bakar pada *LTO cycle*, dan *non LTO cycle* (mendarat dan lepas landas) fase konsentrasi emisi pesawat HC, CO, CO_2, NO_x, SO_x, dan untuk pemetaan emisi pergerakan pesawat terbang. Hasil penelitian menunjukkan bahwa konsumsi bahan bakar pada siklus LTO adalah 7307 kg, 5482 kg, 3338 kg dan 2135 kg untuk taksi / idle, *approach, climb out dan take-off* masing-masing. Konsumsi bahan bakar siklus non-LTO adalah 24396 kg, 2060 kg untuk *climb* dan operasi fase *descent* masing-masing, nilai-nilai ini dihasilkan berdasarkan jenis pesawat di Bandara Internasional Juanda. Konsentrasi emisi pada siklus LTO dari pesawat untuk HC, CO, NOx, CO_2, SO_x, selama jam sibuk adalah 24 kg, 175 kg, 253 kg, 57530 kg dan 18 kg masing-masing. Jumlah total emisi HC, CO, NOx, CO_2 dan SOx selama *climb* adalah 10 kg, 24 kg, 449 kg, 76887 kg, 24 kg masing-masing dan selama descent adalah 10 kg, 28 kg, 13 kg, 6490 kg dan 2 kg masing-masing. Emisi pesawat mempengaruhi kualitas udara di sekitar bandara dan perubahan iklim.

Kata Kunci: Emisi Pesawat, Bandara, Kualitas udara, Penerbangan, Pergerakan pesawat

"This page is intentionally left blank"

ACKNOWLEDGEMENT

"This page is intentionally left blank"

TABLE OF CONTENT

ATTACHMENTS

BIOGRAPHY

"This page is intentionally left blank"

LIST OF FIGURES

LIST OF TABLES

CHAPTER 1

INTRODUCTION

1.1 Background

Since Orville and Wilbur Wright made the first successful powered flight in 1903 air transport demand continues to increase. Indonesia as among ASEAN country the growth of aviation industry is tremendously high this is due to availability of low-cost carriers (LCCs) and the multilateral agreements of Single aviation market commonly known as ASEAN open sky. According to Hooper, (2005) there is an increasing prospects with the experiences on low cost carriers in other main markets in this active area would be duplicated due to a surge of low-cost carriers.. Air transport mode is efficient, reliable and time saving, these attributes contribute to the great demand on this mode year to year compare to other means of transport like sea and land transport. According to Airbus, (2012); Boeing, (2013), world-wide aviation grown at an average yearly amount of 5% in current years and this growth is predicted to continue.

As a result of increased air traffic growth rate leads to the increase of both air and noise pollution near airports. The fuel burned by aircraft emits pollutants such carbon dioxide (CO_2), carbon monoxide (CO), water vapours (H_2O), hydrocarbons (HC) nitrous oxide (NO_X), sulphur dioxide which are the key to the environmental impact on the atmosphere. The emitted gases affect air quality in the vicinity of airport and also contribute to the global climate change. In 2012, aviation corresponds to 13% of all EU transport CO_2 emissions, and 3 percent of the total European CO_2 emissions. It was also estimated that European aviation was 22% of global aviation's CO_2 emissions (EEA, 2014). In their research Grampella et al., (2017) used data from 31 Italian airports assembled over a time of ten years revealed that a 1% rise in an aircraft size and airport's yearly movements produces a 1.8% and 1.05% increase in environmental effects, respectively. Fan et al., (2012) in 2010 assessed twenty-nine commercial airlines of China during their working time of domestic flights shows that

emissions of SO_2, CO, CO_2, NO_x, and HC are 9700 tons, 39700 tons, 38.21 million tons, 154100 tons, and 4600 tons respectively.

Surabaya city is located in the East Java of Indonesia, is the second largest and most industrialized city in Indonesia, with a population of about 2.765.487 million (census 2010). The metropolitan city has always been an important business centre since it is located on major trade route. The Surabaya city is bordered by Gresik region on the west, Madura Island on the North and East, the Sidoarjo region on the South.

The number of airports in Indonesia by Airport Usage are 27 and 264 for International and domestic airports respectively (Ministry of Transportation, 2016). The main airport located near the metropolitan city of Surabaya is Juanda International airport it is about 15km from the city centre of Surabaya. The airport is located in Sidoarjo, East Java, Indonesia at the coordinate 07°22′47″S 112°47′13″E. The airport provides aviation services and facilities; the demand for aviation services is relatively high. The airport not only known as one of the busiest airport in Indonesia in terms of aircraft movement and passenger numbers but also serves the fifth busiest route in the world that is Surabaya- Jakarta route.

The airport opened on 1964 as naval airbase of Indonesia, similarly to many major airports in the world, this airport also is the source of pollutant emission generated by aircraft engines exhaust combustion. The aircraft emissions affect the air quality around the vicinity of airport and climate change. The emissions of greenhouse gases (GHG) such as CO_2 and water vapor impact on global climate change include higher average temperatures, sea level rise, ocean warming, ocean acidification, changes in precipitation, decreasing sea ice, and changes in physical and biological systems. Indonesia as part of South East Asia, particularly the deeply-populated mega delta areas will be at risk from flooding. Around 30% of Asia's coral reefs are expected to be lost in the next 30 years because of numerous stresses and climate change. Diarrheal diseases will increase due to changes in rainfall and this is mainly associated with droughts and floods (UNEP, (2009) ; IPCC, 2007).

2

There have been a few studies on aircraft pollutant emissions at airports. There has been no detailed study to determine the pollutant emissions from aircraft gas turbines generated from LTO cycle, climb and descent at Airports in Surabaya. In the literature, many studies focused on the estimation of pollutant emissions from aircraft at airports during LTO cycles, there is still a knowledge gap on total the aircraft emissions concentrations originated from Juanda International Airport during both landing, take-off, climb and descent phase. Kurniawan and Khardi, (2011) in their research compared different methodologies on estimating emissions pollutant near to the airport. The researchers evaluate the reliable methods to use in terms of accuracy, application, capability and problem of the uncertainty data and model. Mochamad, (2016) computed emission load of CO, HC and CO_2 per LTO cycle using exponential smoothing and econometric methods. The research used population to estimates the aircraft movement at Juanda International airport. Emissions from passenger aircraft at Kayseri Airport, Turkey was estimated by Yılmaz, (2017), this research showed that the LTO pollutant emissions are 177.90 tons per year (102.64 tons per year for NO_x, 66.90 tons per year for CO and 8.4 tons per year for HC) at Kayseri Airport in 2010. It is also calculated that a decrease of 2 min in taxiing time results a decrease of nearly 4% in landing and take-off emissions. Vujović and Todorović, (2017) assessed the aircraft pollutant emission at Nikola Tesla Belgrade using an advanced approach using a landing and take-off cycle (LTO) method recommended by ICAO. Their results showed that the number of LTO cycles increased by 54% which cause the increase of local air pollution. The cause and effect diagram (fishbone) of aircraft emissions is shown on Figure1.1
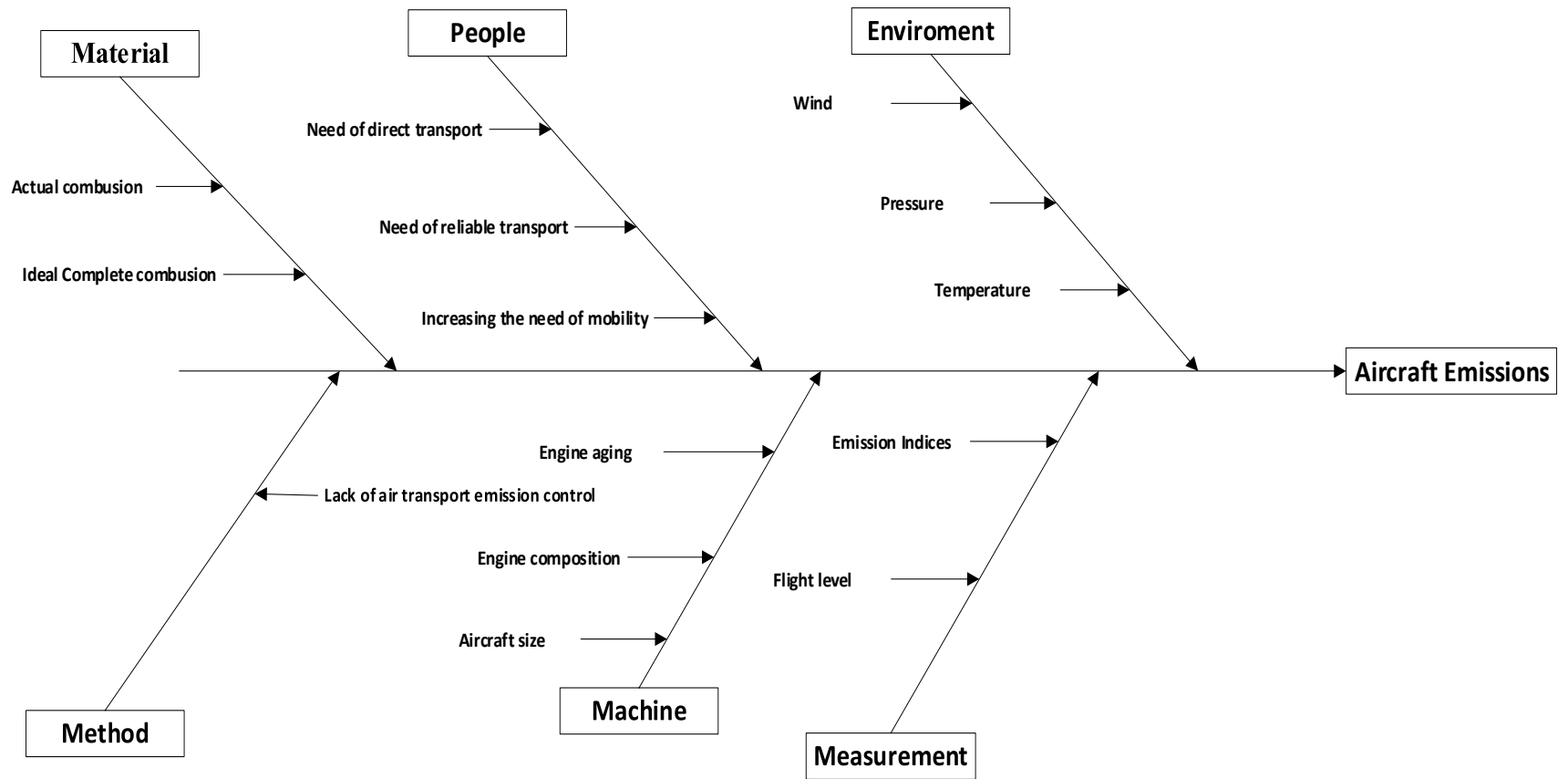
Figure 1. 1. Fishbone diagram.

1.2 Problem Statement

In order to know the extent to which action is required, it is necessary to determine the level of air pollution near the airport. In accordance with **Presidential Regulation Republic of Indonesia No. 61 of 2011**, which aims to reduce the levels of greenhouse gases, only by 26% -46% in all areas, it is necessary to control gas emissions in every activity. Land transportation modes have got much attention to reduce gas emissions. Load emission of CO by motor vehicle in Surabaya 2014-2015 was 0.0646 million ton/year while the target is 0.079 million tons per year therefore referring to the President Decree related to the National Movement of reducing the greenhouse gas effect, the targets is to decrease by 26% per year (Ofrial et al., 2016). Therefore, there is a need to identify the other sources of emission.

This research estimates the concentration of HC, CO, CO_2, NO_X, SO_2 during both landing and take-off (LTO) cycle (taxi/idle, approach, climb out, take-off), non LTO cycle (climb and descent) phases generated by aircraft movements from Juanda International Airport. Therefore, research questions are as following:

1. What is the amount of fuel consumptions produced during LTO cycle, climb and descend operations by type of aircrafts at Juanda International airport?
2. What is the aircraft pollutant emissions concentration load of HC, CO, CO_2, NO_X, SO_2 generated by each aircraft during LTO cycle, climb and descent operation phase at Juanda International Airport?
3. How the emission of aircraft movements at Juanda ca be pictured?

1.3 Objectives

The main objectives of this research are:

1. To estimates fuel consumption on LTO cycle, climb and descent phase operations by type of aircrafts at Juanda International airport.
2. To estimates aircraft emissions concentration of HC, CO, CO_2, NO_X and SO_2 on LTO cycle and non LTO cycle (climb and descent).
3. Mapping the emission of aircraft movements at Juanda Intl. Airport.

1.4 Scope

The following are the limits on conducting this research

1. All flights fly as planned according to flight plan.
2. All flights fly in the standard atmosphere.
3. The emissions are sum up simply, neglecting the drift, chemical reaction, and diffusion of the pollutants in the atmosphere.
4. The types of aircraft used for analysis are passenger aircraft and cargo, not military.
5. The emissions analysed are the result of engine activity or the burning of aircraft materials, not due to ground equipment, aircraft refuelling or engine start-up.
6. There is not designing of the airport layout.
7. The phases of operation, time spent and engine thrust setting are as follows: Take-off process demands 100% engine thrust and takes 42 s, climb process demands 85% engine thrust and takes 2.2 min, cruise process needs 70 percent of engine thrust, approach process demands 30% engine thrust and takes 4 min; Taxiing and idle process demands 7% engine thrust and takes 26 min.
8. The aircraft emission estimated on turbofan engine only.
9. There is no analysis of emission dispersion.

1.5 Research Significance

The research results may give a picture on how much emission has been loaded into the air from aircraft movement. This load may cause other symptoms related to human health. However, the load cannot be detected from the carbon detector (Mochamad, 2016). This research attempts to bring awareness to the emission load added every day.

The research is expected to be helpful in different areas, such as the Government of Indonesia and non-governmental agency on formulating environmental policies and regulations on air transport emissions. Results of the aircraft emissions load analysis can be a reference for the development and operation of airport with an

environmentally eyes. The study will provide data to other researchers who may develop an interest in conducting the research at the same field or any other, not only the researchers, but also the students, learners, managers or directors and other employers in any organization. It is partial requirement to fulfil master award in Civil Engineering Department in Institut Teknologi Sepuluh Nopember (ITS). It is very beneficial for future references.

"This page is intentionally left blank"

CHAPTER 2

LITERATURE REVIEW

2.1   Introduction

Air transport plays a great role in transportation sector. As we know air transport is one which contributes the largest movement of peoples, and goods from one place to another. The Civil aviation transport industry has experienced fast growth while creating another problem; aircraft pollutant emissions, which affect both air quality in the vicinity of airport and regional impact on climate change. This chapter aims at providing a review to different issues, theories, problems and research done by various authors in the area with the main objective of adding knowledge, familiarizing the researcher with any relevant information about the problem being studied. It covers most important journals, articles, books and other relevant publications, presenting the theory of the subject, and linking research already done in the aircraft emissions.

2.2   Air Traffic

This section provides the basic theory of air traffic and how it related to aircraft emissions. It is found that NOx parameters may also be highly sensitive to aircraft mass and cruise altitude. The types of flight rules and flight levels are well discussed.

2.2.1   Flight rules

Aircrafts usual are performed according to two flight rules, Instrument flight rules (IFR) and visual flight rules (VFR). Kalivoda and Kudrna, (1997) categorized three main classes of air transport that can be distinguished when assessing its operational and emission related characteristics:

1) Flights performed under IFR.
2) Military operational air traffic.
3) Flights performed under VFR.

According to Kalivoda and Kudrna, (1997) about 60% to 80% of emissions coming from IFR flights. Normally IFR flights are operated as flights controlled by Air Traffic

9

Services (ATS) within controlled airspace only and generally flights with civil aircraft emission indices for IFR flights.

Visual flight rule (VFR) flights commonly are not operated as controlled flights hence, none of a *Flight Plan* or complete information on the route flown is available. On the other hand, VFR flights correspond to less than five percent of fuel consumption plus pollutant emissions produced by air traffic are mainly emitted at lower altitudes than IFR flights frequently likewise within the planetary boundary layer (Kalivoda and Kudrna, 1997). Most of large and jet aircrafts performed IFR flights such as B747 and E190 while small aircraft usual fly under VFR flights for example C206 and C208.

2.2.2 Flight level.

Flight level (FL) is the 100s of feet of altitude above mean sea level. To maintain standard separation of air traffic in the airspace, air traffic controller assigns flight altitudes to aircraft based on their direction, or more precisely magnetic heading, of flight and whether or not they are flying under Visual Flight Rules (VFR) versus Instrument Flight Rules (IFR).

Aircraft flying under IFR are typically assigned altitudes of odd thousand feet (example 10000 ft, 30000 ft, etc.) Above Mean Sea Level (AMSL) while to East bound (magnetic compass heading of 0° to 179°) that can be presented in flight level (FL) for instance 100FL,300FL and even-thousand feet (example 40000 ft, 60000 ft, etc.) in flight level can be written as 400FL, 600FL etc. while on a western bound (magnetic compass heading of 180° to 359).

Aircraft flying using VFR assigned odd thousands of feet plus 500 ft. of altitude for the one heading East example 5500 ft. AMSL (055FL), and even thousands of feet plus 500ft for the West bound heading example 6500ft AMSL (065FL).

2.3 Aircraft characteristic.

Physical dimensions and performance characteristics vary in each types of aircraft. Aircraft can be operated for general aviation, commercial air service or cargo.

The aircraft characteristic is important when assessing the emissions since it is assisting to obtain the number of engines and its type. More detailed review of relation of the engine types to the emission production discussed on **section 2.5**. Horenjeff (2010) provides summary of some important aircraft characteristics of commercial airline fleet and general aviation aircraft as shown in the Table 1 and Table 2 respectively.

Table 2. 1. Characteristic of commercial service aircraft.

Turboprop							
Aircraft	**Wingspan**	**Length**	**MSTOW (lb)**	**# Engines**	**avg. # Seats**	**Runway Required (ft)**	
Beach 1900C	54'06"	57'10"	16,600	2	19	3,300	
Shorts 360	74'10"	70'10"	27,100	2	35	4,300	
Dornier 328-100	68'10"	68'08"	27,557	2	30	3,300	
SAAB 340B	70'04"	64'09"	28,500	2	37	4,200	
AT-42-300	80'06"	74'05"	36,815	2	45	3,600	
EMB 120	64'11"	65"7"	26,433	2	30	5,200	
Jet Aircraft Less than 100,000 lb MSTOW (Regional Jets)							
Aircraft	**Manufacturer**	**Wingspan**	**Length**	**MSTOW (lb)**	**# Engines**	**Avg. # Seats**	**Runway Required (ft)**
ERJ 135	Embraer	65'9"	86'5"	41,887	2	35	5,800
ERJ 140	Embraer	65'9"	93'4"	44,313	2	40	6,100
ERJ 145	Embraer	65'9"	98'0"	46,275	2	50	7,500
CRJ 200	Bombardier	69'7"	87'10"	51,000	2	50	5,800
CRJ 700	Bombardier	76'3"	106'8"	72,750	2	70	5,500
CRJ 900	Bombardier	81'6"	119'4"	80,500	2	90	5,800

Source: Robert Horonjeff et al., 2010

Table 2. 2. Characteristic of Commercial service aircraft (continued)

Jet Aircraft Less than 100,000 lb MSTOW† (Regional Jets)									
Aircraft	Manufacturer	Wingspan	Length	MSTOW (lb)	# Engines	avg. # Seats	Required (ft)		
BAe-RJ70	British Aerospace	86'00"	78'9"	89,999	2	95	4,700		
BAe-RJ85	British Aerospace	86'00"	86'11"	92,999	2	110	5,400		
Bae-RJ100	British Aerospace	86'00"	94'10"	97,499	2	110	6,000		

Jet Aircraft between 100,000 and 250,000 lb MSTOW† (Narrow Body Jets)									
Aircraft	Manufacturer	Wingspan	Length	Wheel Base	Wheel Track	MSTOW (lb)	# Engine	Avg. # Seats	Required)ft)
A-319	Airbus Industrie	111'25"	111'02"	41'33"	24'93"	141,095	2	140	5,800
MD-87	McDonnell-Douglas	107'10"	130'05"	62'11"	16'08"	149,500	2	135	7,600
MD-90-30	McDonnell-Douglas	107'10"	152'07"	77'02"	16'08"	156,000	2	165	7,600
A-320-200	Airbus Industrie	111'03"	123'03"	41'05"	24'11"	158,730	2	160	5,700
B-737-800	Boeing	112'06"	124'11"	50'09"	18'8"	172,445	2	175	
B-727-200	Boeing	108'00"	153'03"	63'03"	18'09"	184,800	3	165	8,600
B-757-200	Boeing	124'10"	155'03"	60'00"	24'00"	220,000	2	210	5,800
Jet Aircraft Greater than 250,000 lb MSTOW (Wide Body Jets)									
A310-300	Airbus Industrie	144'00"	153'01"	49'11"	31'06"	330,690	2	240	7,500
B-767-300	Boeing	156'01"	180'03"	74'08"	30'06"	345,000	2	275	8,000
A-300-600	Airbus Industrie	147'01"	175'06"	61'01"	31'06"	363,765	2	310	7,600
L-1011-500	Lockheed	164'04"	164'03"	61'08"	36'00"	510,000	3	290	9,000
B-777-200	Boeing	199'11"	209'01"	84'11"	36'00"	535,000	2	375	8,700
DC-10-40	McDonnell-Douglas	165'04"	182'03"	72'05"	35'00"	555,000	3	325	7,600
A-340-200	Airbus Industrie	197'10"	195'00"	62'11"	16'09"	558,900	4	320	7,600
DC-10-30	McDonnell-Douglas	165'04"	182'03"	72'05"	35'00"	572,000	3	320	9,290
MD-11	McDonnell-Douglas	170'06"	201'04"	80'09"	35'00"	602,500	3	365	9,800
B-747SP	Boeing	195'08"	184'09"	67'04"	36'01"	630,000	4	315	7,000
B-747-400	Boeing	213'00"	231'10"	84'00"	36'01"	800,000	4	535	8,800

Source: Horenjeff,2010

Table 2. 3. Characteristic of General Aviation Aircraft

Piston and Turbo-Prop Engine Aircraft							
Aircraft	Manufacturer	Wingspan	Length	MSTOW (lb)	# Engines	Avg. # Seats	Runway Required*
PA28-Archer	Piper	35′00″	23′09″	2,550	1	4	1,660
DA-40	Diamond	39′06″	26′09″	2,645	1	4	1,198
PA28-Arrow	Piper	35′05″	24′08″	2,750	1	4	1,525
C-182 Skylane	Cessna	35′10″	28′01″	2,950	1	4	1,350
SR20-G2	Cirrus	35′07″	26′00″	3,000	1	4	1,446
SR-22	Cirrus	38′04″	26′00″	3,400	1	4	1,028
PA-32 Saratoga	Piper	36′02″	27′08″	3,600	1	6	1,760
Corvalis 400	Cessna	36′01″	25′02″	3,600	1	4	2,600
DA-42 Twin Star	Diamond	44′06″	28′01″	3,748	2	4	1,130
C-310	Cessna	37′06″	29′07″	5,500	2	6	1,790
BN2B-Islander	Britten-Norman	49′00″	35′08″	6,600	2	9	1,155
C-402c	Cessna	44′01″	36′05″	6,850	2	10	2,195
Cheyenne IIIA	Piper Aircraft	47′08″	43′05″	11,200	2	10	2,400
Super KingAir	Beechcraft	54′06″	43′09″	12,500	2	12	2,600
C-208 Grand Caravan	Cessna	52′01″	41′07″	8,750	1	14	1,500

Very Light Jet Aircraft							
Aircraft	Manufacturer	Wingspan	Length	MSTOW (lb)	# Engines	Avg. # Seats	Runway Required*
Mustang	Cessna	43″2″	40′7″	8,645	2	5	3,100
Eclipse 500	Eclipse	33′6″	33′6″	5,995	2	5	2,400
Hondajet	Honda	39′10″	41′8″	9,200	2	5	3,100
Business Jet Aircraft							
Citation CJ1	Cessna	46′11″	42′7″	10,800	2	5	3,300
Citation X	Cessna	56′4″	52′6″	36,400	2	10	3,560
Lear 45 XR	Bombardier	47′9″	57′6″	21,500	2	9	5,040
Lear 60 XR	Bombardier	43′9″	58′6″	23,500	2	9	3,400
Hawker 850 XP	Beechcraft	54′04″	51′02″	28,000	2	8	5,200
G-IV	Gulfstream	77′10″	88′04″	73,200	2	19	5,000
G-550	Gulfstream	93′06″	96′05″	85,100	2	19	5,150

Source: Horenjeff, 2010

2.3.1 Aircraft Weight.

An aircraft will usual be measured with a certain number of weight measurements which depend on its level of loading with crew, payload and fuel, more often assigned maximum allowable weight values for take-off, landing, and at rest

(Horenjeff, 2010). ICAO categorized three types of aircraft according to their wake turbulence weight as following:

1. Light (L) – aircraft types of 7000 kg or less.
2. Medium (M) – all aircraft types less than 136000 kg but more than 7000 kg.
3. Heavy (H) - all aircraft types of 136000 kg or more.

During landing, the total weight of an aircraft is equal to the sum of the weight when it is empty operated, the payload, and the fuel reserve, assuming that the aircraft is not diverted to an alternate airport and lands at its destination. The landing weight cannot exceed the maximum structural landing weight of the aircraft. The take-off weight equal to the sum of the landing weight and the trip fuel. This weight cannot surpass aircraft's maximum structural take-off weight.

2.4 Aircraft operation/performance

According to EEA/EMEP, (2009) aircraft operation can be branched into two parts, namely landing and take-off (LTO) cycle and the cruise part. The LTO cycle well defined by ICAO, (1993) as all the operations that occur when aircraft is below 3000 ft above field elevation (equivalent to 914 m) over a specific range of certifiable operating conditions. LTO cycle contains **four modes** in which both typical engine thrust settings (stated as a percentage of highest rated thrust, F_{00}) and time in every specific mode of operation (time-in-mode, TIM) is given. For the first ICAO LTO stage aircraft goes down from cruising level continues to the runway and landing at the airport. The stage is known as *approach*. After landing, the aircraft enters in the idle stage which includes all the ground-based operations. It is then *taxi-in* at a low speed toward the gate and stays stand-by for the unloading and loading operations, after that continues for take-off towards the runway (*taxi-out*). The following operating phases contain the *take-off* with engines pushed to the full thrust, and then *climb* until to the height of 3000 ft. One LTO cycle equal to summation of one landing and one take-off operation, ICAO document 9889 (ICAO (International Civil Aviation Organization), 2011). The ICAO LTO cycle is shown in the Figure 2.1
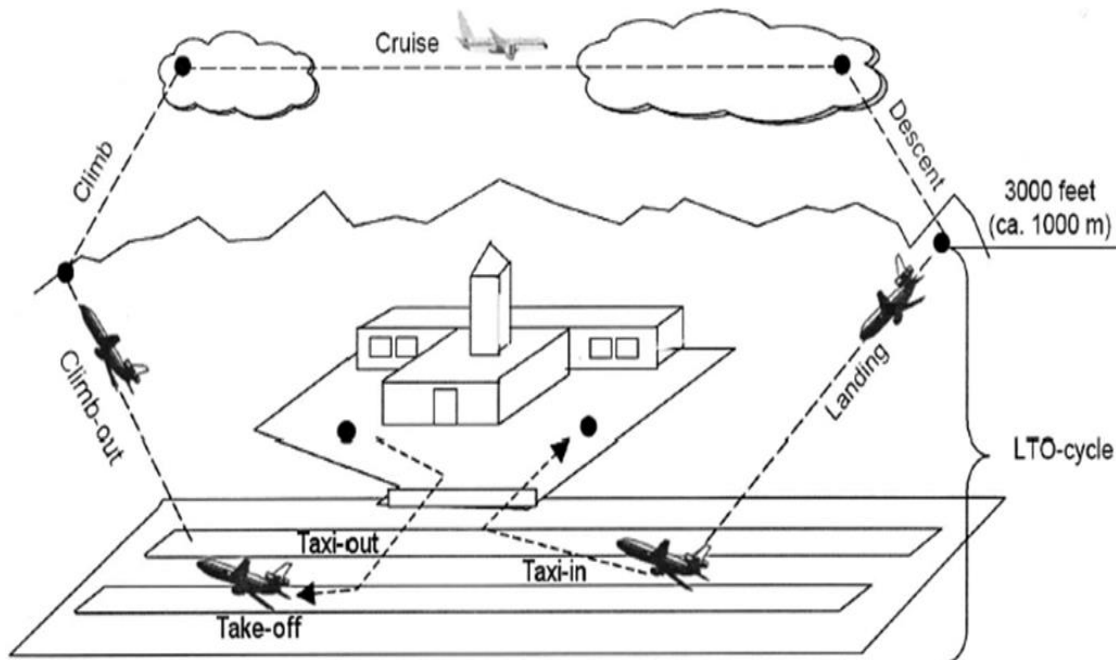
Figure 2. 1. Standard ICAO LTO cycle. (ICAO 1993)

All activities that occur at altitude above 3000 ft (914 m) are known as **cruise**, no upper limit level is offered. Cruise contains climb from the end of climb-out mode in the LTO cycle, then proceed to the cruise level, after that the aircraft cruise, and finally descent from cruise altitudes to the start of LTO operations of landing. The typical aircraft performance of Boeing 735 is shown on Figure 2.2. Barrett et al., (2010) predicted that presently aircraft operations at cruise altitude (about 80%) attributes approximately 10,000 premature mortalities per year and the landing and take-off cycle (LTO) (about 20%). However Krzyzanowski and Cohen, (2008) in their research estimated 0.8 million premature mortalities worldwide as a result of anthropogenic air pollution, which is equal to 1% of (Barrett et al., 2010). In other research Ratliff et al., (2009) estimated that about 160 annual cases of premature mortality in the United States caused by airport operations (aircraft landing and take-off (LTO) cycle and auxiliary power units (APUs)) attribuTable to particle matter ($PM_{2.5}$) exposure.
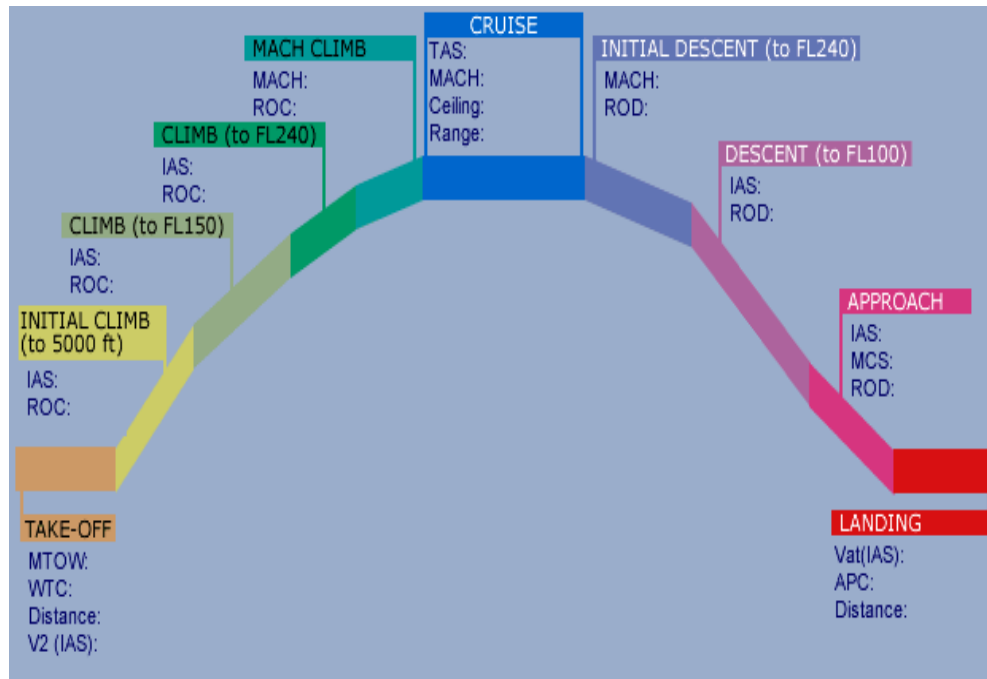
Figure 2. 2. Actual Boeing 735 flight path phases. (Source: Aircraft Performance Database v3.0 www.eurocontrol.int)

2.5   Aircraft engine.

Aircraft engine is an important component on aircraft performance. However, aircraft engine is one of significant factor during assessing the emissions generated by aircraft engine exhaust. Table 2.4 shows the engines family commonly mounted on aircraft. Most of general aviation and civil aviation are equipped with three different types of engine namely:

a. Turbofan (jet) engine.
b. Turboprops.
c. Piston engine.

The *turbofan* or jet engine has reference to those aircraft which are not dependent propellers for thrust, but which obtain the thrust directly from a turbine engine. The *turboprop* engine refers to propeller-driven aircraft powered by turbine

engines. The *piston engine* is applying to all proper driven aircraft. General aviation and small aircraft mostly use piston engines while historically jet engines have been used to power larger general aviation and commercial service aircraft, jet engines recently have been increasingly produced for smaller "regional jet" commercial service aircraft, and even smaller "very light jet" general aviation aircraft (Horenjeff 2010). According to ICAO (2011) the turboprop and turbofan engines are powered by aviation kerosene also known as jet fuel while piston engines are fuelled by aviation gasoline also known as avgas. The main difference between jet and piston engines is in combustion. In jet engine the combustion is continuous while in piston engines the combustion   is intermittent (Masiol and Harrison, 2014)

A turbojet engine made of a compressor, combustion chamber and a turbine at the rear of the engine. For adding and igniting fuel an inlet compressor, a combustion section of a turbojet is used and the   turbines accounTable for getting energy from the exhaust gas in expansion and moving the compressor. Thrust is generated by acceleration of exhaust gas from exhausts nozzle. A turbofan is primarily a turbojet engine to which has been added large-diameter blades, usually located in front of the compressor. A single and two rows of blades are referred to as single stage and multistage respectively. The blades are commonly known as fan. Based on Horenjeff (2010) in dealing with turbofan engines, the main reference is made to **bypass ratio** which is defined as the ratio of the mass airflow through the fan to the mass airflow through the core of the engine or the turbojet portion. In civil aviation high-bypass ratios are favoured for a good fuel efficiency and low noise (Masiol and Harrison, 2014). A simplified diagram of turboprop engine is show in diagram 1 The jet fuel which is a combination of different hydrocarbons combusts in an aircraft engine therefore various chemical species are emitted. CO_2 and water vapour are released when a complete combustion occur (Masiol and Harrison, 2014). However, incomplete burning of fuel can happen because of a deficiency of oxygen and low temperatures near the walls of the engine's combustion chamber. Based on Knighton et al., (2009); Masiol and Harrison, (2014), unburned hydrocarbons are emitted because the

17

conversion of fuel to CO_2 and H_2O in jet turbine engines is not completely efficient. Products of this process result in additional species as NO_x, CO, SO_2, unburned hydrocarbons, and particulate matter. Engines advancement in technology are focused toward the development of *propfan* engines for short and medium haul aircraft and ultrahigh bypass ratio turbofan engines for long haul aircraft.

Table 2. 4. Engines family used in most aircraft. The number of engines is given on brackets

Manufacturer	Engine family	Main aircraft and number of engines
General Electric	CF6 series	A300(2); A310(2); A330(2); B747(4); B767(2); MD DC-10(3); MD-11 (3)
	CE90 series	B777 (2)
	GEnx series	B747 (4); B787 (2); replacing CF6 series
CMF International	CFM56 series	A318 (2); A319(2); A320(2); A321(2); A321(2); A340(4); B737(2); MD DC-8(4)
Pratt and Whitney	JT8D series	B707(4); B727(3); B737(2); MD DC-9(2); MD80(2);
	JT9D series	A300(2); A310(2); B747(4); B767(2); MD DC-10(3)
	PW 4000 series	A300(2); A310(2); B747(4); B767(2); B777(2); MD DC-11(3)
Rolls-Royce	RB211 series	B747(4); B757(2); B767(2); L1011(3); Tu-204(2)
	Trent series	A330(2); A340(4); A380(4); B777(2); B787(2)
BMW Rolls- Royce	BR700 series	B717(2)
International Aero Engines	V2500 series	A319(2); A320(2); A321(2); MD-90(2)
Aviadvigatel' Solov'ev	D30 series	Tu-154(3)

Source: Masiol and Harrison, 2014
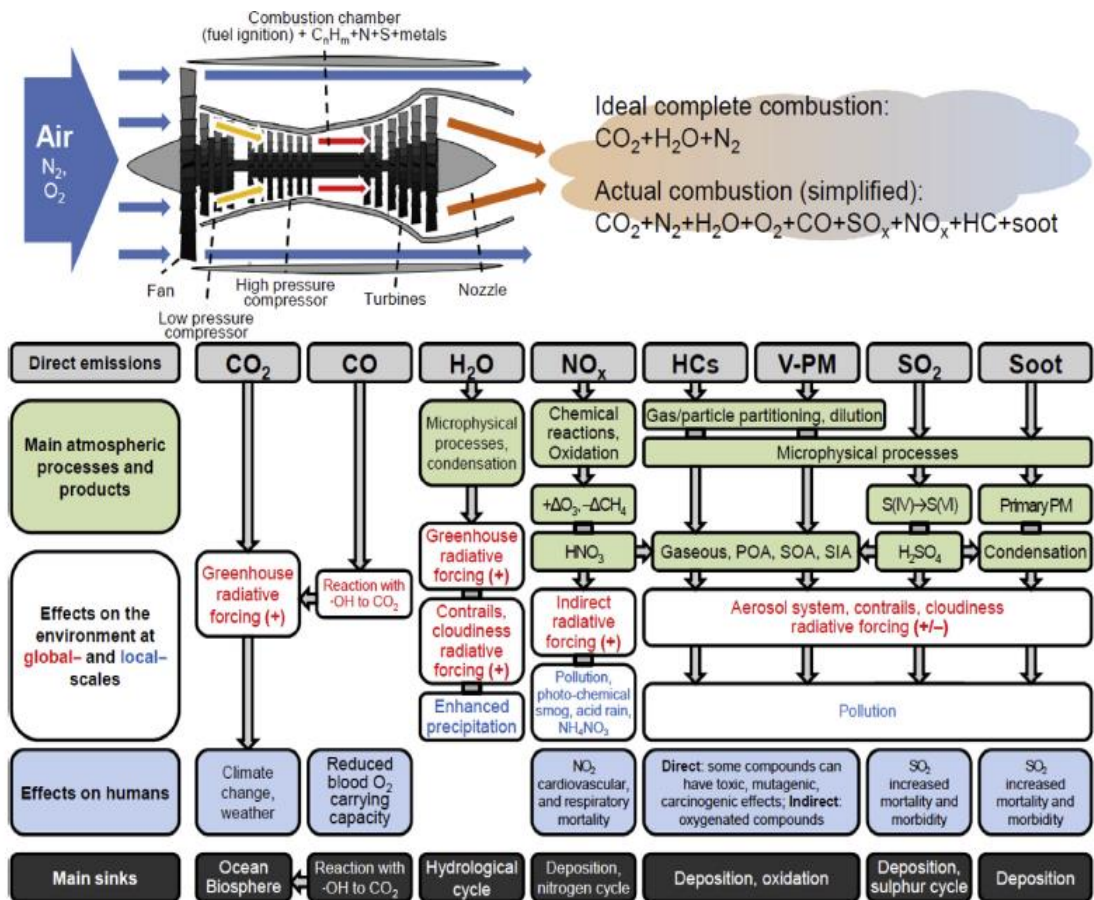
Figure 2. 3. Upper left- a simplified diagram of a turbofan engine; Upper right-products of ideal and actual combustion in an aircraft engine; and at the bottom-related atmospheric processes products, environmental effects, human health effects and sinks of emitted compounds. (Maslow and Harrison 2014).

2.5.1 Emission Indices.

Emission Index (EI) is described as mass of the pollutant released per unit mass of fuel burned for a particular engine. The emission indices depend on conditions and measurements procedure during aircraft engine certifications. Certificated engine emission indices which are given by the engine manufacturers and reported in ICAO engine emission database usually are used to calculate the aircraft emission inventory. The ICAO emission index data bank contains emission indices of HC, NO_x and CO

with several types of jet engines measured under the International Standard Atmosphere (ISA) condition at sea level. Zaporozhets and Synylo, (2017) described that under real circumstances these conditions during aircraft certification result in the value of certificated engine Indices may vary and deviate due to the following three factors:

a) Life expectancy (age) of aircraft. The average period of 30 years the aircraft engine emissions might vary very significantly.

b) Type of an engine installed on an aircraft. The modification of engines for example like combustions chambers may also result different value of emission because of aircraft using different engine during certification.

c) Metrological conditions. The pressure of ambient air, temperature and humidity can be different during certification conditions.

2.6   Aircraft Emissions.

Aircraft emissions have been an interested subject to the researchers especial considering the rapid growth of air transportation industry and its effects to the environment and human health. Researchers have been conducting many researches in LTO cycle and few researches on non LTO cycle due to the complexity of the subject especial on attained data from real environment. This research will use available methodology on determining aircraft emissions from LTO cycle and non LTO cycle (climb and descent.). The summary of the current researches conducted on this topic is given in Table 2.9. This section provides a review of the main parameters on dealing with aircraft engine exhaust emissions. Comparison of available methodologies described on Table 2.8 research done by (Kurniawan and Khardi, 2011).

2.6.1   Time in Mode (TIM).

Time which aircraft spends in one of the specific phases of operation that is time-in-mode (TIM) and is proportional to the amount of emissions during that phase of the LTO cycle. The standard default ICAO LTO cycle is shown in Table 2.5. In each aircraft size category there is a variation in time in mode. For example London

Stansted, Heathrow, and Gatwick airports which empirical data available uncertainty in TIM is approximate as ±10% and ±20 percent for those where TIMs were approximated using the method represented in (Watterson et al., 2004). Patterson et al., (2009) noticed similar order of variations in TIMs with deviations of 10% to 20% for take-off, climb-out and 15% to 20% for approach. According to Stettler et al.,(2011) found that there is a deviation of ±10% for all phases compared with the ICAO LTO cycle.

Table 2. 5. The time mode in LTO cycle

Operation mode	ICAO default LTO cycle		
	Phase	Time in mode TIM (s)	Thrust setting (%)
Arrival	Approach	240	30
	Taxi in	420	7
Departure	Taxi out	1140	7
	Take-off	42	100
	Climb out	132	85

Source: ICAO, 1995

2.6.2 Thrust Setting and Fuel flow.

As pollutant emissions are positively correlated with the fuel consumption (Fan et al., 2012). As stated by Wey et al., (2006) fuel flow to the engine is almost linearly proportional to engine thrust setting which is explained as a percentage of maximum rated thrust . The variations between in real environment computations of emissions indices for a specific LTO phase and those listed in the ICAO engine emissions databank relative to the default ICAO LTO cycle It is distinctly possible that differences in thrust setting are the fundamental source (Herndon et al., 2009: Herndon et al., 2008:Schürmann et al., 2007) The thrust level applied in the real taxi operation

as recommended by Wood et al., (2008) can be depicted by two discrete modes; firstly *ground idle* with thrust settings approximate to 4 percent vice the 7 percent explained by the default ICAO LTO cycle and secondly *taxiway acceleration* with thrust settings until 17 percent.

Fuel consumptions extending between 3 and 10% due to engine ageing which influence engine fuel flow and emissions by lower the capability of the engine (Curran, 2006; Lukachko and Waitz, 1997). To assist air-conditioning and supply airframe power service, involving an amount of the engine's power output, hence commercial aircraft most of the time use engine bleed flow (Baughcum et al., (1996); Herndon et al., 2009).In due course, fuel flow to the engine is mount for a given thrust output and correction factors proposed by Baughcum et al., (1996) have been *used*. Koudis et al., (2017) in their research on impact of aircraft take-off thrust setting on NO_X emissions, shows that reduction of 32% per take-off roll on mass of NO_X emissions. In spite of this, factors for instance wind speed, wind direction and take-off weight (TOW), which impact TIM may affect the capability of using reduced thrust take-off.

2.6.3   HC and CO emissions

Hydrocarbons (HC) are produced due to incomplete fuel combustion by an engine while carbon monoxide (CO) is formed due to the incomplete combustion of the carbon in the fuel. As stated by Knighton et al., (2009) unburned hydrocarbons are emitted because the conversion of fuel to CO_2 and H_2O in jet turbine engines is not completely efficient. Emission index EI(HC) and EI(CO) decrease with increasing thrust.

Emissions of HC and CO are regulated by ICAO international standards and engine manufacturers must provide emission indices for these pollutants during an LTO cycle (ICAO, 2008). Sutkus Jr et al., (2001) suggested that total hydrocarbon EIs and CO emissions indices are highest at low power settings where combustor temperatures and pressures are low and combustion is less efficient. In their research

Anderson et al., (2006) found EI(CO) for in-use commercial engines included in the ICAO databank at take-off power, range from 0.6 g kg Fuel^{-1} to 31 g kg Fuel^{-1} at idle.

2.6.4 CO$_2$ emissions

Carbon dioxide and water vapour emitted when complete fuel combustion occurs. Under complete combustion the EI(CO$_2$) complete depends on the ratio of carbon to hydrogen. Hileman et al., (2010) found that in aviation fuel the ratio of carbon to hydrogen lies within the range of 3148-3173g kg Fuel^{-1}, The results is similar to (Lewis et al., 1999: Lee et al., 2010) which EI(CO$_2$) for complete combustion was 3160± 60 g kg Fuel^{-1}. However Wey et al., (2006) mentioned that incomplete combustions cause a decrease of EI(CO$_2$) at low thrust, relative to assuming complete combustion as EI(CO) and EI(HC) increased non-linearly. Carbon dioxide is the greenhouse gases which has a great effect on earth climate warming (IPCC, 1999).

Carbon dioxide is not listed on ICAO engine certification database. The main anthropogenic sources are the combustions of fossil fuels. Le Quéré et al., (2009) estimated CO$_2$ emissions from fossil fuel combustion, with small influences from gas flaring and cement production to be 8.7 ± 0.5 Pg C yr^{-1} in 2008 an increase of 2% from 2007 and 29% , 2000 and 41% from 1990.In addition, Peters et al., (2012) study indicated that global CO$_2$ emissions from cement production and fossil fuel combustion further grew by 5.9% in 2010, surpassing 9 Pg C yr^{-1} mainly due to the solid emissions growth in emerging economies. The obtained results of Macintosh and Wallace, (2009) proposed that, international aviation carbon dioxide (CO$_2$) emissions will rise over 110 percent between 2005 and 2025 (in the middle of 876 and 1013 Mt from 416 Mt) also it is very improbable that emissions could be stabilized at stages consistent with risk opposed climate targets without restricting demand. Similarly Olsthoorn, (2001) projected that international aviation CO$_2$ emissions will be 86–144% above 1995 levels by 2020 (or 383–503 Mt) and 187–513% above 1995 levels by 2050 (591–1263 Mt) if carbon is not priced. These outcomes indicate that by 2025, emissions will be nearly 100–190% above 1995 levels (~410–600 Mt CO$_2$).

2.6.5 SO_x emissions

When small quantities of Sulphur present in hydrocarbon, fuels mix with oxygen from the air during combustion, Sulphur oxides are produced. SO_2 is the major S-species in aircraft exhaust emissions, however can be oxidized to produce S(IV) as SO_3 and H_2SO_4 (Lee et al., 2010). Sulphur dioxide is proportional to the fuel and is the function of fuel Sulphur content (FSC). Exposure to SO_2 has health effect such as cardio-vascular admissions especial for ischaemic heart disease (Sunyer et al., 2003a; Sunyer et al., 2003b). Moreover SO_2 has indirect influence on climate (Masiol and Harrison, 2014).

Sulphur dioxide is also not listed on ICAO engine certification database. (Lewis et al., 1999; Kim et al., 2007; Lee et al., 2010; Presto et al., 2011) reported that for complete combustion, emission index of SO_x (SO_2) as 0.8- 1.3gram per kilogram fuel.

2.6.6 NO_x emissions

Nitrogen oxides are produced when air passes through high temperature or high-pressure combustion and nitrogen and oxygen present in the air combine to form NO_x (FAA, 2005). Hence NO_x formation is sensitive to combustor pressure, temperature, flow rate, and geometry (Sutkus Jr et al., 2001). Same as to fuel-related parameters, it is found that NOx parameters may also be highly sensitive to aircraft mass and cruise altitude. For example a five tons heavier aircraft or cruising at a 2000 ft higher altitude causes extra 11.2% NOx emissions, 12.3% NO_x intensity or fewer 2.7% NOx emissions 2.4% NO_x intensity (Turgut and Usanmaz, 2017).

ICAO Certification parameters included NO_X as $NO_X = NO+NO_2$. Most of the time is termed as NO_2 unless specified otherwise. According to Timko et al., (2010) at high thrust situations (thrust settings of 65 to 100%) with NO_2/NOx less than 10% for majority of engines, NO is the predominant types while at low thrust setting NO_2 becomes dominant, with NO_2/NO_x varying between 75 and 98% at 4% thrust (Timko et al., 2010; Wood et al., 2008)

2.6.7 Summary of LTO cycle emissions

Summary of emissions during LTO cycle at take-off, climb out, approach and taxi/idle can be seen on Table 2.6 below. The emission is given by total percentage of pollutant on each mode.

Table 2. 6. Summary of LTO emissions

Gas	% emissions				Resources
	Take-off	Climb out	Approach	Taxi/Idle	
CO_2	12%	30%	18%	40%	
SO_2	12%	30%	18%	40%	
NOx	24%	48%	14%	14%	
CO	1%	1%	4%	94%	
HC	1%	2%	2%	95%	(Liu et al., 2019)
SO_2	9.90%	35%	21.20%	33.80%	
NOx	20.50%	55.50%	14.10%	9.90%	
CO	1%	2.40%	5%	91.60%	
HC	1%	3.80%	3%	92.20%	(Yang et al., 2018)
NOx	25%	49%	13%	13%	
CO	1%	2%	4%	93%	
HC	1%	3%	3%	93%	(Yılmaz, 2017)

2.7 Air pollution and Climate change

This section provides overview of the environmental impacts caused by emissions generated from aircraft engine exhaust. The pollutant emitted on aircraft engine has various health effects and one the source of climate change. The link between poor air quality and health impacts was well studied.

2.7.1 Air quality Impact.

. The pollutants emitted from aircrafts are considered very harmful to the public health and the environment. Health impacts of pollutant such as carbon monoxide, nitrogen oxides and Sulphur dioxides are summarized in the Table 2.7.

Table 2. 7. Air quality pollution health effects

Pollutant	Health Effect
Particulate matter (PM)	• Premature mortality • Aggravated respiratory and cardiovascular disease • Lung function impairment
Nitrogen oxides (NO_x)	• Lung irritation • Lower resistance to respiratory infections
Unburned hydrocarbons (UHCs)	• Eye and respiratory tract infections • Headaches/dizziness/memory impairment
Ozone (O_3)	• Lung function impairment • Lower resistance to respiratory infections
Carbon monoxide (CO)	• Aggravation of cardiovascular disease

Source: Richard de Neufville et al., 2013

2.7.2 Climate Change

Climate change is a world issue in nowadays, aviation as other sector plays an important role on contribution to the climate change by adding pollutant such as carbon dioxide and water vapours to the atmosphere. On the other end aviation produces 3 percent of anthropogenic carbon dioxide emissions however special attention has been placed on it because the highest growth of the aviation industry and deposing of pollutant at higher altitudes. Fuglestvedt et al., (2010) on the research Transport impacts on atmosphere and climate: Metrics indicated one damage caused by climate change is wealth loss as shown in the Figure 2.4 Pollutant emitted from aircraft engine exhaust has several impacts on climate change such increasing of global warming (caused by greenhouse gas (GHGs) CO_2), sea level, ice/snow cover, and precipitation patterns. NO_x gas pollutant are not GHGs, but through atmospheric processes they lead to ozone (O_3) production and methane (CH4) destruction, both of which are strong GHGs, so these processes have warming and cooling effects. SO_X when suspended in atmosphere not only cause cooling effect by reflect the sun light but also warming

26

effect by trap infrared radiation. Indonesia average annual expenditures related to climate change is US $15.7 billion as shown on Figure 2.5. (CPEIR).

Increasing relevance

Increasing uncertainty

Emissions (E)

(CO_2, CH_4, HFC, PFC, NO_X, SO_2…)

↓

Atmospheric concentrations (C)

↓

Radiative forcing (RF)

↓

Climate changes

Temperature (ΔT), precipitation (Δp), winds, soil moisture, extreme events, sea level (ΔSL)

↓

Impacts

Agriculture and forestry, ecosystems, energy production and consumption, social effects

↓

Damages

Welfare loss (e.g. monetary units)

Figure 2. 4. Cause and effect chain of the potential; climate effect emissions (Fuglestvedt et al., 2010)
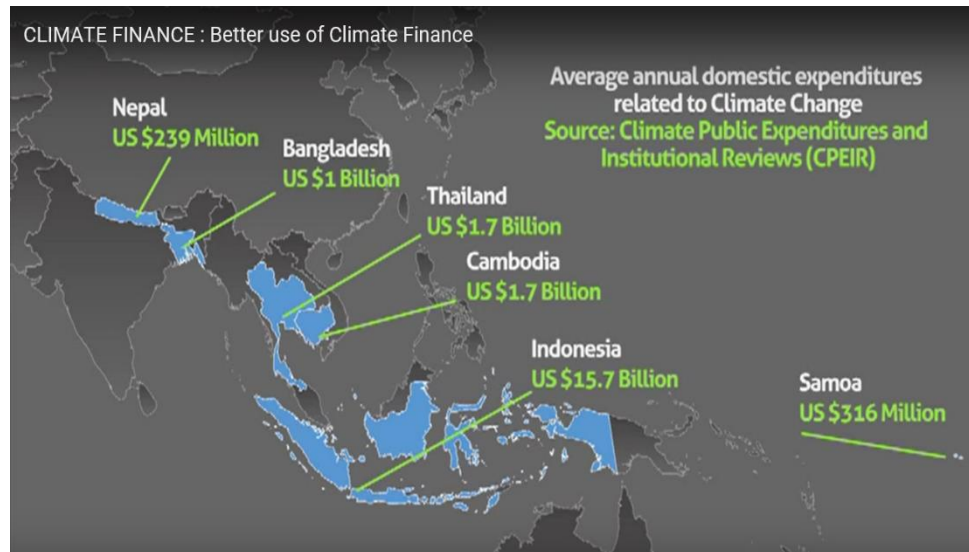
Figure 2. 5 Average annual domestic expenditures related to climate change (Source: Climate Public Expenditures and Institutional Reviews (CPEIR Database)

2.8   The International standard atmosphere (ISA)

The features of the atmosphere are different all over the world, atmosphere is a gaseous envelope surrounding the earth. International standard atmosphere (ISA) is the set of standard average condition based on mean sea level. The ICAO emission data bank contains emission indices of HC, NOx and CO with different types of jet engines determined under the ISA (International Standard Atmosphere) at mean sea level. Under ISA condition the temperature, pressure and density are given below:

a) Temperature equal to 15°C

b) Pressure at 1013.25 hPa (29.92 Hg)

c) Standard density of the sea level is 1.225 kg/m^3

2.8.1   Temperature

The atmosphere is divided in troposphere, stratosphere, mesosphere and thermosphere, usual civil aircrafts fly at altitudes between 8 km and 12 km while light aircraft mainly fly at low altitudes up to 1.5 km (Romano et al., 1999). Temperature

28

decreases with increasing altitude at constant rate of -6.5°C/1000m or -1.98°C/1000ft until to the tropopause which is located at altitude of 11000m. The temperature remains at constant at -56.5°C from tropopause to the higher altitudes (Airbus, 2002) The characteristic of temperature is shown on Figure 2.6 below:
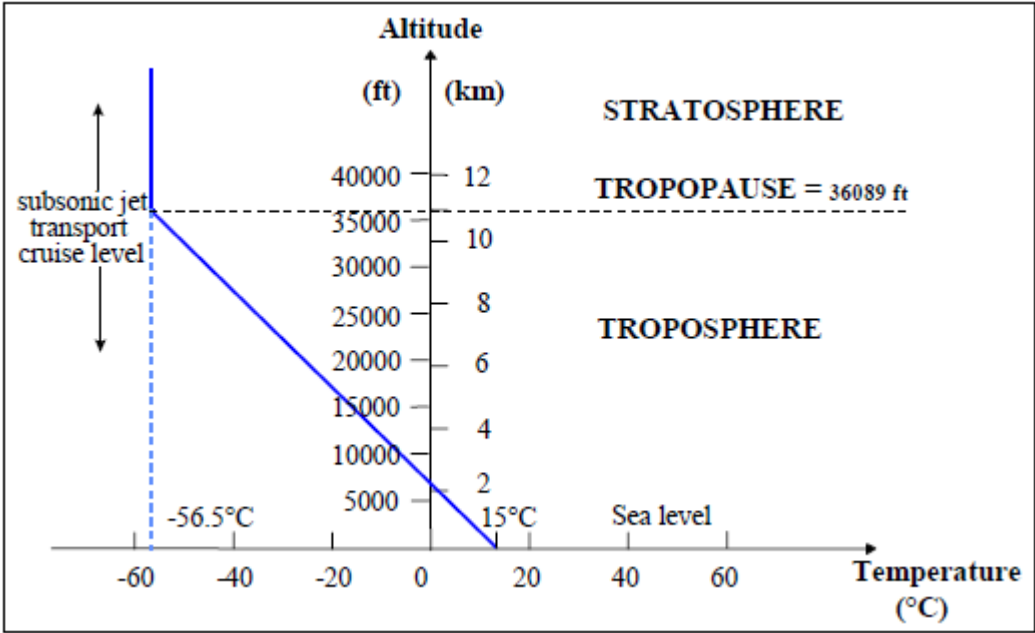
Figure 2. 6. Temperature variations (Source Airbus, 2002)

These parameters temperature, density and pressure are very important because the values of emission factors are different at mean sea level and at high altitude, this lead also to affect emission calculation. The formula for calculation of temperature, pressure and density above mean sea level can be seen on attachment.

Table 2. 8 Comparison of different methodologies

Parameter	ICAO			EPA	EEA/EMEP			MEET	ALAQS	SOURDINE II
	Simple approach	Advanced approach	Sophisticated approach		Tier 1	Tier 2	Tier 3			
Fleet aircraft/engines combinations	Identification of aircraft types	Identification of aircraft and engine types	Actual fleet composition in terms of aircraft types and engine combination	Identification of aircraft types and engine combination	Identification of Aircraft fuel consumption by domestic and international flight separately	Identification of aircraft types and fuel consumption for both domestic and international flight	Actual flight movement data in terms of aircraft types and flight distance	Identification of aircraft types and engine performance	Identification of aircraft types and engine types in actual flight movement data	Identification of aircraft types and engine types
TIM	N/A (indirectly accounted for via UNFCC LTO emission factors)	ICAO Databank Certification values adjusted if possible to reflect airport specific information	Refined values (e.g. with consideration of performance)	Adjustment calculation of mixing height (duration of climb out and approach) from ICAO Databank	ICAO databank			ICAO databank	ICAO databank	ICAO databank
Emission factor	UNFCC LTO Emission Factors by Aircraft type	ICAO Databank Certification values	Refined values using actual performance and operational data	Refined values using weighted average emission factor per aircraft type per LTO	EEA/EMEP emission factor databank			ICAO databank and Emission Indices Sheets of MEET	ICAO databank	ICAO databank
Pollutants										
NO$_x$	Yes	Yes	Yes	Yes	Yes	Yes	Yes	Yes	Yes	Yes
CO	Yes	Yes	Yes	Yes	Yes	Yes	Yes	Yes	Yes	Yes
HC	Yes	Yes	Yes	Yes	Yes	Yes	Yes	Yes	Yes	Yes
SO$_2$	Yes	No	No	Yes	Yes	Yes	Yes	Yes	No	Yes
CO$_2$	Yes	No	No	No	Yes	Yes	Yes	Yes	No	Yes
SO$_x$	No	No	No	No	No	No	Yes	No	Yes	Yes
VOC	No	No	No	Yes	Yes	Yes	Yes	No	No	Yes
CH$_4$	No	No	No	No	Yes	Yes	Yes	No	No	No
N$_2$O	No	No	No	No	Yes	Yes	Yes	No	No	No
PM$_{10}$	No	No	No	No	Yes	Yes	Yes	No	Yes	No
PM$_{2.5}$	No	No	No	No	Yes	Yes	Yes	No	No	No
H$_2$O	No	No	No	No	No	No	Yes	Yes	No	Yes
TOG	No	No	No	No	No	No	No	No	No	Yes
LTO	Yes			Yes	Yes			Yes	Yes	Yes
Fuel flow	UNFCC LTO Emission Factors by Aircraft type	ICAO Databank Certification values	Refined values using actual performance and operational data	Refined values using performance and operational data	EEA/EMEP databank			ICAO databank and Emission Indices Sheets of MEET using Air Traffic Emission Simulation	ICAO databank	ICAO databank
Movements	Number of aircraft movement by aircraft type	Number of aircraft movement by aircraft engine combination	Number of actual aircraft movement by aircraft engine combination	Number of aircraft movement by aircraft engine combination	Number of aircraft movement by domestic and international flight	Number of aircraft movement by domestic and international flight	Number of actual aircraft movement by domestic and international flight	Number of aircraft movement by aircraft type and engine combination	Number of aircraft movement (actual/generated simulation) by aircraft type, engine type, date, time, type of operation, gate and runway.	Number of aircraft movement by aircraft type and engine type
Uncertainty	High uncertainty in representative engine type, TIM	uncertainty if actual performance and operational data not available	uncertainty if actual performance and operational data not available	uncertainty in forecast of growth aircraft activity	20–30% for LTO factor and 20–45% cruise factor	High uncertainty associated with the emission factor	5–10% for LTO factor and 15–40% cruise factor	uncertainty in ageing of engine	uncertainty in consistency of data used	emission indices vary linearly with thrust level
GIS information	No	No	No	No	No	No	No	No	Yes	No

Source Kurniawan and Khardi, 2011

Table 2. 9. Current researches on aircraft emissions

No	Reference	Parameters	Method
1	Fan et al., 2012	HC, CO, NO$_X$, CO$_2$ and SO$_2$	Based on the 2010's China flight schedule, aircraft/engine combination information, and revised emission indices from the ICAO emission data bank with meteorological data, The emissions of HC, CO, and NOx are calculated by using the Boeing Fuel Flow Method 2 (BFFM2)
2	Yılmaz, 2017	HC, NO$_X$, HC and CO	The estimation of aircrafts emissions in 2010 during landing and take-off cycle described by ICAO is presented using flight data recorded by the State Airports Authority for Kayseri Airport, Turkey. The ICAO – Engine emission data bank is used for the emission calculations.
3	Koudis et al., 2017	NO$_X$	Sophisticated ICAO method.
4	Vujović and Todorović, 2017	NO$_X$, CO, HC, SO$_X$, Particle matter	An advanced approach using a landing and take-off cycle (LTO) method recommended by ICAO was employed to assess emissions Emissions of both volatile and non-volatile particulate matter are estimated using the new First-Order Approximation methodology.

Hence, the current study was developed from pervious researches shown on Table 2.9 Most studies focus on the estimation of pollutant emission during LTO cycle this study will focus on both emission pollution from LTO cycle and non LTO cycle (climb and descend) by using two methodologies Advanced approach by ICAO (2011) for LTO cycle, this methodology is accurate and have been used in most airport all over the world due to ICAO is the key and repuTable authority on aviation industry (Grampella et al., 2017; Liu et al., 2019; Vujović and Todorović, 2017). Methodology of estimating emission from air traffic (EIS MEETS) for non LTO cycle, this method has advantage of calculation of emission at regional base above 3000 ft. (Kurniawan and Khardi, 2011) Also, this study will map the pollution around Juanda international Airport. Table 2.10 summarizes the study parameters and methodology.

Table 2. 10. Short summary from current study

Reference	Parameters	Method
Current study (Freddy)	HC, CO, CO_2, NO_X and SO_2	• ICAO Advanced approach method. • Methodology of estimating emission from air traffic (EIS MEET) • Mapping of emission concentration at Juanda airport

CHAPTER 3

RESEARCH METHODOLOGY

3.1 Introduction

This chapter describes the research methods that the researcher is going to use in the process of carrying out the research study. This section contains the following parts: research location, nature of data, data collection techniques, data analysis and research flow chart.

3.2 Research location

Research location for assessing aircraft emissions based on flight path will be conducted on Juanda International Airport, Road Ir. Haji Sidoarjo, East Java Indonesia. The location is as shown on the Figure 3.1.
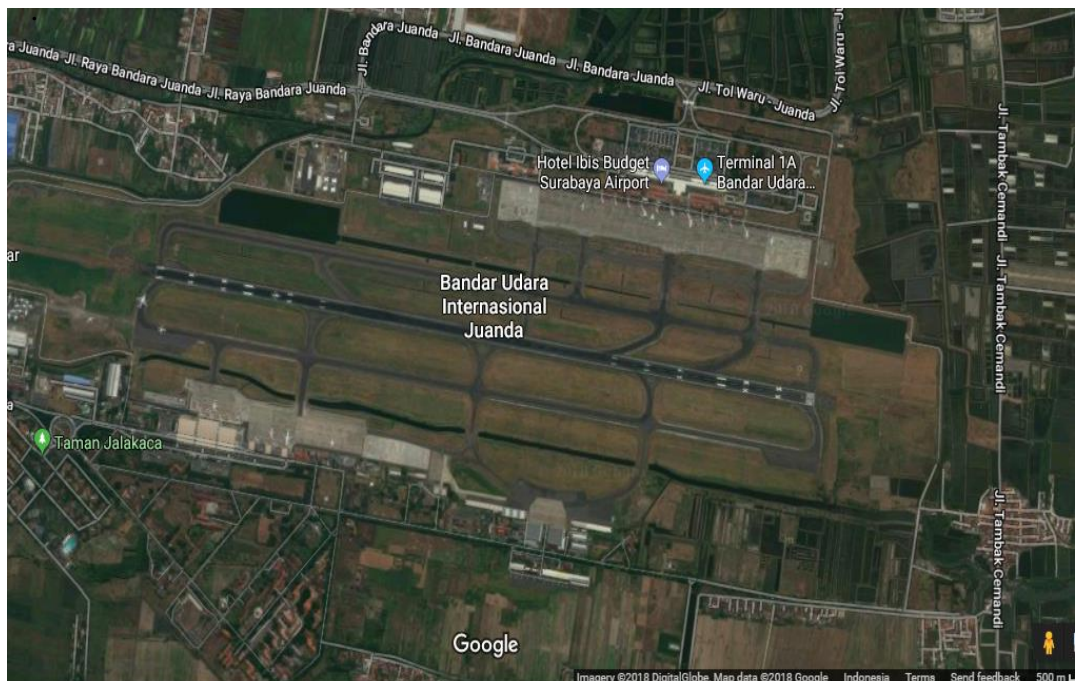
Figure 3. 1. Juanda International Airport (Source Google map 2018).

3.3 Literature Review

Literature review was explained in the chapter 2. It is contained the review of the basic theory and conventional framework. This stage is useful in develop understanding on the nature of aircraft movements and those effects to the

environment. The literatures also give reference in shaping the methodology to achieve research goal.

3.4   Data Collection.

Method used for data collection on this research will be based on survey of literature review of reference books, and journal which relevant to the research.

3.4.1   Types of Data

Type of the data that used on this research is secondary data. Data that could yield from other data, actual the data is available from the past researches, internet, documents and from library. It used because it has strong connection to the previous in term of saving money. It helps the researcher to broaden the database. It is much less expense than other ways of collecting data. Data required is as listed below:

a) Schedule Database

The schedules used in this research are from the planning schedules of the airlines. The airline name, flight number, airplane type, flight date, starting place and time, terminal place and time, are given for each flight. Some errors like flight double counting have been avoided by arranging the flight in the form of city to pair.

b) Aircraft Engine Combination

Aircraft/engine combinations are obtained from official websites of aircraft manufacturers. For the same airline, aircrafts of one specific type may be equipped with different types of engines. Usually the detailed aircraft/engine combination information is difficult to approach. Information from the aircraft manufacturers and the ICAO emission data bank ICAO, (2018) was used to analysed and selected the most typical engine combinations mounted on the aircraft.

c) Engine Emission Indices

The ICAO emission data bank contains CO, NO_x and HC emission indices of several kinds of jet engines measured under International Standard Atmosphere (ISA) condition at sea level. In addition, the CO_2 and SO_2 emission indices used in this research are taken from   Kalivoda and Kudrna, (1997) as 3150 g kg^{-1} and 1g kg^{-1} respectively. Also, emission index

sheet from methodology of estimating emission from air traffic (EIS MEET) will be used to assess emission indices apart from LTO cycle that is climb and descent.

d) Determination of LTO cycle.

One LTO cycle is the summation of one landing and one take-off operation. An LTO cycle contains one landing and one take-off, and so the number of landings and take-offs at an airport should be equal If there is a difference then the greater number should be used. The total number of either landings or take-offs may be treated as the number of LTOs. (ICAO doc 9889)

3.5 Data Process

The researcher reduced data into manageable size in order to get clear set of conclusion and findings. The calculation of fuel consumption, calculation of emission concentration and analysis emission pollutant from aircrafts were conducted. Method used to calculate the fuel flow during LTO cycle is based on ICAO emission indices databank 2018, during climb and descent using methodology for estimating emission from air traffic (MEET) method. Methods used for Emission pollutant calculation of HC, CO, CO_2, SO_2 and NO_x for this research are two methods. ICAO LTO cycle method used to calculate emission from landing, taxi in, taxi out and take-off. MEET used to calculate emission from climb and descent. ArcGIS used to map ground pollution concentration at Juanda International airport.

3.5.1 Calculation of Fuel consumptions

The fuel consumptions we are dealing with consists of two parts: the LTO fuel consumptions and the climb and descent fuel consumption and can be calculated as following.

a) LTO fuel consumptions

The LTO fuel flow of engines has been given in the ICAO emission data bank 2018.

$$Fuel\ consumption = Fuel\ flow \times flight\ duration\ .\ ....(3.1)$$

35

Therefore, to get total fuel consumption by aircraft the fuel consumption in equation (3.1) is multiplied by number of engines and LTO cycles. Flight duration in each phase is given in the Table 3.1

b) Fuel consumption during climb and descent.

The coefficients of fuel flow c1, c2, c3, and c5 during climb and descent given by emission index sheet EIS MEET. The following equation is used

Fuel per engine = $c1+c2\times(CRALT)+c3\times(CRALT)^2+c4\times(CRALT)^3$………....(3.2)

Where, CRALT = Cruising altitude.

Therefore, total fuel consumptions obtained by multiplying equation (3.2) with number of engine and aircrafts.

Table 3. 1. Time in Mode in LTO cycle.

Operation mode	ICAO default LTO cycle		
	Phase	Time in mode TIM (min)	Thrust setting (%)
Arrival	Approach	4	30
	Taxi in	7	7
Departure	Taxi out	19	7
	Take-off	0.7	100
	Climb out	2.2	85

Source: ICAO ,2011

3.5.2 Calculation of Emission Concentration.

Calculation of LTO emissions, climb and descent emissions conducted as following;

a) LTO cycle emissions

Advanced approach returns an increased level of improvement concerning about aircraft types, emission indices calculations and TIM. Estimations of aircraft engine emissions on this approach signified more accurate compared to the simple

approach and studies the pollutant emissions of HC, CO and NO_x. The calculation of emission concentration follows equation 3.2 (ICAO 2011)

$$Eij = (TIM \times 60) \times \left(\frac{FFjk}{1000}\right) \times EIjk \times NEj \dots\dots\dots\dots\dots\dots\dots\dots\dots\dots\dots\dots (3.3)$$

Where:

Eij   total emissions of pollutant i (for example HC, CO_2, or NOx), in grams, produced by aircraft type j for one LTO cycle.

TIMjk time-in-mode for mode k in minutes, for aircraft type j.

FFjk   the fuel flow mode in k in kilograms of fuel per second (kg/s) for each engine used on the aircraft type j.

EIjk   the emission factor for pollutant i given in grams of pollutant per kilogram of fuel (g/kg fuel) in mode k (during take-off, climb, taxi/idle and approach) for each engine used on the aircraft type j.

NEj   Number of engines used on aircraft type j.

b) Descent and Climb out emissions

Emission Indices of CO and HC in descent mode are calculated by using Equation. (3.4) and (3.5), where a1, a2, b1 and b2 are the coefficients provided by EIS MEET.

$$a1 + a2 \times \ln(CRALT)\dots\dots\dots\dots\dots\dots\dots\dots\dots\dots\dots\dots\dots\dots\dots\dots (3.4)$$

$$b1 + b2 \times \ln(CRALT) \dots\dots\dots\dots\dots\dots\dots\dots\dots\dots\dots\dots\dots\dots\dots\dots\dots (3.5)$$

Emission Indices of CO and HC in climb out mode are calculated by using equations (3.6) and (3.7), where a1, a2, b1 and b2 are the coefficients provided by EIS MEET.

$$a1 + \frac{a2}{CRALT} \dots\dots\dots\dots\dots\dots\dots\dots\dots\dots\dots\dots\dots\dots\dots\dots\dots\dots\dots\dots (3.6)$$

$$b1 + b2/(CRALT) \dots\dots\dots\dots\dots\dots\dots\dots\dots\dots\dots\dots\dots\dots\dots\dots\dots (3.7)$$

Emission indices of NOx in descent and climb out mode are calculated by using equation (3.8), where d1, d2, d3 and d4 are the coefficients provided by EIS MEET.

$$d1 + d2 \times (CRALT) + d3 \times (CRALT)^2 + d4 \times (CRALT)^3 \dots\dots\dots\dots\dots\dots\dots (3.8)$$

Where;

(CRALT) is cruising altitude

c) Calculation for SO_X and CO_2 emissions

Emission of pollutant SO_X and CO_2 are calculated by multiplying fuel consumption with its respective specific emission factor because emission indices of CO_2 and SO_2 based on fuel composition.

3.5.3 How to map the pollution.

ArcGIS software used to map the pollutant around Juanda International airport. The working steps are described as following

1. Digitized Area Juanda airport.

This process aims to create a polygon in the Juanda Airport area by interpreting it from ESRI's Basemap Imagery.

2. Airport Buffer Area.

This process forms a new polygon by enlarging in all directions as far as radius distance (d) from the Polygon Airport Area. The distance from the polygon is calculated by consider approaching speed, glide path angle (GPA) and height of 3000ft (LTO) equation (3.9). as described below:

ILS Approach

Instrument landing system (ILS) is a ground-based radio navigation system giving pilot the lateral and vertical guidance toward the runway. The following are key concepts of ILS as defined by ICAO Annex 10 volume I (Aeronautical Telecommunication - Radio navigation Aids)

ILS glide path that focus points in the vertical plane containing the runway centre line at which difference in depth modulation (DDM) is zero, which of all such loci is the closest to the horizontal line.

ILS Glide path angle (GPA) the angle between a straight line which represents the mean glide path with horizontal. Preferred ILS Glide path angle is 3 degrees.

ILS reference datum (Point "T") a point at a specified height located above the intersection of the runway centre line and the threshold and through the downward extended straight portion of the ILS glide path passes.

ILS divided into three categories as explained below:

Facility Performance Category I — ILS. An ILS which provides guidance information from the coverage limit of the ILS to the point at which the localizer course line intersects the ILS glide path at a height of 60 m (200 ft) or less above the horizontal plane containing the threshold.

Facility Performance Category II — ILS. An ILS which provides guidance information from the coverage limit of the ILS to the point at which the localizer course line intersects the ILS glide path at a height of 15 m (50 ft) or less above the horizontal plane containing the threshold.

Facility Performance Category III — ILS. An ILS which, with the aid of ancillary equipment where necessary, provides guidance information from the coverage limit of the facility to, and along, the surface of the runway.

According to Aeronautical Information Publication (AIP) Indonesia volume II, Juanda International airport is in *ILS category I* as seen on Table 3.2.

Table 3. 2. Radio navigation and Landing Aids at Juanda Airport

1	2	3	4	5	6	7
Type of Aid and Category	ID	Frequency	Hours of Operation	Site of Transmitting Antenna Coordinates	Elevation of DME Transmitting Antenna	Remarks
VOR/DME	SBR	113.4 MHz/ CH-81X	H – 24	07 22 26.18 S 112 46 16.39 E		VOR/DME "SBR" unusable areas beyond:
ILS/LLZ	ISBY	110.10 MHz	H – 24	07 22 56.83 S 112 48 10.92 E		160° - 210° BLW 14000 ft. 210° - 230°
GP		334.40 MHz	H – 24	07 22 45.10 S 112 46 34.02 E		BLW 11000 ft.
OM		75 MHz	H – 24	07 22 00.84 S 112 42 25.16 E		ILS/LLZ "ISBY" for RWY 10 (category
MM		75 MHz	H – 24	07 22 34.39 S 112 45 53.36 E		1) located 300 M FM end of RWY 10, angle 3°.
Radar Head				07 22 27.53 S 112 48 01.85 E		Coverage range : MSSR 200 NM PSR 70 NM

Source AIP Indonesia volume II, website www.aimindonesia.dephub.go.id

The ILS shall comprise the following basic components

    a) Very High Frequency (VHF) localizer equipment, associated monitor system, remote control and indicator equipment.

    b) Ultra-High Frequency (UHF) glide path equipment associated monitor system, remote control and indicator equipment.

    c) VHF marker beacons or distance measuring equipment (DME) together with associated monitor system, remote control and indicator equipment.

Based on the assumption that the aircraft is heading directly toward the facility equation 3.9 is applied.

$$tan\ \theta = \frac{3000}{d} \quad\text{.. (3.9)}$$

Where

θ is glide path angle (GPA) and (d) radius distance from runway of the airport.
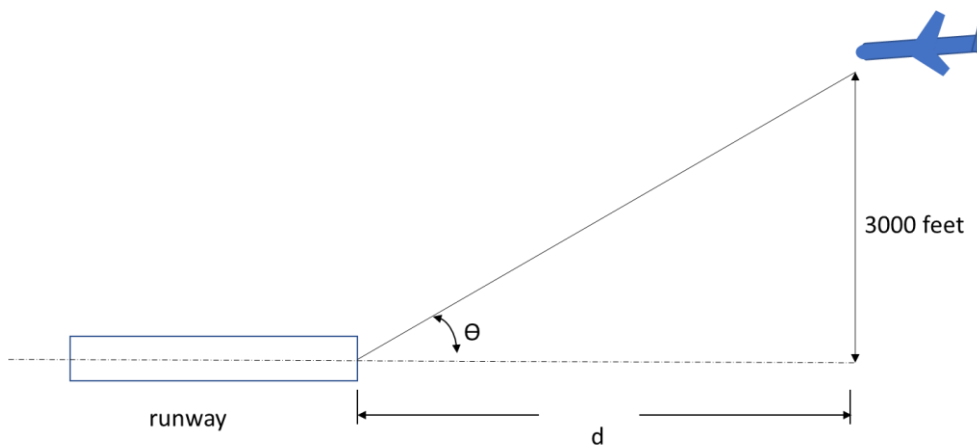
Figure 3. 2. Illustration of aircraft approach.

  After that, separate the polygons that are in the direction of the plane path and which are not. In this polygon the value that is in the direction of the direction of the plane path is 10 while the one that is not in the direction is valued at 20. This value is entered in the FID field.

3. Polygon to Raster.

      This process aims to change the Polygon Buffer which is vector data into raster data. The raster generated in this process uses a cell size of 5 meters (raster

pixel size of 5 meters). The value field used is FID, the FID value is 0 so the value of all pixels in this raster is 0.

4. Cost distance.

This process analyses how far the range of pollutant is. In this process 2 input sources and raster costs are needed, source is polygon which becomes the beginning of distribution while cost raster is a raster that determines the value of how far a pixel is to be reached from source. Maximum distance which is the amount of pollutant at Juanda Airport.

5. Raster calculator.

This process changes the value of Cost Distance Raster to become an Affected Raster Area. Because Cost Distance calculates how far a pixel is from the source, the farther away from the source, the greater the pixel value, while in this analysis the distance from the airport should be (the source) the less pollutant. Then do the Raster Calculator with the equation [(- "Cost Distance Raster") + pollutant].

6. Raster Affected by pollutant at Juanda Airport

Then Affected Raster symbology was done so that the area is divided into 4 classes less affected, affected and high affected and highest affected. After that make a layout.

Mapping work flow can be seen on Figure 3.3 below:
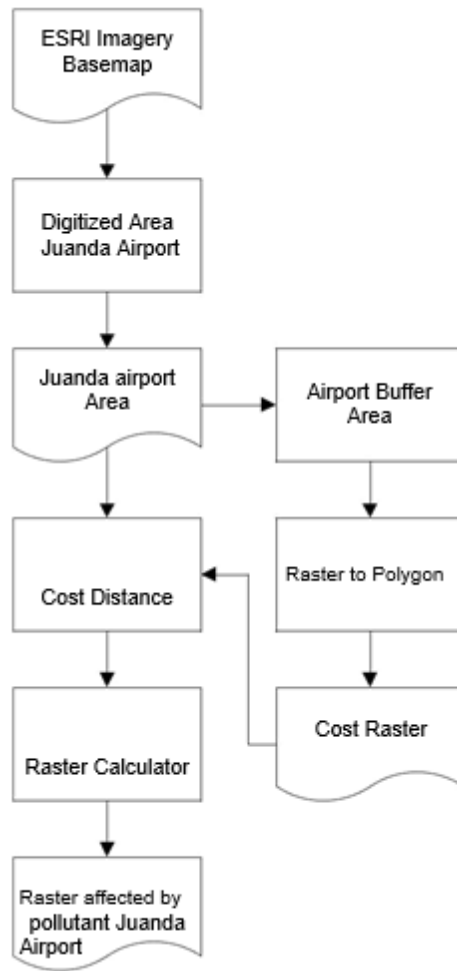
Figure 3. 3. Mapping of pollution work flow.

	WORKING STAGE	INPUT	WORKING DETAIL	OUTPUT
START	**Stage I** **Introduction and Collecting Informaton** ●Identification of problems: 1.Flight movement increase in Indonesia 2.The impact of of incresed air traffic movement on enviroment.		Literature Review Data Collection	● Research problems. ● Variables identification. ● Methodology and calculation method.
PROCESS	**Stage II** **Research Implementation Process** ● Analysis of fuel consumptions on LTO cycle and non LTO cycle ●Analysis of aircraft emissions ●Analysis of mapping the emission of aircraft movements	Secondary Data Fuel Flow, Time in mode, aircraft engine combination, aircraft time, arrival, departure. Secondary Data Engine emission Indices, Aircraft engine comibination, Time in mode, Aircraft type, flight path,Thrust settings, number of engiine, cruising Altitute Calculation Method 1. ICAO Advanced approach. 2. MEET Approach. Data aircraft emissions concentations	Data Prrocessing Fuel consumption calculation Calculation of aircraft emissions concentration Mapping of emission of aircraft movements	● Fuel consumed at approach, taxi, takeoff, climb out, descend and climb ●LTO cycle emissions ● Descent and Climb emissions ●Map of the emission of aircraft movements at Juanda Intl. Airport
FINISH	**Phase III** **Study Results** Analysis	The results of data analysis and estimation of commercial aircraft emission at Juanda International Airport based on flight path	Conclusions and recommendations	●Research problems answered ●Suggestions for upcoming research and development

Figure 3. 4. Research flow chart.

"This page is intentionally left blank"

CHAPTER 4

ANALYSIS AND DISCUSSION

4.1 Introduction

This chapter deals with the analysis of data and presentation of findings. This is the most important chapter in which the findings of the study are discussed and analysed in details relating to the objectives of the study. It is from this chapter where the answer of the Estimation of Aircraft Engine Emissions from Commercial Aircraft at Juanda International Airport based on flight path will be disclosed and analysed.

4.2 Peak Hour

Peak hour is the busiest hour obtained in the busiest month in a year. Determination of peak hour in this research is intended as reference data to be used in determining the most critical conditions for emissions concentration. In this calculation, flight departure-arrival schedule data is needed for Juanda International Airport. The peak hour data was taken from the movement data for seven days by taking the data on month of September 2018, then the busiest day in the week was determined and final the busiest hour on the busiest day has been found. Data of schedule of aircraft movement for seven days at Juanda International airport is listed in the attachment.

Table 4. 1. Peak Day Data

Day	Traffic Movement			LTO cycles
	Arrival	Departure	Total	
Sunday 16/09/2018	177	147	324	177
Monday 17/09/2018	189	165	354	189
Tuesday 18/09/2018	209	187	396	209
Wednesday 19/09/2018	223	194	417	223
Thursday 20/09/2018	249	248	497	249
Friday 21/09/2018	250	252	502	252
Saturday 22/09/2018	202	169	371	202

Table 4.1 shows that during seven consecutive days the peak day was on Friday 21 September 2018 which has 250 arrival aircrafts and the number of departed aircraft was 252. The sum of one arrival and one departure aircraft make one LTO cycle, according to ICAO doc 9889 if the number of departure and arrival are not the same take the maximum number between the two. The maximum number of LTO cycles was 252. (Source www.flightradar24.com)

Table 4. 2. Peak Hour Data

Traffic Movement		Peak hour	
Arrival	Departure	Time (Local time)	Total
1	18	05:00am - 05:59am	19
8	21	06:00am - 06:59am	29
17	15	07:00am - 07:59am	32
9	15	08:00am - 08:59am	24
17	14	09:00am - 09:59am	31
16	16	10:00am - 10:59am	32
16	19	11:00am - 11:59am	35
21	15	12:00pm - 12:59pm	36
6	16	01:00pm - 01:59pm	22
19	11	02:00pm - 02:59pm	30
16	13	03:00pm - 03:59pm	29
12	15	04:00pm - 04:59pm	27
21	12	05:00pm - 05:59pm	33
19	21	06:00pm - 06:59pm	40
13	13	07:00pm - 07:59pm	26
14	6	08:00pm - 08:59pm	20
17	6	09:00pm - 09:59pm	23
7	6	10:00pm - 10:59pm	13

Table 4.2 shows that the peak hour was from 06:00- 06:59 pm on Friday 21st September 2018.Row one of traffic movement of arriving and departing aircrafts, peak hour in the middle column. The traffic movement was 19 on arrival aircrafts and the number of departed aircrafts was 21. The sum of arrival and departure gives total number of movements of aircraft and was 40 during peak hour, others determined the same This data gives the number of landing and take-of (LTO) cycle, aircraft type during peak hour. (Source www.flightradar24.com)

4.3   Calculation and analysis of fuel consumption.

Fuel consumptions on this research consist of two parts. First part is calculation of fuel consumptions during LTO cycle that is taxi/idle, approach, take off and climb out. The second part is calculation of fuel consumption during non LTO cycle climb and descent phase. Type and registration of aircraft operated during peak hour at Juanda International airport shown on Table 4.3

Table 4. 3. Aircraft types during peak hour

No	Aircraft	ICAO code	Aircraft Registration
1	Airbus 330-343	A333	PK-GPX
2	CRJ-1000ER	CRJX	PK-GRN
3	Boeing 737-900	B739	JT642
4	Airbus 320-251N	A20N	PK-GTF
5	Boeing 737-800	B738	PK-LPU
6	Airbus 320-251N	A20N	PK-GTI
7	Boeing 737-800	B738	PK-LKV
8	Boeing 737-800	B738	PK-GFN
9	Boeing 737-800	B738	PK-LKJ
10	Airbus 320-214	A320	PK-LAV
11	Boeing 737-300	B733	SJ259
12	Airbus 320-214	A320	PK-GQE
13	Boeing 737-300	B738	PK-GFK
14	Airbus 320-214	A320	9V-SLP
15	Boeing 737-900	B739	PK-LGW
16	Boeing 737-800	B738	PK-LPQ
17	CRJ-1000ER	CRJX	PK-GRC
18	Airbus 320-214	A320	PK-AXH
19	Boeing 737-500	B735	SJ227
20	Airbus 737-800	B738	PK-CRH
21	Airbus 320-214	A320	PK-GLA

Table 4.3 shows the types and registration of aircraft operated during peak hour at Juanda International airport. There were 19 aircrafts on arrival and 21 aircrafts on departure ICAO suggested that for simplification of calculation take the maximum number between departure and arrival if it is not the same. The total numbers of LTO for calculation used in this research were 21 LTO cycles.

After obtained data from Table 4.3 then using aircraft manufactures website, the engine type mounted on each aircraft operated at Juanda International airport and number of LTO cycles was found and listed as shown in the Table 4.4 below.

Table 4. 4. Aircraft Engine type

Aircraft type	Number of Engine	Type of Engine	Manufactures	Number of LTO cycles
A320	2	CFM56-5B4/P	CFM international	5
B739	2	CFM567B27	CFM international	2
B735	2	CFM56 3C1	CFM international	1
B738	2	CFM56 7B27	CFM international	7
B733	2	CFM56 3B2	CFM international	1
A333	2	CF680E1A4	GE Aircraft Engine	1
A20N	2	LEAP 1A26	CFM international	2
CRJ-1000ER	2	CF34-8C5A2	GE Aircraft Engine	2

Data from Table 4.4 shows the aircraft types and typical engines mounted on each aircraft. Most of aircraft mounted with engines manufactured by CFM international. It is important to identified different engine types mounted on aircraft because each engine has different fuel flow and emission factors which will be used for calculation of fuel and emissions. Example A320 has CFM56-5B4/P engine. grouping each type of aircraft from table to get LTO cycles, example 5 for A320.

4.3.1 Calculation of fuel consumption at LTO cycle

Fuel consumption during LTO cycles calculated by using equation 3.1 The time in mode and thrust setting used was as shown on Table 4.5 The data for fuel flow obtained from Engine Exhaust emission Databank (ICAO, 2018) hosted by European Safety Aviation agency (EASA) at   https://www.easa.europa.eu/easa-and-you/environment/icao-aircraft-engine-emissions-databank steps are as follows

Table 4. 5. Standard time in mode and Thrust setting at LTO cycle

Phase	Time in mode TIM (min)	Thrust setting (%)
Approach	4	30
Taxi/Idle	26	7
Take-off	0.7	100
Climb out	2.2	85

Source ICAO, 2011

Table 4. 6. A320 Fuel flow per engine used

Mode	TIME	Fuel flow per engine used
	min	kg/s
Taxi/Idle	26	0.104
Approach	4	0.312
Climb out	2.2	0.935
Takeoff	0.7	1.132

Source ICAO, 2018

Calculation of fuel consumption for Airbus 320 is shown below and repeated the same procedure for other aircrafts using data from Table 4.4, 4.5 and Table 4.6 for number of engines, number of LTO cycles, time in mode and fuel flow respectively

$$Fuel\ consumption = Fuel\ flow \times flight\ duration$$

$$Fuel\ consumption\ taxi = 0.104 \times 26 \times 60 \times 2 \times 5$$

Therefore, fuel consumption during taxi/idle mode = 1622 kg

$$Fuel\ consumption\ Approach = 0.312 \times 4 \times 60 \times 2 \times 5$$

Therefore, fuel consumption during approach mode is equal to 749 kg

$$Fuel\ consumption\ Climb\ out = 0.935 \times 2.2 \times 60 \times 2 \times 5$$

Therefore, fuel consumption during climb out mode is 1234 kg

$$Fuel\ consumption\ Takeoff = 1.132 \times 0.7 \times 60 \times 2 \times 5$$

Therefore, fuel consumption during take-off is same as 475 kg

Table 4. 7. A320 fuel consumption

Mode	TIME	Fuel flow per engine used	Fuel consumption
	min	kg/s	kg
Taxi/Idle	26	0.104	1622
Approach	4	0.312	749
Climb out	2.2	0.935	1234
Takeoff	0.7	1.132	475

Table 4.7 presents the fuel consumption of aircraft A320 during one LTO cycle. The taxi/idle phase has the maximum number of fuel consumptions followed by climb, approach take off phases respectively.

Table 4. 8. B738 fuel consumption

Mode	TIME	Fuel flow per engine used	Fuel consumption
	min	kg/s	kg
Taxi/Idle	26	0.116	2533
Approach	4	0.349	1173
Climb out	2.2	1.043	1927
Takeoff	0.7	1.284	755

Table 4.8 presents the fuel consumption of aircraft B738 during one LTO cycle. The taxi/idle phase has the largest number of fuel consumptions followed by climb out, approach take-off phases respectively.

Table 4. 9. B739 fuel consumption

Mode	TIME	Fuel flow per engine used	Fuel consumption
	min	kg/s	kg
Taxi/Idle	26	0.116	724
Approach	4	0.349	335
Climb out	2.2	1.043	551
Takeoff	0.7	1.284	216

Table 4.9 presents the fuel consumption of aircraft B739 during one LTO cycle. The taxi/idle phase has the largest number of fuel consumptions followed by climb out, approach take-off phases respectively.

Table 4. 10. B735 fuel consumption

Mode	TIME	Fuel flow per engine used	Fuel consumption
	min	kg/s	kg
Taxi/Idle	26	0.124	387
Approach	4	0.336	161
Climb out	2.2	0.954	252
Takeoff	0.7	1.154	97

Table 4.10 presents the fuel consumption of aircraft B735 during one LTO cycle. The taxi/idle phase has the largest number of fuel consumptions followed by climb out, approach take-off phases respectively.

Table 4. 11. B733 fuel consumption

Mode	TIME	Fuel flow per engine used	Fuel consumption
	min	kg/s	kg
Taxi/Idle	26	0.119	371
Approach	4	0.314	151
Climb out	2.2	0.878	232
Takeoff	0.7	1.056	89

Table 4.11. presents the fuel consumption of aircraft B733 during one LTO cycle. The taxi/idle phase has the largest number of fuel consumptions followed by climb out, approach take-off phases respectively.

Table 4. 12. A333 fuel consumptions

Mode	TIME	Fuel flow per engine used	Fuel consumption
	min	kg/s	kg
Taxi/Idle	26	0.227	708
Approach	4	0.744	357
Climb out	2.2	2.337	617
Takeoff	0.7	2.904	244

Table 4.12 presents the fuel consumption of aircraft A333 during one LTO cycle. The taxi/idle phase has the largest number of fuel consumptions followed by climb out, approach take-off phases respectively.

Table 4. 13. A20N (A320-251N)

Mode	TIME	Fuel flow per engine used	Fuel consumption
	min	kg/s	kg
Taxi/Idle	26	0.088	549
Approach	4	0.242	232
Climb out	2.2	0.705	372
Takeoff	0.7	0.855	144

Table 4.13 illustrates the fuel consumption of aircraft A20N during one LTO cycle. The taxi/idle phase has the largest number of fuel consumptions followed by climb out, approach take-off phases respectively.

Table 4. 14. CRJ1000ER fuel consumptions

Mode	TIME	Fuel flow per engine used	Fuel consumption
	min	kg/s	kg
Taxi/Idle	26	0.066	412
Approach	4	0.188	180
Climb out	2.2	0.563	297
Takeoff	0.7	0.691	116

Table 4.14 presents the fuel consumption of aircraft CRJ1000ER during one LTO cycle. The taxi/idle phase has the largest number of fuel consumptions followed by climb out, approach take-off phases respectively.

After calculation of each aircraft fuel consumption during LTO cycles the results summary can be seen on the following Table 4.15.

Table 4. 15. Fuel consumptions during LTO by each aircraft

Number of LTO cycles	Aircraft	Fuel consumption (kg)			
		Taxi/Idle	Approach	Climb out	Takeoff
5	A320	1622	749	1234	475
7	B738	2533	1173	1927	755
2	B739	724	335	551	216
1	B735	387	161	252	97
1	B733	371	151	232	89
1	A333	708	357	617	244
2	A20N	549	232	372	144
2	CRJ	412	180	297	116
21	TOTAL	7307	3338	5482	2135

In Table 4.15 number of LTO cycles and aircraft obtained from table 4.4, Fuel consumption is the results of table 4.7 to 4.13 After we obtained the fuel consumption of each aircraft, the following step is to sum up all fuel consumption from each aircraft so as to get the total fuel consumption on each operating mode such as taxi/idle, approach, climb out and take-off. Fuel consumption of jet aircraft engines favours being expressed in pounds (lb) preferred than in gallons (gal). This is due to the volumetric expansion and contraction of fuel with changes in temperature can be misleading in the amount of fuel which is available (Robert Horonjeff et al., 2010). The results of fuel consumptions can be seen of table below;

Table 4. 16. Fuel consumption during LTO cycle at Juanda International airport

Mode	Fuel consumptions (kg)
Taxi/Idle	7307
Approach	3338
Climb out	5482
Takeoff	2135

Table 4.16 shows the total fuel consumptions during LTO cycle at Juanda international Airport. Taxi/Idle mode has a largest number of fuel consumptions of 7307 kg compare to other approach, climb and take off modes. The take-off approach was the lowest mode in fuel consumptions of 2135 kg.
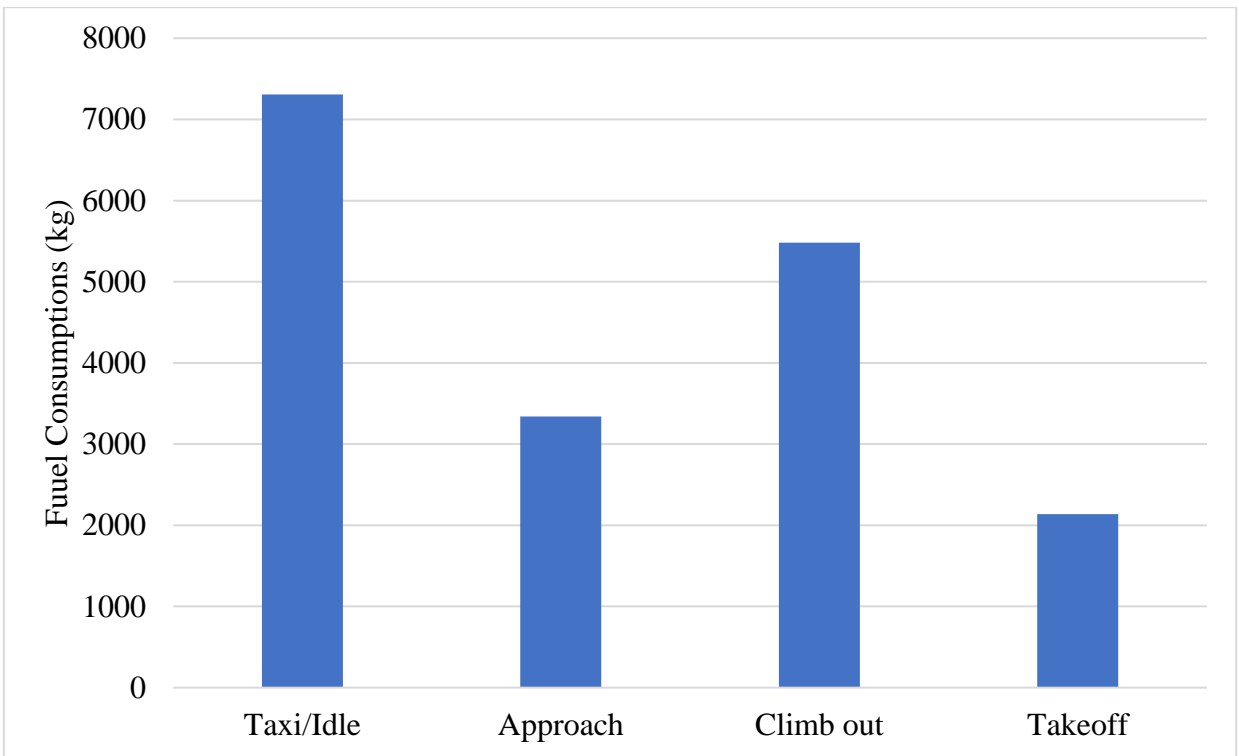
Figure 4. 1. Total fuel consumptions during LTO cycle at Juanda International airport.

Figure 4.1 and Figure 4.2 show the total fuel consumptions during LTO cycle at Juanda international Airport. Taxi/Idle mode has a largest number of fuel consumptions which was 40% of total amount compare to other approach 18%, climb out 30% and take off modes. The take-off was the lowest mode in fuel consumptions which was 12%.

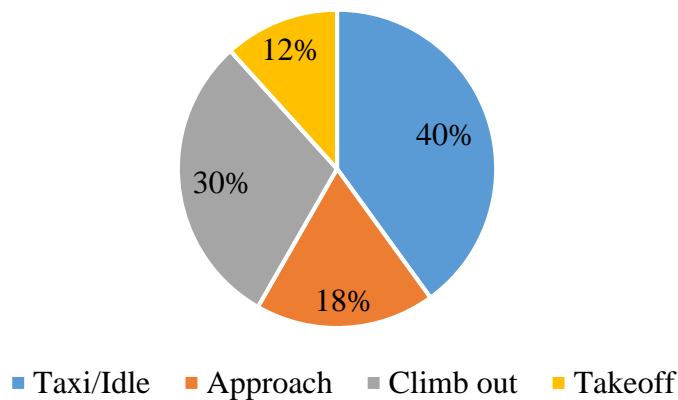Figure 4. 2. Distribution of fuel consumption at Juanda international airport.

4.3.2 Calculation of fuel consumption at climb and descent phase

This part deal with calculation of fuel consumption of non LTO cycle that is climb and descent. The MEET methodology was used to calculate the fuel consumption for A320, B733, B735, B738, B739. Aircraft type A333 and CRJX the consideration of ROC, time and average fuel consumption method was used because these types of aircrafts not covered by MEET methodology. Fuel consumed calculated up to FL150 (15000 ft) and descent from FL150(15000 ft to FL30(3000 ft) because this level will cover all flight international and domestic flight even those which fly to near destination so they do not need to climb to high altitude.

Calculation for A320 is shown below as an example. The coefficient of fuel c1, c2, c3 and c4 are given by emission index sheet (EIS). Equation 3.2 was used by calculation for climb and descent respectively.

Climbing from 3000ft to 15000 ft means cruising altitude used (CRALT) equal to 12000 ft same as descent from 15000 ft to 3000 ft.

Fuel during Climb

Fuel during climb up to 15000 ft for calculation the following data was used

c1 $= -6.438 \times 10^{1}$

c2 $= 6.045 \times 10^{-2}$

c3 $= -9.614 \times 10^{-7}$

c4 $= 1.921 \times 10^{-11}$

CRALT = 12000 ft

Number of engines= 2

Number of aircraft= 5

$$c1 + c2 \times (CRALT) + c3 \times (CRALT)^2 + c4 \times (CRALT)^3$$

Fuel = $-6.438 \times 10^{1} + 6.045 \times 10^{-2} \times 12000 + -9.614 \times 10^{-7} \times 12000^2 + 1.921 \times 10^{-11} \times 12000^3$

Fuel per engine used = 555.87328 kg

To get fuel consumption multiply fuel per engine used with number of engine and aircraft as follow

Fuel consumption = 555.87328×2×5

$\qquad$ =5558.7328 kg

Therefore, the total fuel consumption used by A320 from climb 3000ft to 15000ft equal to 5558.7328 kg.

Fuel during descent

Fuel during climb up to 15000 ft for calculation the following data was used

c1 $\quad = 5.745 \times 10^0$

c2 $\quad = 3.541 \times 10^{-3}$

c3 $\quad = -7.306 \times 10^{-8}$

c4 $\quad = 3.493 \times 10^{-12}$

CRALT = 12000 ft

Number of engines= 2

Number of aircraft= 5

$$c1 + c2 \times (CRALT) + c3 \times (CRALT)^2 + c4 \times (CRALT)^3$$

Fuel = $5.745 \times 10^0 + 3.541 \times 10^{-3} \times 12000 + -7.306 \times 10^{-8} \times 12000^2 + 3.493 \times 10^{-12} \times 12000^3$

Fuel per engine used = 43.752264 kg

To get fuel consumption multiply fuel per engine used with number of engine and aircraft as follow:

Fuel consumption = 43.752264 ×2×5

$\qquad$ = 437.52264 kg

$\qquad$ Therefore, the total fuel consumption used by A320 to descent from 15000 ft to 3000 ft equal to 437.52264 kg

Calculation for other aircraft A20N, B733, B735, B738, B739 follow the same procedure as for A320 and the results are shown on Table 4.17

Calculation of fuel consumption for CRJX (CRJ1000ER) and Airbus 300-300

To calculate the fuel consumption for CRJX and A333 we used the concept of rate of climb, rate of descent, time and distance. The forces acting on aircraft shown on Figure 4.3. The calculation was conducted as following:
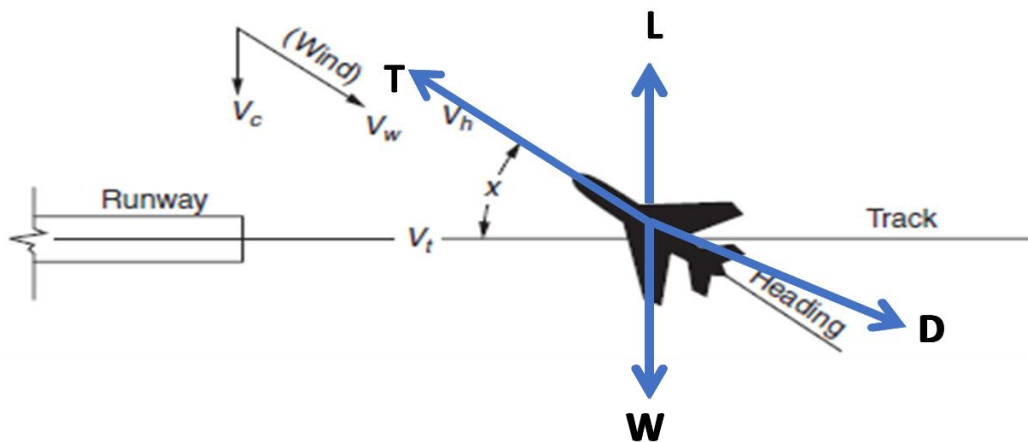
Figure 4. 3. Common forces acting on aircraft (Source *Robert Horonjeff et al., 2010)*

$$T - D - WSin\theta = m\frac{dV}{dt} .... (4.1)$$

Assumptions

   a) Thrust and velocity on same direction
   b) Mass is constant.
   c) Static performance

We get;

$$T - D - WSin\theta = 0$$

$Sin\theta = \frac{T-D}{W}$, multiply both side by V

$$VSin\theta = \frac{TV - DV}{W}$$

From definition

TV = Power available from an engine at given altitude

DV = Power required.

Hence, TV-DV = Excess power, and

$VSin\theta$ = Rate of climb (ROC)

$$Rate\ of\ climb = \frac{excess\ power}{W}$$

Where;

T   = Thrust

D   = Drag force

W   = Weight of aircraft

M   = Mass of aircraft

L   = Lifting force

θ   = Angle of climb

V   = Velocity

In this research we used rate of climb (ROC) and rate of descent (ROD) from aircraft performance database as shown in the following Figure 4.4 and 4.5 for A333 and CRJX.
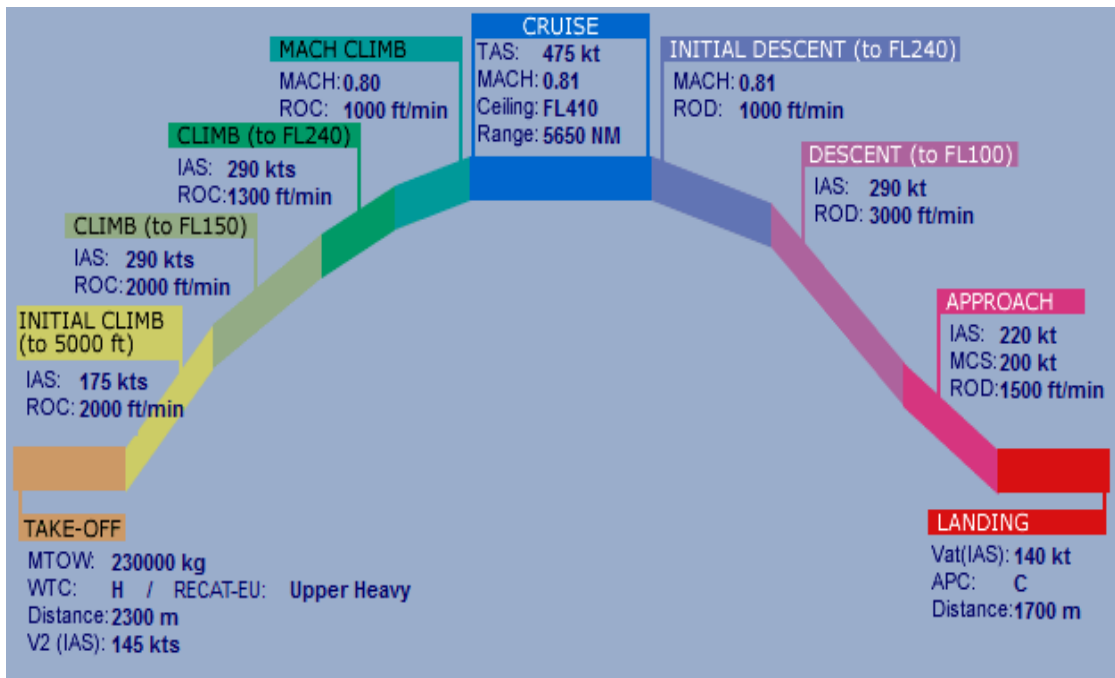
Figure 4. 4. A333 Flight path (Source Aircraft performance database v3
www.eurocontrol.int).
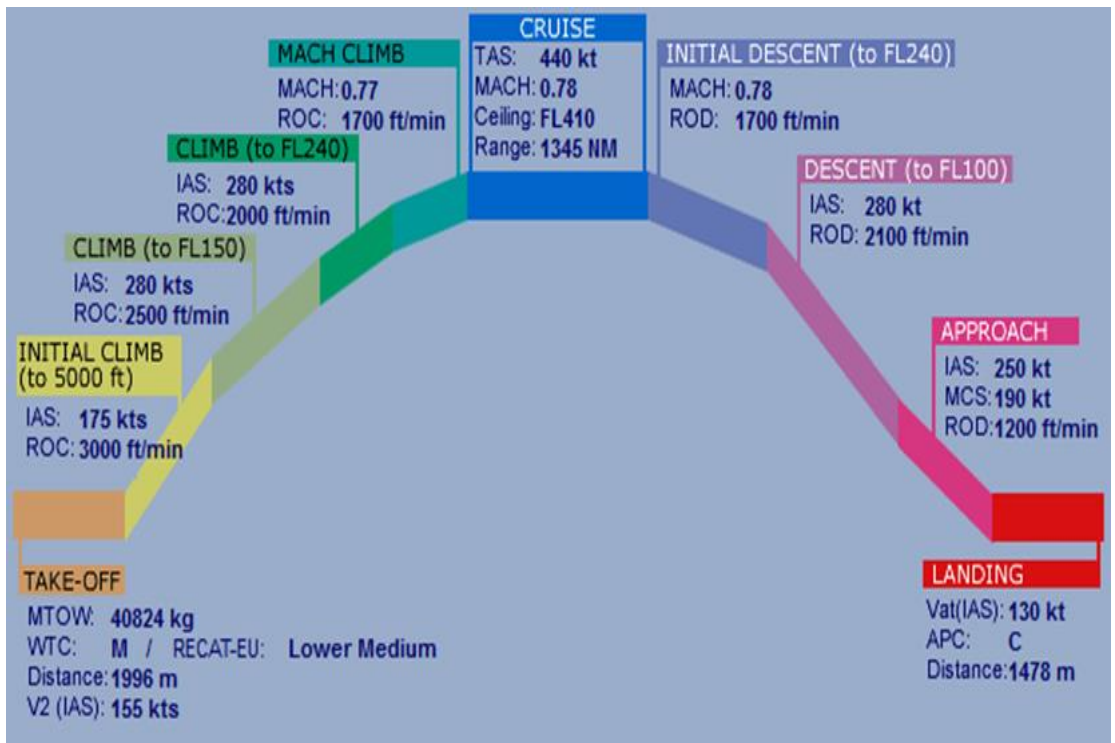
Figure 4. 5. CRJX flight path (Source aircraft performance database v3
www.eurocontrol.int).

Figure 4.4 and Figure 4.5 show the complete flight profile of aircraft Airbus A300-300 (A333) and CRJ1000ER (CRJX). The rate of climb (ROC) from 3000ft to 5000 ft is 2000 ft/min, 3000 ft/min for A333 and CRJX respectively. The rate of descent (ROD) from 15000 ft to 5000 ft is 3000 ft/min, 2100 ft/min respectively. The rate of descent from 5000 ft to 3000 ft is 1500 ft/min, 1200 ft/min for A333 and CRJX respectively.

Example of calculation of fuel consumption during climb and descent for A333 and CRJX is shown below using A333 as an example:

Fuel during Climb.

Using data from the Figure 4.4 we calculated the time required to climb from 3000ft to 5000 ft with rate of climb equal to 2000 ft/min and from 5000 ft to 15000 ft with rate of climb equal to 2000 ft/min.

Time to climb to 15000 ft = Time to climb 2000ft + Time to climb 10000 ft

$$Velocity = \frac{Distance}{Time}$$

Therefore,

$$Time = \frac{Distance}{Velocity}$$

Velocity used in this research is rate of climb, hence time required to climb up to 15000ft calculated as following;

$$Time = \frac{2000}{2000} + \frac{10000}{2000}$$

Time = 6 minutes

After obtained the time required to climb to 15000 ft, we multiply it by average fuel consumption which is 5900kg/h (Source aircraft operations manual) for A333 and 1349.35 kg/h for CRJX.

$$Fuel\ consumption = Time\ \times average\ fuel\ consumption$$

Fuel consumption = 6÷ 60× 5900

$$= 590 \text{ kg}$$

Therefore, fuel required to climb up to 150FL (15000 ft) for A333 is 590kg.

Fuel during Descent.

Using data from the Figure 4.4 we calculated the time required to descent from 15000 ft to 5000 ft with rate of descent (ROD) equal to 3000 ft/min and from 5000 ft to 3000ft with rate of descent equal to 1500 ft/min.

Time $= \frac{10000}{3000} + \frac{2000}{1500}$

Time = 4.666666667 minutes

Fuel consumption = 4.666666667÷60×5900

$$= 459 \text{ kg}$$

Therefore, fuel required to descent from 150FL (15000 ft) to 30FL (3000 ft) for A333 is 490 kg.

The same calculation of fuel consumption for climb and descent was used for CRJ1000ER (CRJX) and the results are as shown on Table 4.17

Table 4. 17. Fuel consumption during Climb and Descent from Juanda
International airport

Aircraft	Mode	Fuel consumption
		kg
A320	Climb	5559
	Descent	438
B738	Climb	10063
	Descent	445
B739	Climb	2875
	Descent	127
B735	Climb	1438
	Descent	64
B733	Climb	1438
	Descent	64
A333	Climb	590
	Descent	459
A20N	Climb	2223
	Descent	175
CRJX	Climb	210
	Descent	289

Table 4.17 illustrates the fuel consumptions during climb from 30FL (3000ft)
to 150FL (15000 ft) and descent from 150 FL (15000 ft) to 30FL (3000ft) from
Juanda International airport during peak hour. The maximum and minimum fuel
consumption during climb was 10063 kg and 210 kg by B738 and CRJX
respectively while maximum and minimum fuel consumption during descent was
459 kg and 64kg by A333 and B733/B375 respectively,

The distribution of fuel consumption by each aircraft can be seen in the
following Figure.
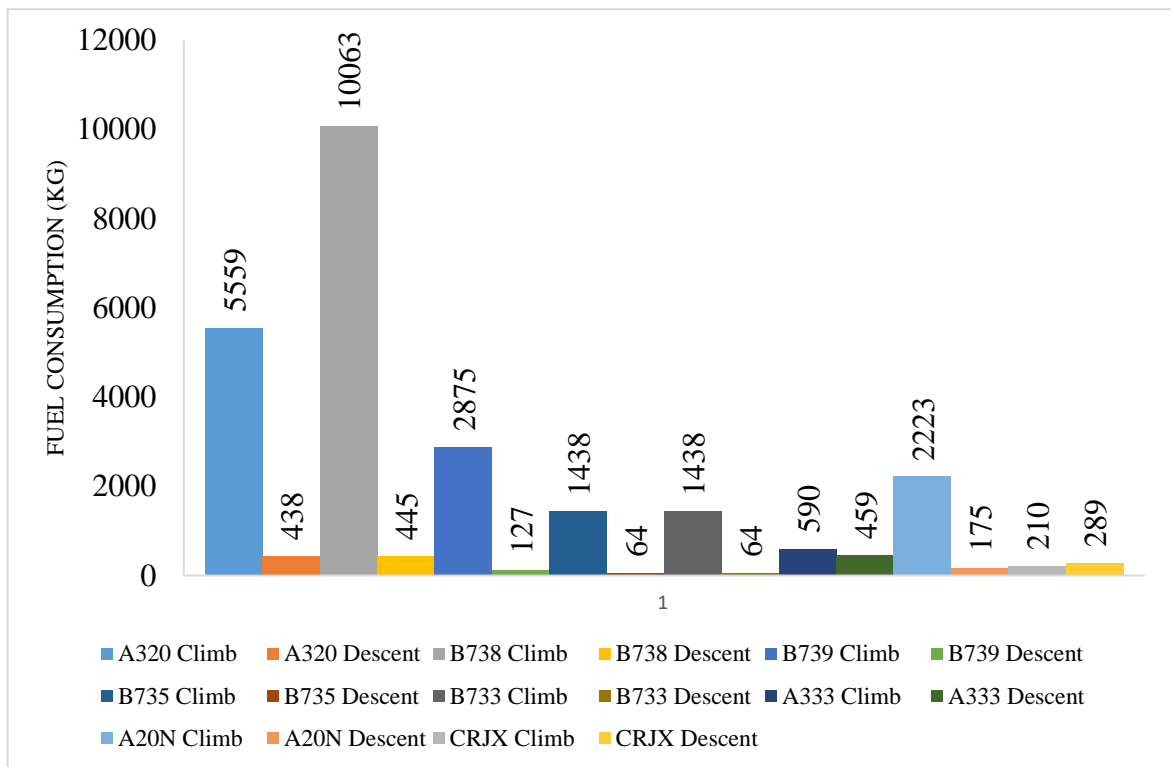
Figure 4. 6. Fuel consumption by each type of aircraft during climb and Descent

Fuel consumption by each time of aircraft from Juanda International airport during peak hour can be seen on the Figure 4.6. Many aircraft used more fuel during climb than descent except for CRJX which used less fuel during climb than descent. The total fuel consumption obtained by adding up the fuel used by each aircraft as shown on the following Table 4.18

Table 4. 18. Total fuel consumption during climb and descent

Mode	Fuel consumption kg
Climb	24396
Descent	2060

The aircraft operated at Juanda international airport during peak hour generated fuel consumption during climb from 3000 ft up to 15000 ft and descent

from 15000 ft to 3000 ft as shown on Table 4.18. The fuel consumption during climb was more than descent.

The total distribution of percentage of fuel used by each type of aircraft during climb and descent can be seen on the Figure below
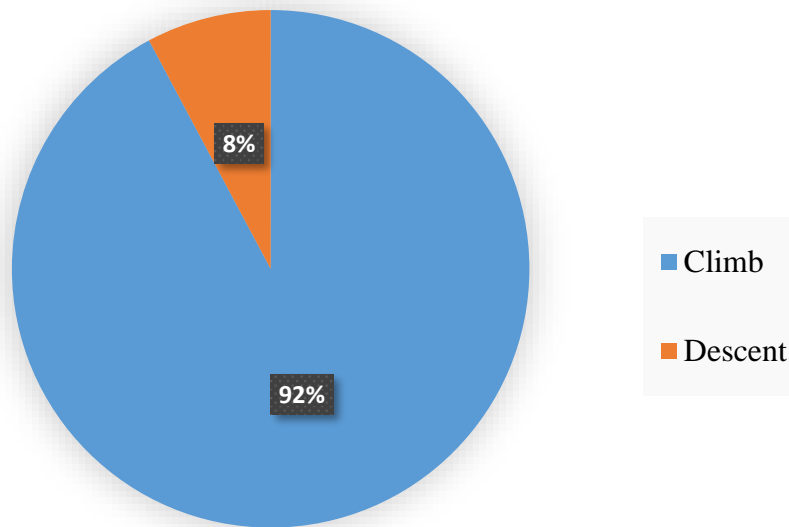
Figure 4. 7. Distribution of total fuel consumption during. climb and descent.

The fuel consumption distribution from aircraft operated at Juanda international airport during peak hour generated fuel consumption during climb from 3000 ft up to 15000 ft and descent from 15000 ft to 3000 ft as shown on Table 4.18. The fuel consumption during climb was 92% more than descent which was 8% of total fuel consumption as seen on Figure 4.7.

4.4   Calculations and analysis of emissions

After estimations of fuel consumptions during LTO and non LTO the next step is to calculate emission concentrations. The emission from taxi/idle, approach, climb out and take-off calculated using ICAO methodology while from non LTO cycle estimated using MEET methodology.

4.4.1 Calculation of emissions on LTO cycle

ICAO Advanced approach method was used to calculate emissions at different phase during LTO cycle. The emission factors were provided by ICAO engine exhaust emission index databank 2018 hosted by European Union Safety Agency (EASA) at (https://www.easa.europa.eu/easa-and-you/environment/icao-aircraft-engine-emissions-databank) and time in mode by (ICAO, 2011) Table 4.5. Equation 3.2 was used for calculation.

$$Eij = (TIM \times 60) \times \left(\frac{FFjk}{1000}\right) \times EIjk \times NEj$$

Where:

Eij   Total emissions of pollutant i (for example HC, CO_2 for HC), in grams, produced by aircraft type j for one LTO cycle.

TIMjk time-in-mode for mode k in minutes, for aircraft type j.

FFjk   the fuel flow mode in k in kilograms of fuel per second (kg/s) for each engine used on the aircraft type j.

EIjk   the emission factor for pollutant i given in grams of pollutant per kilogram of fuel (g/kg fuel) in mode k (during take-off, climb, taxi/idle and approach) for each engine used on the aircraft type j.

NEj   Number of engines used on aircraft type j.

A320 used as example on how to calculated emission of HC on different phases. The other aircrafts followed the same procedures.

Emission during taxi/idle mode:

Time in mode = 21 minutes (taken from (ICAO, 2011)

Fuel flow = 0.104 kg/s per engine used (source ICAO, 2018)

Emission indices = 4.6 g/kg of fuel (source ICAO, 2018)

Number of engines = 2 (from Table 4.4)

Number of LTO cycles = 5 (from Table 4.4)

Emission during taxi/idle = 21 × 60 × 0.104× 4.6 ×2× 5

Therefore, emission of HC during taxi/idle = 7463 g

Emission during approach mode:

Time in mode = 4 minutes

Fuel flow = 0.312 kg/s per engine used

Emission indices = 0.5 g/kg of fuel

Number of engines = 2

Number of LTO cycles = 5

Emission during approach = 4 × 60 × 0.312× 0.5 ×2× 5

Therefore, emission of HC during approach = 374 g

Emission during Climb out mode:

Time in mode = 2.2 minutes

Fuel flow = 0.935 kg/s per engine used

Emission indices = 0.2 g/kg of fuel

Number of engines = 2

Number of LTO cycles = 5

Emission during climb out =2.2 × 60 × 0.935× 0.2 ×2× 5

Therefore, emission of HC during climb out = 247 g

Emission during take-off mode:

Time in mode = 0.7 minutes

Fuel flow = 1.132 kg/s per engine used

Emission indices = 0.2 g/kg of fuel

Number of engines = 2

Number of LTO cycles = 5

Emission during take-off = 2.2 × 60 × 1.132× 0.2 ×2× 5

Therefore, emission of HC during take-off = 95 g

The emissions of each types of aircraft during LTO cycle operated at Juanda International airport are shown on the Tables 4.19 to 4.26 below;

Table 4. 19. A320 LTO cycle emissions

Mode	Total emission (g)				
	HC	CO	NO$_X$	CO$_2$	SO$_X$
Taxi/Idle	7463	37964	6976	5110560	1622
Approach	374	1722	7488	2358720	749
Climb out	247	1111	28633	3887730	1234
Takeoff	95	428	13312	1497636	475
TOTAL	8179	41225	56410	12854646	4081

Table 4. 20. B738 LTO cycle emissions

Mode	Total emission (g)				
	HC	CO	NO$_X$	CO$_2$	SO$_X$
Taxi/Idle	4307	45349	12161	7980336	2533
Approach	117	1642	12899	3693816	1173
Climb out	193	964	45681	6071512	1927
Takeoff	75	151	23329	2378225	755
TOTAL	4692	48105	94070	20123888	6389

Table 4. 21. B739 LTO emissions

Mode	Total emission (g)				
	HC	CO	NO$_X$	CO$_2$	SO$_X$
Taxi/Idle	1231	12957	3474	2280096	724
Approach	34	469	3685	1055376	335
Climb out	55	275	13052	1734718	551
Takeoff	22	43	6666	679493	216
TOTAL	1341	13744	26877	5749682	1825

Table 4. 22. B735 LTO emissions

Mode	Total emission (g)				
	HC	CO	NO_X	CO_2	SO_X
Taxi/Idle	1106	10368	1664	1218672	387
Approach	13	500	1468	508032	161
Climb out	13	227	4483	793346	252
Takeoff	5	87	2007	305348	97
TOTAL	1137	11182	9621	2825399	897

Table 4. 23. B733 LTO emissions

Mode	Total emission (g)				
	HC	CO	NO_X	CO_2	SO_X
Taxi/Idle	650	11176	1522	1169532	650
Approach	11	512	1311	474768	11
Climb out	11	209	3871	730145	11
Takeoff	3	80	1721	279418	3
TOTAL	675	11976	8425	2653862	675

Table 4. 24. A333 LTO emissions

Mode	Total emission (g)				
	HC	CO	NO_X	CO_2	SO_X
Taxi/Idle	7330	26977	3272	2230956	708
Approach	6	475	3618	1124928	357
Climb out	43	185	18694	1943449	617
Takeoff	15	83	10526	768398	244
TOTAL	7395	27720	36110	6067732	1926

Table 4. 25. A20N LTO emissions

Mode	Total emission (g)				
	HC	CO	NO_X	CO_2	SO_X
Taxi/Idle	154	11751	2542	1729728	549
Approach	9	637	2014	731808	232
Climb out	7	101	4154	1172556	372
Takeoff	3	32	2696	452466	144
TOTAL	173	12520	11407	4086558	1297

Table 4. 26. CRJ1000ER emissions

Mode	Total emission (g)				
	HC	CO	NOx	CO_2	SO_X
Taxi/Idle	54	7125	1936	1297296	412
Approach	11	731	1996	568512	180
Climb out	6	169	3909	936382	297
Takeoff	2	82	1835	365677	116
TOTAL	73	8108	9676	3167867	1006

The results from Table 4.19 - 4.26 show the emissions of pollutant during taxi/idle, approach, climb out and take-off of different types of aircraft operated at Juanda International airport. The pollutant CO_2 was the largest pollutant emitted on most aircraft while SO_x was the smallest emitted pollutant by aircraft during LTO cycle.

The results of pollutant from each aircraft were added up to get the total emissions on taxi/idle, approach, climb out and take-off phase. There is a difference between landing and take-off emissions, all pollutants (HC, CO_2 and SO_X) have greater emissions at landing than take-off except NOx which depend on altitude and power setting. The total emissions from each pollutant are shown of the following Table;

Table 4. 27. LTO cycle emissions at Juanda International Airport

Mode	emission (g)				
	HC	CO	NOx	CO$_2$	SOx
Taxi/Idle	22294	163666	33547	23017176	7586
Approach	576	6688	34479	10515960	3199
Climb out	575	3240	122477	17269837	5262
Takeoff	220	986	62092	6726661	2050
TOTAL (kg)	24	175	253	57530	18

The emissions pollutant during LTO cycle at Juanda International airport is shown in Table 4.27. As seen in the Table 4.27 the CO$_2$ was the largest pollutant emission in the magnitude of 57530 kg. The lowest emission was by SO$_x$ which total of 18 kg.

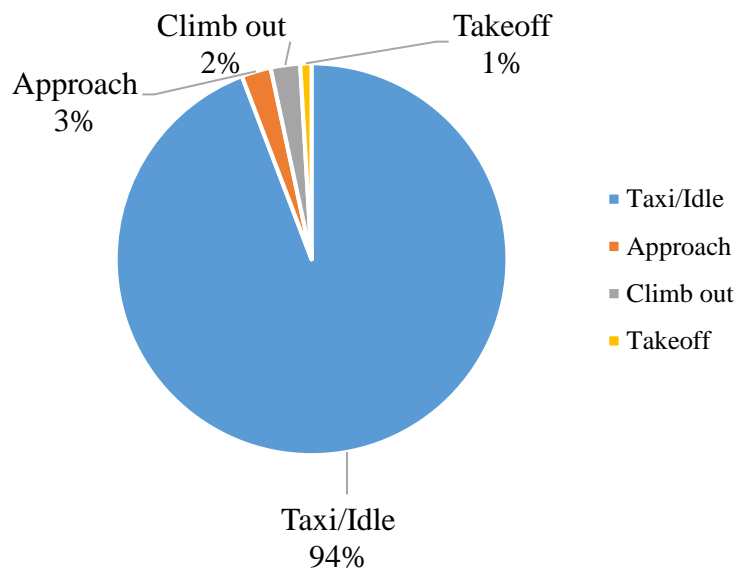Figure 4. 8. Distribution of LTO emission for HC at Juanda International airport.

Distributions of LTO emissions during taxi/idle, approach, climb out and take-off for Hydrocarbons (HC) is shown on Figure 4.8. As seen on the Figure 4.8 the taxi/idle constitutes the biggest portion of total LTO emissions at 94%. The climb out, approach made up 2%, 3% respectively. The lowest emission was during take-off operation mode which was 1%.

Figure 4. 9. Distribution of LTO emission for CO at Juanda International airport.

Figure 4.9 depicts the distribution of LTO emissions for carbon monoxide CO during taxi/idle, approach, climb out and take-off at Juanda International Airport. As illustrated on the Figure 4.3 the taxi/idle constitutes the biggest portion of total LTO emissions at 93%. The climb out, approach made up 2%, 4% respectively. The lowest emissions for CO was during take-off operation.
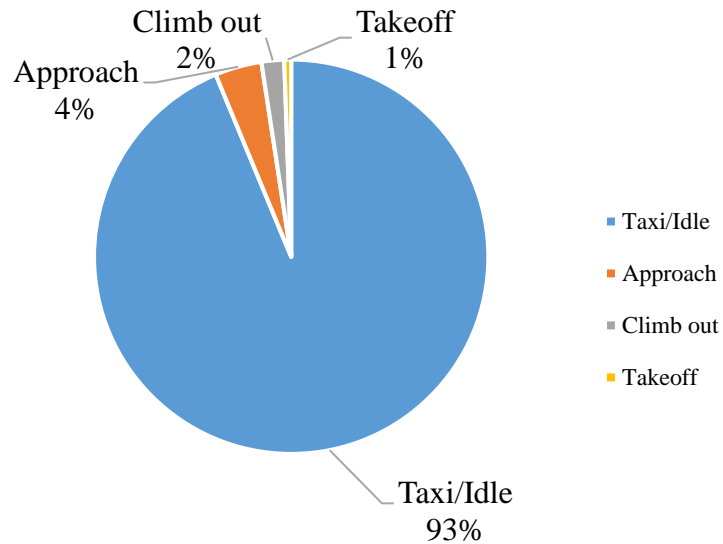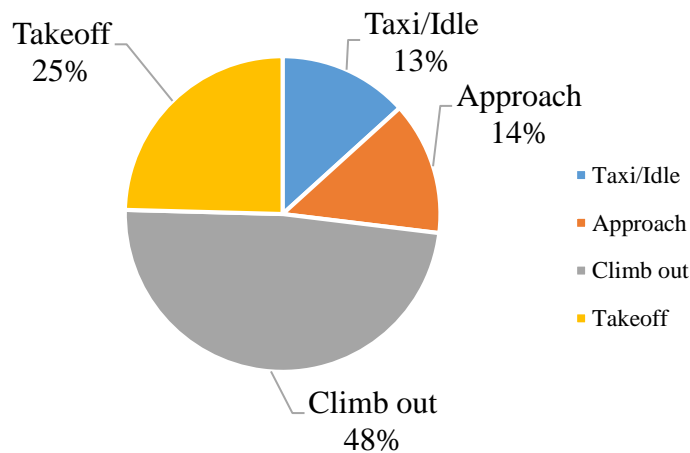

Figure 4. 10. Distribution of LTO emission for NOx at Juanda International airport.

At Juanda International Airport the distribution of LTO emissions for Nitrogen dioxide (NOx) during taxi/idle, approach, climb out and take-off is revealed in the Figure 4.10. As seen on Figure 4.10 the emissions of NOx were largest at 48% of total emissions during climb out phase while lowest emissions at 13% were emitted during taxi/idle.
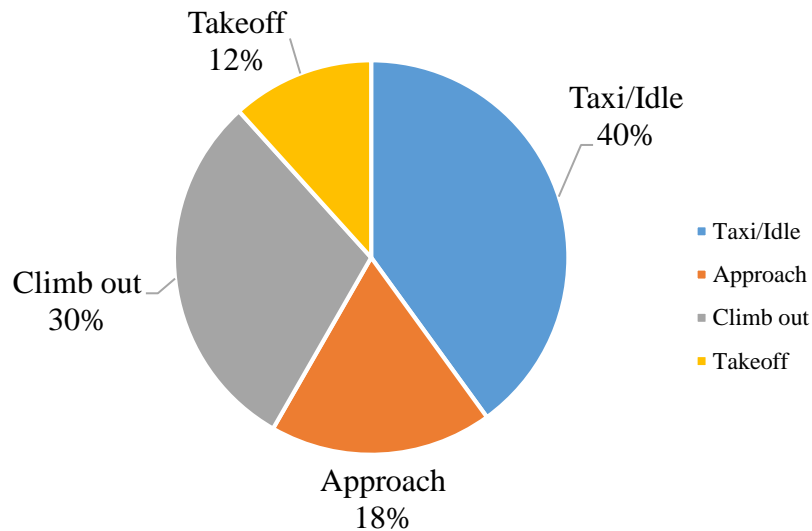
Figure 4. 11. Distribution of LTO emission for CO_2 at Juanda International airport.

Emissions during taxi/idle, approach, climb out and take-off at Juanda International airport were shown in Figure 4.11. We can see from Figure 4.11 the emissions of carbon dioxide CO_2 during taxi/idle were the largest which constitutes 40% of the total emissions during LTO cycle. The emissions of CO_2 for climb out, approach and take-off were 30%,18% and 12% respectively.
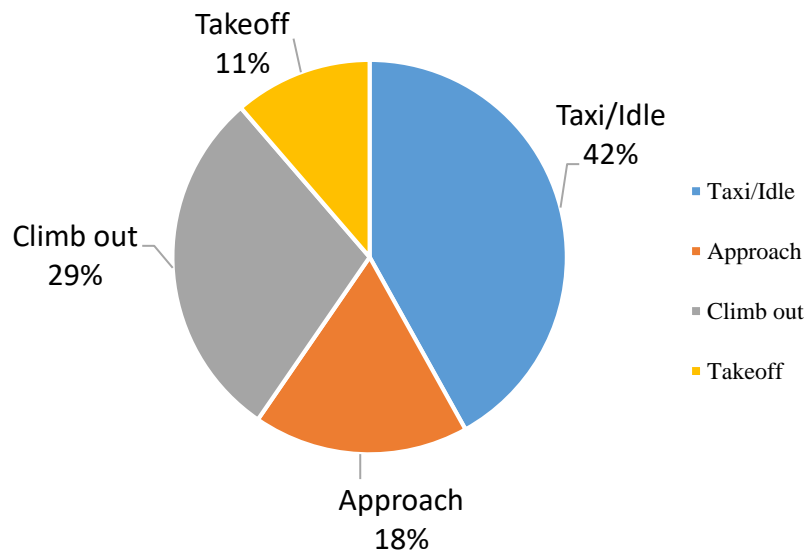
Figure 4. 12. Distribution of LTO emission for SOx at Juanda International airport.

Figure 4.12 illustrates the distribution of LTO emissions for SO_X during taxi/idle, approach, climb out and take-off at Juanda International Airport. As depicted on the Figure 4.12 the taxi/idle constitutes the biggest portion of total LTO emissions at 42%. The climb out, approach made up 29%, 18% respectively. The lowest emissions for SO_x were during take-off operation at 11%.

4.4.2 Calculation of emissions during climb and descent

Methodology for estimating air traffic emission (MEET) was used to calculate emissions at different phase during climb and descent phases for aircraft types A320, A20N, B733, B735, B736, B738 and B739.Method used for calculation emission on aircraft type A333 and CRJX was multiplying fuel consumption by average emission factors because these two aircrafts were not covered by MEET method.

A320 was used as example for calculation of emissions during climb from 3000 ft to 15000ft and during descent from 15000 ft to 3000 ft using MEET methodology as following.

73

Emission during climb

The coefficient of emission factors was provided by emission index sheet (EIS) (Kalivoda and Kudrna, 1997). Given the coefficient d1, d2, d3 and d4 of NOx for example and altitude 12000 ft using equation 3.8 The emission factor of NOx (EI NOX) during climb can be found.

$$d1 + d2 \times (CRALT) + d3 \times (CRALT)^2 + d4 \times (CRALT)^3$$

d1   = 32.88

d2   = -0.001033

d3   = 3.559E-08

d4   = -5.197E-13

CRALT= 12000 ft

Fuel consumption = 5558.7328 kg

EI NOX = $32.88 + -1.033 \times 10^{-3} \times 12000 + 3.559 \times 10^{-8} \times 12000^2 + -5.197 \times 10^{-13} \times 12000^3$

       $= 25.60895998 \text{ g kg}^{-1}$

After we obtained emission factor of Nitrogen oxides, we multiply by total fuel consumption during climb to get the emission of NOx during climb as following.

Emission during climb = $5558.7328 \times 25.60895998$

                 $= 142353.3658 \text{ g}$

Therefore, the emission of NO_X from A320 during climb equal to 142353g.

Emission during descent

The coefficient of emission factors was provided by emission index sheet (EIS) (Kalivoda and Kudrna, 1997). Given the coefficient d1, d2, d3 and d4 of NOx for example and altitude 12000 ft using equation 3.8 The emission factor of NOx (EI NO_X) during descent can be found.

$$d1 + d2 \times (CRALT) + d3 \times (CRALT)^2 + d4 \times (CRALT)^3$$

d1   = 6.326

d2   = -0.000569

d3   = 2.86E-08

d4   = -4.274E-13

CRALT= 12000 ft

Fuel consumption = 437.52264 kg

EI NO_X = $6.326+-5.69\times10^{-4}\times12000+2.86\times10^{-8}\times12000^2+-4.27\times10^{-13}\times12000^3$

$\qquad$ =2.8778528 g kg^{-1}

After we obtained emission factor of Nitrogen oxides, we multiply by total fuel consumption during descent to get the emission of NOx during descent as following.

Emission during descent = 437.52264 $\times$2.8778528

$\qquad\qquad$ =1259.1 g

Therefore, the emission of NO_X from A320 during descent equal to 1259.1g.

The same procedure was repeated to calculated the emission of HC, CO, NOx and SOx for A20N, B733, B735, B738 and B739. Th results can be seen on Table 4.29

Calculation of emission for A333 and CRJX

The emissions from A333 and CRJX was calculated by multiply the fuel consumptions during climb and descent with average emission indices provided by *System for assessing Aviation's Global Emissions* (SAGE), The average emissions factor of HC, CO and NOx for six years was used using results from research done by Kim et al., (2007) as shown in the Table 4.28 The emission indices for CO_2 and SO_X was 3150 g/kg and 1 g/kg respectively.

Table 4. 28. Yearly global emissions indices

Year	EI NO$_x$ (g/kg)	EI CO (g/kg)	EI HC (g/kg)
2000	13.8	2.98	0.417
2001	13.8	2.73	0.371
2002	14.1	2.81	0.374
2003	14.1	2.76	0.35
2004	14.3	2.71	0.332
2005	14.2	2.72	0.32
Average	14.1	2.79	0.361

Source: Kim et al., 2007

After we obtained emission indices as shown on Table 4.28 and using fuel consumption for A333 as example during climb and descent as 590 kg, 459 kg respectively. The emission during climb and descent can be calculated as shown in the next step.

Emission during climb

Emission is the function of fuel consumption and emission indices. During climb fuel consumption was 590 kg and emission indices of CO was 2.79 g/kg. Hence the emission of CO was obtained by multiplication of fuel consumption and emission indices as shown below.

Emission of CO = 590×2.79

$$= 1646.1 \text{ g}$$

Therefore, the emission of CO from A333 during climb was 1646.1 g. the same procedure was used to calculate emissions of other pollutant.

Emission during descent

Emission is the function of fuel consumption and emission indices. During descent fuel consumption was 459 kg and emission indices of CO was 2.79 g/kg. Hence the emission of CO was obtained by multiplication of fuel consumption and emission indices as shown below.

Emission of CO = 459×2.79

= 1280.61 g

Therefore, the emission of CO from A333 during descent was 1280.61 g. The same procedure was used to calculate emissions of other pollutant and results shown on Table 4.29

Calculation for emission from CRJX used the same procedure as A333 and the results are shown on Table 4.29

Table 4. 29. Aircraft emission during climb and descent from Juanda international airport

Aircraft	Mode	emission (kg)				
		HC	CO	NOx	CO_2	SOx
A320	Climb	0.95	3.95	142.35	17510.01	5.56
	Descent	0.31	4.46	1.26	1378.20	0.44
B738	Climb	5.27	10.12	147.61	31699.07	10.06
	Descent	3.96	12.40	0.73	1402.50	0.45
B739	Climb	1.50	2.89	42.17	9056.88	2.88
	Descent	1.13	3.54	0.21	400.72	0.13
B735	Climb	0.75	1.45	27.86	4528.44	1.44
	Descent	0.57	1.77	0.10	200.36	0.06
B733	Climb	0.75	1.45	21.09	4528.44	1.44
	Descent	0.57	1.77	0.10	200.36	0.06
A333	Climb	0.21	1.64	8.29	1858.50	0.59
	Descent	0.17	1.28	6.45	1445.50	0.46
A20N	Climb	0.38	1.58	56.94	7004.00	2.22
	Descent	0.13	1.78	0.50	551.28	0.18
CRJX	Climb	0.08	0.58	2.95	661.18	0.21
	Descent	0.10	0.81	4.06	910.81	0.29

The results from Figure 4.29 show the emissions of pollutant during climb from 3000 ft to 15000 ft and descent from 15000 ft to 3000 of different types of aircraft operated at Juanda International airport. The pollutant CO_2 was the largest pollutant emitted on most aircraft during climb and descent phases.

Once the estimation of emission from each aircraft was found, the summation of pollutants was next step and the results as shown below:

Table 4. 30. Total emission during climb and descent from Juanda International Airport

Mode	emission (kg)				
	HC	CO	NO_X	CO_2	SO_X
Climb	10	24	449	76847	24
Descent	7	28	13	6490	2

Emission of pollutant estimation's during climb from 3000ft to 15000 ft and descent from 15000 ft to 3000 ft from Juanda international airport during peak hour was depicted on Table 4.30. The largest emission pollutant during climb was CO_2 with value of 76847 kg followed by NOx, CO and HC with amount of 449 kg, 24 kg and 10 kg respectively. The lowest pollutant emission during descent was SO_X at magnitude of 2 kg while the largest was CO_2 at the quantity of 6490 kg.

The distributions of pollutant HC, CO, NO_X, CO_2 and SO_X during climb and descent is shown on the Figures below

Figure 4. 13. Distribution of climb and descent emission for HC at Juanda International airport

Distributions of non LTO emissions during, climb and descent for Hydrocarbons (HC) is shown on Figure 4.13. As seen on the Figure 4.12 the climb constitutes the biggest portion of total emissions at 59%. The descent made up 41%.

Figure 4. 14. Distribution of climb and descent emission for CO at Juanda International airport

Figure 4.14 depicts the distribution of emissions for carbon monoxide CO during descent and climb at Juanda International Airport. As illustrated on the Figure 4.13 the descent constitutes the biggest portion of total non LTO emissions at 54% while climb at 46% of total emission.

NO$_X$

Figure 4. 15. Distribution of climb and descent emission for NO$_X$ at Juanda International airport

Juanda International Airport the distribution of emissions for Nitrogen dioxide (NOx) during climb and descent is revealed in the Figure 4.15. As seen on Figure 4.15 the emissions of NOx were largest at 97% of total emissions during climb out phase while lowest emissions at 3% were emitted at descent.
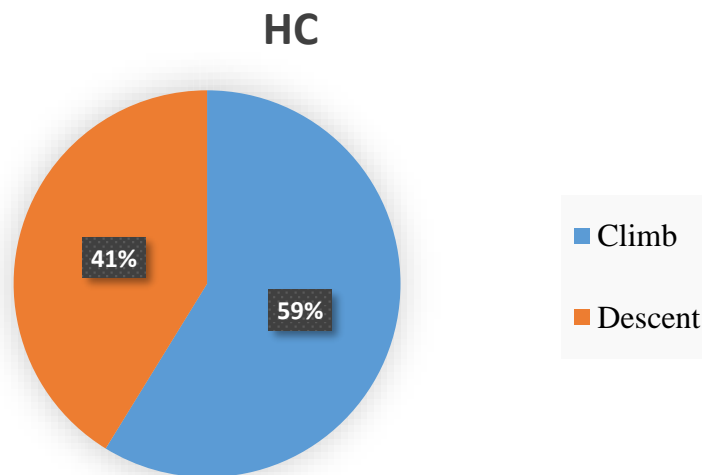

CO$_2$
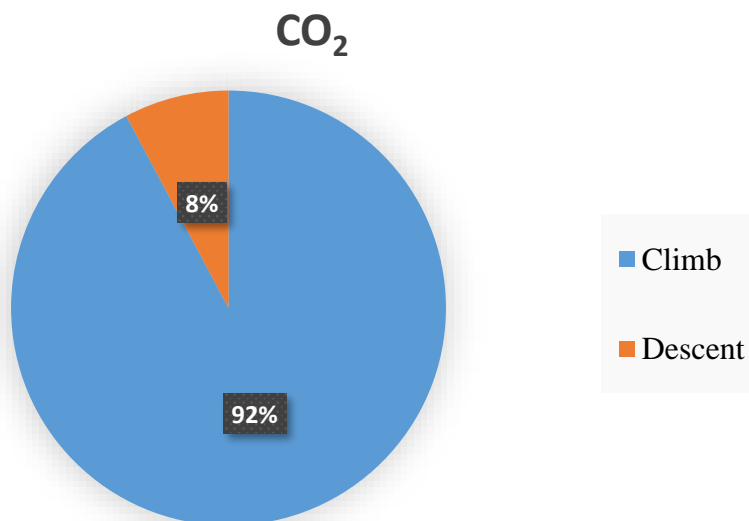
Figure 4. 16. Distribution of climb and descent emission for CO$_2$ at Juanda International airport

Emissions of CO_2 during climb and descent phases at Juanda International airport were shown in Figure 4.16. We can see from Figure 4.16 the emissions of carbon dioxide (CO_2) during climb were the largest which constitutes 92% of the total emissions during non LTO cycle. The emissions of CO_2 for descent, were 8%.
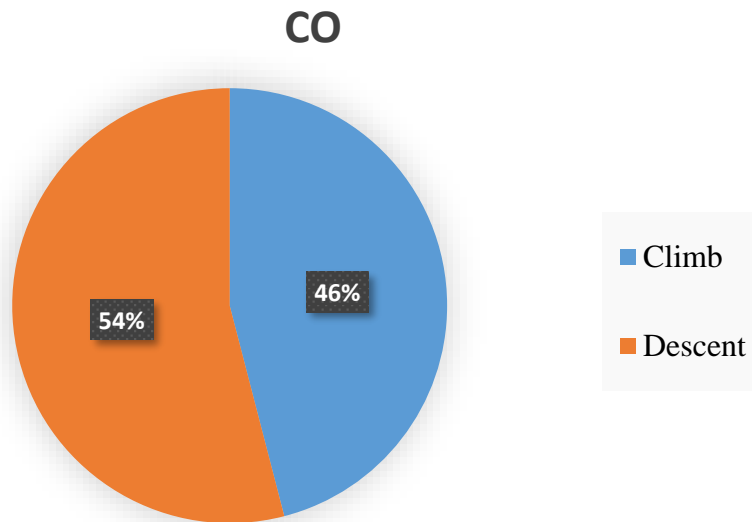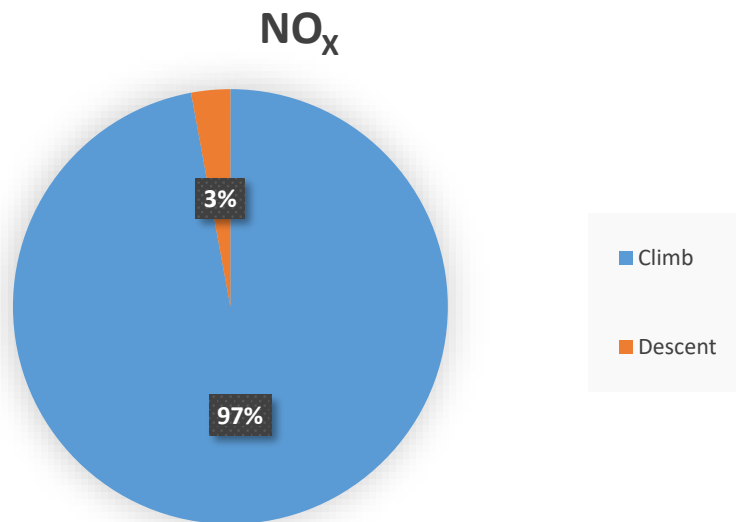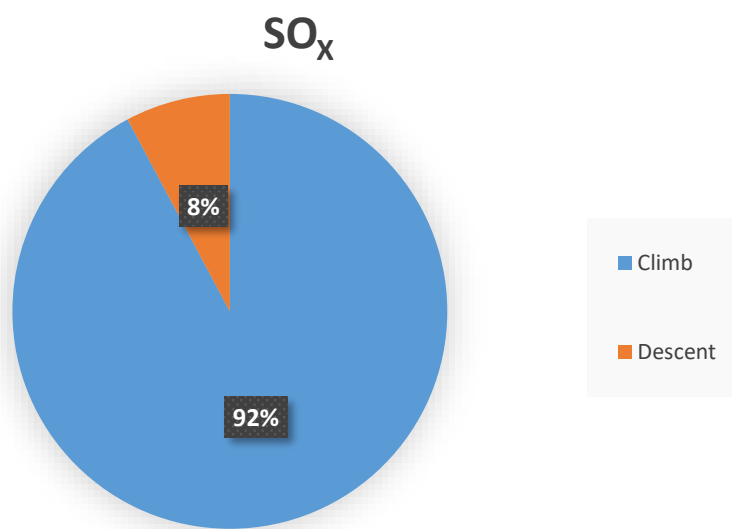

Figure 4. 17. Distribution of climb and descent emission for SO_X at Juanda International airport

Figure 4.17 illustrates the distribution of emissions for SO_X during climb and descent at Juanda International Airport. As depicted on the Figure 4.17 the climb constitutes the biggest portion of total non LTO emissions at 92%. The descent phase made up 8%.

4.5 Mapping

Mapping of emission concentration on LTO cycle was done after calculation of all pollutant during taxi/idle, approach, climb out and take-off. The software ArcGIS was used to map the emission around Juanda International Airport as shown on from Figure 4.20

The aircraft engine typical dimensions of A320, B735, B738, B739, B733, CRJX, A20N and A333 as provided by European aviation Safety agency (EASA) can be seen of Table 4.31 below.

Table 4. 31. Aircraft engine height

Aircraft	Engine type	Height(mm)
A320	CFM56-5B4/P	2105
B735	CFM56-3C1	1817
B738	CFM56-7B27	1829
B739	CFM56-7B27	1829
B733	CF56-3B2	1817
CRJX	CF34-8C5A2	1541
A20N	LEAP1A26	2368
A333	CF6 80E1A4	2873.5

Source European Aviation Safety Agency (EASA)

Illustration of engine exhaust temperature and emissions contours shown on Figure 4.18 during take-off using Airbus 320-200 as an example. The exhaust emitted from engine spread as shown on the Figure 4.18. The temperature is very high at red area with magnitude of 425 K which emitted approximately 50 feet from the engine. The brown area covers the engine exhaust temperature of 370 K which covers until 66 feet from engine nozzle. The yellow area represents the engine exhausts with temperature of 315 K and can reach a distance of approximately 135 feet from the engine. The emissions characteristics of pollutant are different depending on the phase of operation for example during this mode of take-off the emissions of nitrogen dioxide (NOx) and carbon dioxide (CO_2) can be describe high at red area followed by brown and yellow area respectively. The engine exhaust emissions cover the flight path of an aircraft.

The common aircrafts operated during peak hour at Juanda International airport are A320 and B738 which are in approach category C and D respectively. B738 is the most frequent aircraft operated at Juanda International Airport approach speed of category C aircraft. The distance from the polygon was calculated by consider glide path angle (GPA) approaching speed, and height of 3000ft (LTO) as described **section 3.5.3**. The list of approach speed can be seen on Table 4.32.

Table 4. 32. Aircraft approach speed category

Category	Approach Speed. kn
A	<91
B	91-120
C	121-140
D	141-166
E	>166

Source Robert Horonjeff et al., 2010
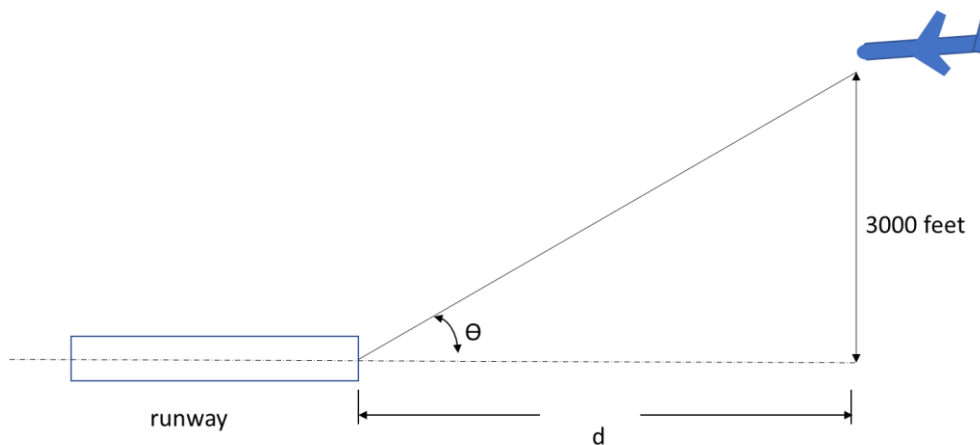
Figure 4. 18. Illustration of aircraft approach

Based on the assumption that the aircraft is heading directly toward the Instrument landing system (ILS) facility equation 3.9 is applied, from Figure 4.18 glide path angle (GPA) angle is given by;

$$tan\theta = \frac{3000}{d}$$

Where

Ө   = glide path angle (GPA).

d   = radius distance from the airport

Hence,

Ө   = 3° (taken from Table 3.2.)

$$tan\ 3° = \frac{3000}{d}$$

d   = 57243.4 feet which equal to 17 km

Therefore, the horizontal distance that covers altitude of 3000ft when aircraft descent and climb is equal to 17 km. This radius distance is used to show the how far the emission of aircraft from the Juanda International airport to surrounding area when aircraft start to descend from 3000 ft and climb up to 3000 ft. The total 57530 kg during landing and take-off LTO cycle of carbon dioxide (CO_2) pollutant emissions which is greenhouse gases was used to map the pollution around Juanda International airport. The following processes were conducted during mapping

1. Digitized Area Juanda airport.

This process aims to create a polygon in the Juanda Airport area by interpreting it from ESRI's Basemap Imagery.

2. Airport Buffer Area.

This process forms a new polygon by enlarging in all directions as far as 17 km from the Polygon Airport Area. After that, separate the polygons that are in the direction of the plane path and which are not. In this polygon the value that is in the direction of the direction of the plane path is 10 while the one that is not in the direction is valued at 20. This value is entered in the FID field

3. Polygon to Raster.

This process aims to change the Polygon Buffer which is vector data into raster data. The raster generated in this process uses a cell size of 5 meters (raster pixel size of 5 meters). The value field used is FID, the FID value is 0 so the value of all pixels in this raster is 0.

4. Cost distance.

This process analyses how far the range of pollutant is. In this process 2 input sources and raster costs are needed, source is polygon which becomes the beginning of distribution while cost raster is a raster that determines the value of how far a pixel is to be reached from source. Maximum distance 57530 which is the total amount of CO_2 at Juanda Airport.

5. Raster calculator.

This process changes the value of Cost Distance Raster to become an Affected Raster Area. Because Cost Distance calculates how far a pixel is from the

source, the farther away from the source, the greater the pixel value, while in this analysis the distance from the airport should be (the source) the less CO_2. Then do the Raster Calculator with the equation [(- "Cost Distance Raster") + 57530].

6. Raster Affected by CO_2 at Juanda Airport

Then the Affected Raster symbology was done so that the area is divided into 4 classes less affected, affected and high affected, highest affected. After that make a layout. The distributions neglecting the effect of wind speed and direction the final results can be seen on Figure 4.20.

As seen from Figure 4.20 the red area is the area which has highest concentrations of pollutant emissions range from 45000 kg-57,530 kg of CO_2, yellow area 30000 kg-45000 kg pollutants emissions, the green area represents emission concentration between 15,000 kg-30,000 kg, and the blue area represent the pollutant emissions of 0-15000 kg of CO_2. It can be seen that the close to the airport the high exposed of pollutant emissions which has various impacts on health and climate changes. More green area on the residential area especial the area with red colour in the map around airport can be implemented to reduce the effect of aircraft engines exhaust pollutions.
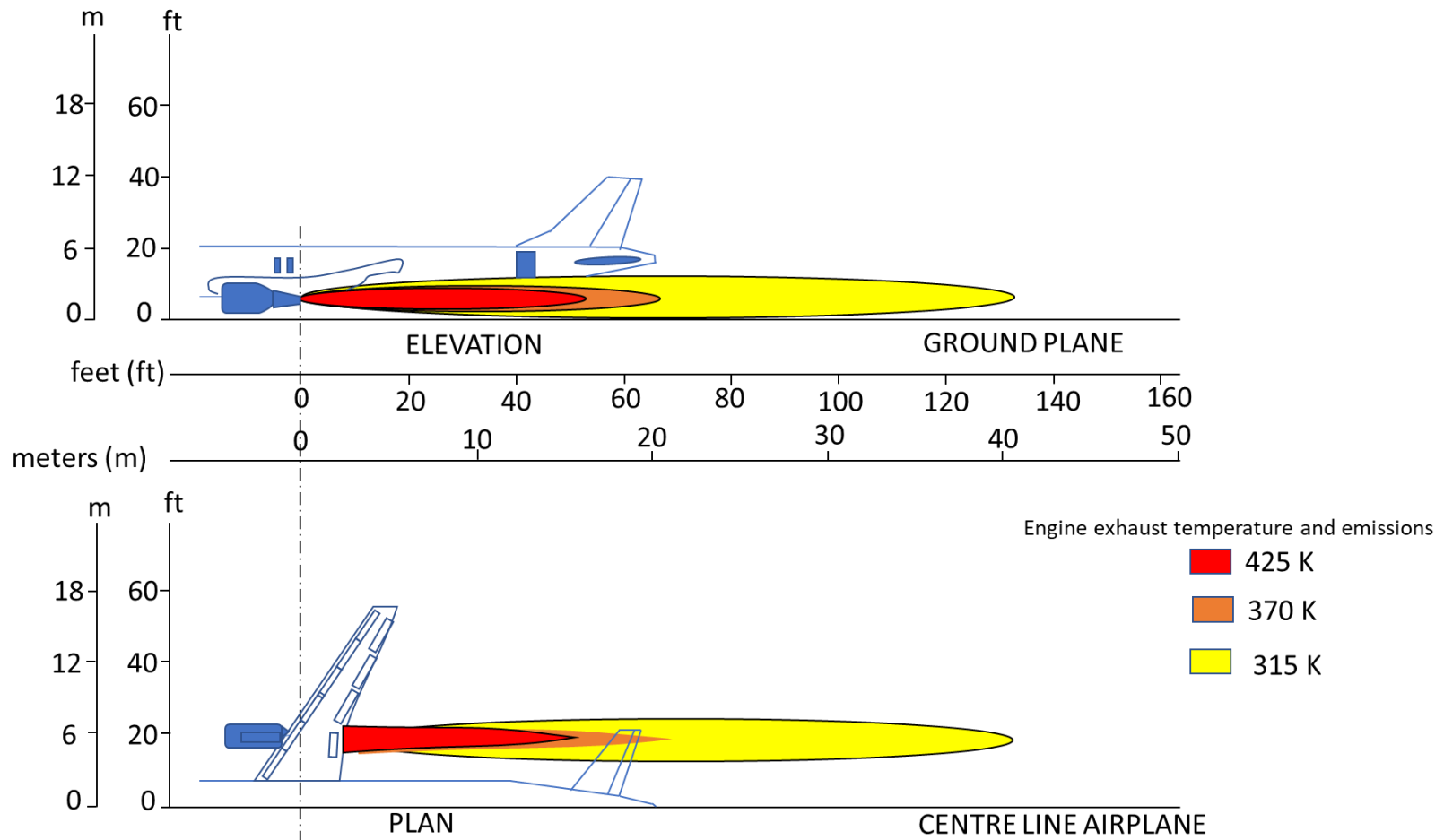
.

Figure 4. 19. Illustration of engine exhaust temperature and emissions of A320 during take-off (Source Airbus, 2005)

Figure 4. 20. Juanda International Airport CO_2 LTO emission map

4.6   Discussions

Fuel consumption is the one important when operating aircraft. The results from Figure 4.1 and Figure 4.2 demonstrated the total fuel consumptions during LTO cycle at Juanda international Airport. Taxi/Idle mode has a largest number of fuel consumptions which was 40% compare to other, climb out 30% and approach 18%, modes. The take-off was the lowest mode in fuel consumptions which was 12%. The largest number of fuel consumption was during taxi/idle due to the time aircraft spend on this mode. The higher time spend the more fuel consumed.

Distributions of LTO emissions during taxi/idle, approach, climb out and take-off for Hydrocarbons (HC) is shown on Figure 4.8. As seen on the Figure 4.8 the taxi/idle constitutes the biggest portion of total LTO emissions at 94%. The climb out, approach made up 2%, 3% respectively. The lowest emission was during take-off operation mode which was 1%. The taxi/idle mode usual aircraft operated at low pawer setting which results the large emissions of HC because the emission factors are high during low power. The results can be comparable to other research by Elbir, (2008) which was around 73% of emissions during taxi/idle. The same results obtained by Yılmaz, (2017) which shows the emissions during taxi/idle, approach, climb out and take-off was 93%, 3%, 3% and 1% respectively.

Figure 4.9 depicts the distribution of LTO emissions for carbon monoxide CO during taxi/idle, approach, climb out and take-off at Juanda International Airport. As illustrated on the Figure 4.2 the taxi/idle constitutes the biggest portion of total LTO emissions at 93%. The climb out, approach made up 2%, 4% respectively. The lowest emissions for CO was during take-off operation. The taxi/idle mode usual aircraft operated at low pawer setting which results the large emissions of CO because the emission factors are high during low power. The results are similar to Kayseri International airport Turkey which shows that emission during taxi/idle at 93%, climb out 2%, approach 3% and take-off 1% of total emissions. (Yılmaz, 2017).

At Juanda International Airport the distribution of LTO emissions for Nitrogen dioxide (NOx) during taxi/idle, approach, climb out and take-off is revealed in the Figure 4.10. As seen on Figure 4.10 the emissions of NOx were

largest at 48% of total emissions during climb out phase, the second was take-off at 25% while lowest emissions at 13% were emitted during taxi/idle and approach was 14%. The emissions during Climb out were the largest because NOx depend largely on altitude and power setting, the power setting was large during take-off and climb. The same results shown by Yilmaz where taxi/idle, approach, climb out and take-off was 49%, 13%,13% and 25% respectively. Liu et al., (2019) on civil aviation in China shows that the emissions of NOx at taxiing and idle, approach, climb out and take of were 48%, 14%,14%,24% for the year 2015 which agree to this research.

Emissions of carbon dioxide (CO_2) during taxi/idle, approach, climb out and take-off at Juanda International airport were shown in Figure 4.11. We can see from Figure 4.11 the emissions of carbon dioxide CO_2 during taxi/idle were the largest which constitutes 40% of the total emissions during LTO cycle. The emissions of CO_2 for climb out, approach and take-off were 30%,18% and 12% respectively. The emissions of CO_2 were largest at taxi/idle because during this phase the largest fuel consumptions were obtained as shown on Figure 4.2. As we know the CO_2 emissions factors depend solely on the fuel content. As pollutant emissions are positively correlated with the fuel consumption (Fan et al., 2012).

Figure 4.12 illustrates the distribution of LTO emissions for Sulphur oxides (SO_x) during taxi/idle, approach, climb out and take-off at Juanda International Airport. As depicted on the Figure 4.12 the taxi/idle constitutes the biggest portion of total LTO emissions at 42%. The climb out, approach made up 29%, 18% respectively. The lowest emissions for SO_x were during take-off operation at 11%. The emissions of SO_x were largest at taxi/idle because during this phase the largest fuel consumptions were obtained as shown on Figure 4.2. As we know the SO_x emissions factors depend solely on the fuel sulphur content. According to Fan et al., (2012). the fuel consumptions are positively correlated with pollutant emissions. The results are well agree with the current study which show the emission of sulphur depend on fuel consumption and fuel sulphur content (Yang et al., 2018)

There is a difference between landing and take-off emissions, all pollutants (HC, CO_2 and SO_X) have greater emissions at landing (approach mode) than take-off except for NOx which has greater emission during take-off than landing due to

its dependence on altitude and power setting. The emissions for CO was much higher during landing about 87% compare to other gases this is due aircraft operated at low power setting during landing compare to take-off, hence the emission factors of CO are high during low power, used 30% of rated thrust during landing compare with 100% rated thrust during take-off. The time in mode (TIM) is also a factor as can be seen from Table 4.33 which was taken from ICAO,2011 the aircrafts need 4 minutes during landing while it takes 0.7 minutes for take-off mode hence more emissions during landing due to the longer time. The graph of the difference between landing and take-off can be seen below on Figure 4.21

Total fuel consumption during climb and descent by each type of aircraft from Juanda International airport during peak hour can be seen on the Figure 4.6. Many aircraft used more fuel during climb than descent except for CRJX which used less fuel during climb than descent. Aircraft took more time to climb due to weight and resistance hence more fuel consumption than during descent while CRJX has high climb rate and it took less time to climb then to descent. The highest fuel consumption during climb was 10063 kg by Boeing 737-800 this due to this aircraft is the most common used than others.

Total emission of pollutant estimation's during climb from 3000ft to 15000 ft and descent from 15000 ft to 3000 ft from Juanda international airport during peak hour was depicted on Table 4.30. The largest emission pollutant during climb was CO_2 with value of 76847 kg followed by NOx, CO and HC with amount of 449 kg, 24 kg and 10 kg respectively. The lowest pollutant emission during descent was SO_x at magnitude of 2 kg while the largest was CO_2 at the quantity of 6490 kg. As seen from the results the emission of carbon dioxide (CO_2) is larger in climb than in descent this is because CO_2 is only depending on fuel consumptions and on climb phase fuel consumption was large compare to descent as depicted on Table 4.18. The same case for SO_x emission which depend also on amount of fuel content. The number of emissions of hydrocarbons (HC) and carbon monoxide (CO) are low during high altitudes because high power setting as we know HC and CO emitted due to incomplete combustion and usual high at low power setting as we have seen during taxi/idle at 7% engine thrust. The amount of nitrogen dioxide (NOx) was

449 kg and 13 kg during climb and descent respectively. NOx emission is mainly depend on engine thrust setting and altitude, at high power setting nitrogen emission is high (Stettler et al., 2011: Koudis et al., 2017: Liu et al., 2019)
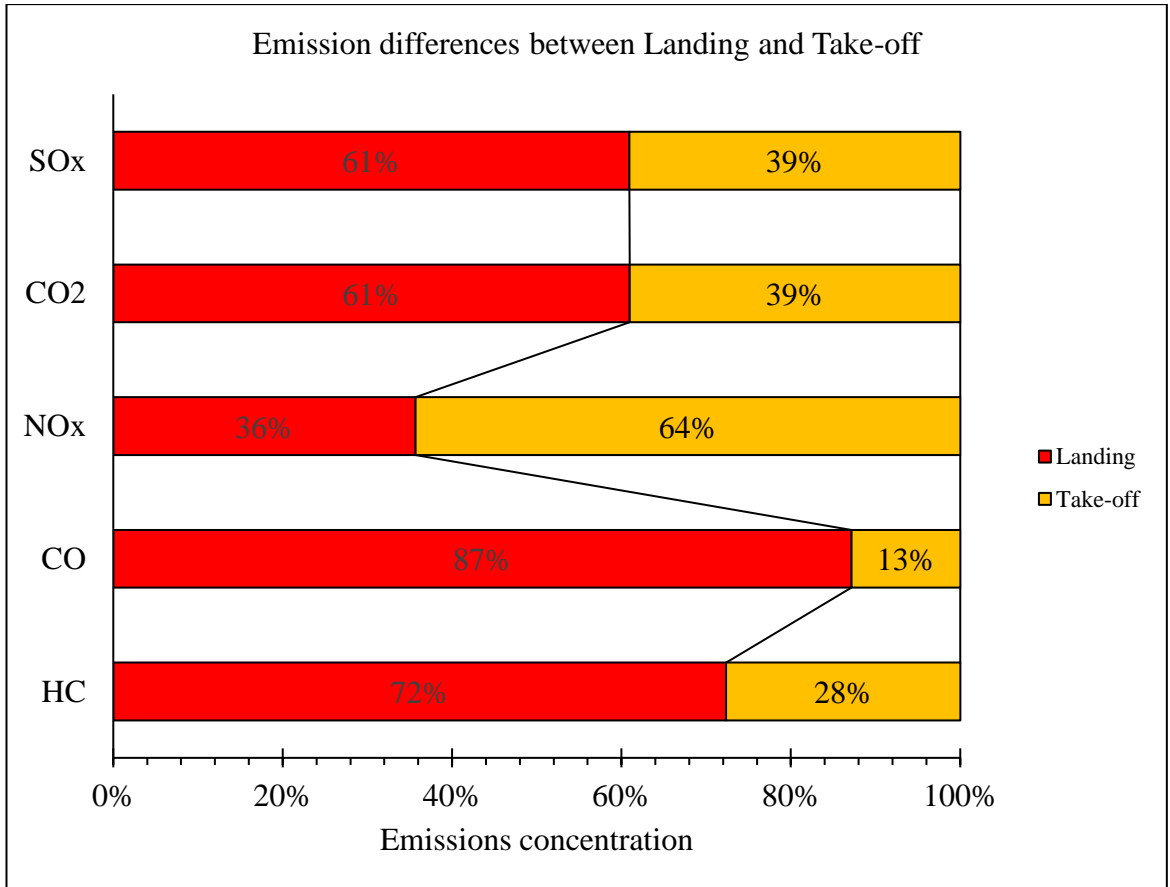
Figure 4. 21. Landing and take-off emissions comparison.

Table 4. 33. Time in mode

Aircraft	Time in mode (minutes)			
	Taxi/Idle	Landing	Climb out	Take-off
A320	26	4	2.2	0.7
B738	26	4	2.2	0.7
B739	26	4	2.2	0.7
B735	26	4	2.2	0.7
B733	26	4	2.2	0.7
A333	26	4	2.2	0.7
A20N	26	4	2.2	0.7
CRJ	26	4	2.2	0.7

"This page is intentionally left blank"

CHAPTER 5

CONCLUSION AND RECOMMENDATION

5.1 Conclusion

This research has estimated the commercial aircraft emissions at Juanda International airport based on flight path. International Civil Aviation Organisation (ICAO) advanced approach methodology was used to calculate fuel consumptions and emissions pollutant at landing and take-off cycle (LTO cycles) and methodology of estimating emission from air traffic (MEET) was used to estimate the fuel consumption and pollutant emissions during non LTO cycle climb and descent phases. ArcGIS was used to map ground concentration of emissions at Juanda International airport. Based on the results of the discussion it can be concluded that pollutant emissions and fuel consumption are positively related to amount of flight operation, flight duration in each phase and engine configuration. The results obtained are as follow

1   The estimated fuel consumption on LTO cycle, climb and descent phase operations by type of aircrafts at Juanda International airport are as follow:

   a. Total fuel consumptions during LTO cycle at Juanda international Airport from aircraft operation, taxi/Idle mode has a largest number of fuel consumptions which was 7307 kg equal to 40% of total fuel consumption compare to climb out modes 5482 kg same as 30%, approach 3338 kg composite of 18%, The take-off was the lowest mode in fuel consumptions which was 2135 kg same as 12%. The largest number of fuel consumption was during taxi/idle due to the time aircraft spend on this mode. (Table 4.15, Table 4.16, Figure 4.1 and Figure 4.2).

   b. The estimation fuel consumption from aircraft operated at Juanda international airport during peak hour at non LTO cycle climb from 3000 ft up to 15000 ft and descent from 15000 ft to 3000 ft was 24396 kg and 2060 kg respectively. Fuel consumption during climb was 92% more than descent which was 8% of total fuel consumption. Aircrafts took more time to climb

93

due to weight and drag force hence more fuel consumption than during climb mode (Table 4.18 and Figure 4.7).

2   The estimated aircraft emissions concentration of HC, CO, CO_2, NO_X and SO_2 on LTO cycle and non LTO cycle (climb and descent) are

    a. The amount of hydrocarbon (HC) emission during taxi/idle constitutes the biggest portion of total LTO emissions at 22 kg (94%). The climb out, approach made up 0.575 kg (1%), 0.576 kg (1%) respectively. The lowest emission was during take-off operation mode which was 2 kg (6%). The taxi/idle mode usual aircraft operated at low pawer setting which results the large emissions of HC due to emission factors of HC decreasing with increasing thrust, the emission factors are high during low power (Table 4.27 and Figure 4.8).

    b. The amount of carbon monoxide (CO) emission during taxi/idle constitutes the biggest portion of total LTO emissions at 164 kg (93%). The climb out, approach made up 3 kg (2%), 7 kg (4%) respectively. The lowest emissions for CO was during take-off operation 1 kg (1%). The taxi/idle mode usual aircraft operated at low pawer setting which results the large emissions of CO because the emission factors are high during low power. The emission factor of CO decreasing with increasing thrust. (Table 4.27 and Figure 4.9).

    c. The emissions of Nitrogen dioxide (NOx) were largest at 122 kg (48%) of total emissions during climb out phase, the second was take-off at 62 kg (25%) while lowest emissions at 34 kg (13%) were emitted during taxi/idle. The emissions during Climb out were the largest due to NOx emissions depend largely on altitude and power setting, the power setting was large during take-off and climb 100% and 85% of engine thrust (Table 4.27 and Figure 4.10).

    d. Carbon dioxide (CO_2) emissions during taxi/idle were the largest which constitutes 23017 kg (40%) of the total emissions during LTO cycle. The emissions of CO_2 for climb out, approach and take-off were 17270 kg (30%), 10516 kg (18%) and 6727 kg (12%). Respectively. The emissions of CO_2 were largest at taxi/idle because during this phase the largest fuel consumptions were obtained as shown on Figure 4.2. Based on the fact that

94

the CO_2 emissions factors depend solely on the fuel content (Table 4.27 and Figure 4.11).

e. Taxi/idle was the biggest portion of total LTO emissions at 8 kg (42%) of sulphur dioxide (SO_x). The climb out, approach made up 5kg (29%), 3kg (18%) respectively. The lowest emissions for SO_x were during take-off operation at 2 kg (11%). The emissions of SO_x were largest at taxi/idle because during this phase the largest fuel consumptions were obtained as shown on Figure 4.2. As the matter of fact, the SO_x emissions factors does not depend atmosphere or engine technology only on the fuel content. According to Fan et al., (2012). the fuel consumptions are positively correlated with pollutant emissions (Table 4.27 and Figure 4.12).

f. The total amount of HC, CO, NO_x, CO_2 and SO_x emission during Landing and take-off cycle (LTO cycle) at Juanda International Airport during peak hour was 24 kg, 175 kg, 253 kg, 57530 kg and 18 kg respectively (Table 4.27).

g. Emission of pollutant estimation's during climb from 3000ft to 15000 ft and descent from 15000 ft to 3000 ft from Juanda international airport during peak hour was depicted on Table 4.30. The largest emission pollutant during climb was CO_2 with value of 76847 kg followed by NO_x, CO and HC with amount of 449 kg, 24 kg and 10 kg respectively. The lowest pollutant emission during descent was SO_x at magnitude of 2 kg while the largest was CO_2 at the quantity of 6490 kg. As seen from the results the emission of carbon dioxide (CO_2) is larger in climb than in descent this is because CO_2 is only depending on fuel consumptions and on climb phase fuel consumption was large compare to descent as depicted on Table,4.18. The same case for SO_x emission which depend also on amount of fuel content. The number of emissions of hydrocarbons (HC) and carbon monoxide (CO) are low during high altitudes because high power setting as we know HC and CO emitted due to incomplete combustion and usual high at low power setting as we have seen during taxi/idle at 7% engine thrust. The amount of nitrogen dioxide (NO_x) was 449 kg and 13 kg during climb and descent respectively. NOx emission is mainly depending on engine thrust setting

and altitude, at high power setting nitrogen emission is high (Stettler et al., 2011: Koudis et al., 2017: Liu et al., 2019).

    c.   The total amount of $HC.CO.NO_X$, CO_2 and SO_x emission during climb was 10 kg, 24 kg, 449 kg, 76887 kg, 24 kg and during descent was 10 kg, 28 kg, 13 kg, 6490 kg and 2 kg respectively (Table 4.30).

3   The area near Juanda International Airport around radius distance 17 km from the airport for LTO cycle affected by emissions from the aircraft engine. The near to the airport the high possibility of exposed to health problems. More green area on the residential area around airport can be implemented to reduce the effect of aircraft engines exhaust pollutions (Figure 4.20).

5.2   Recommendation

Aircraft emissions at airport need a serious consideration from the stakeholders due to the rapid growth of aviation industry. As seen from the results pollutant emission around airport mainly depend on time of operation of the aircraft the following steps can be taken to reduce emissions and fuel consumption of the aircraft; controlling the use of auxiliary power unit (APUs), using single-engine during taxi, extended towing of aircraft, better runway assignment and airfield design intended at reducing taxiing time and distances. Airports can also promote other ground, departure, and approach/landing flight phase operational improvements. Surface congestion management approaches are chiefly applicable at reducing taxi fuel burn and associated air quality and greenhouse gas (GHG) emissions. Improving of airport operation procedures, engines of high combustion efficiency, shifting to low-emission transportation mode are better strategies to reduce pollutant emissions from aircraft at Juanda International Airport.

More research on emission inventory around other airports in Indonesia is needed. The research can cover the full flight path and calculate the emissions associated with each aircraft also distribution analysis of emissions.

There is a need for research of emissions load generated by overflights aircraft that is aircraft that operated on airspace of Indonesia without landing.

REFERENCES

Airbus, 2012. Global Market Forecast 2012-2031.

Airbus, 2005. Aircraft characteristics-Airport and Maintenance Planning.

Airbus, 2002. Getting Grips with Aircraft Performance.

Anderson, B.E., Chen, G., Blake, D.R., 2006. Hydrocarbon emissions from a modern commercial airliner. Atmos. Environ. 40, 3601–3612. https://doi.org/10.1016/j.atmosenv.2005.09.072

Barrett, S.R., Britter, R.E., Waitz, I.A., 2010. Global mortality attribuTable to aircraft cruise emissions. Environ. Sci. Technol. 44, 7736–7742.

Baughcum, S.L., Tritz, T.G., Henderson, S.C., Pickett, D.C., 1996. Scheduled civil aircraft emission inventories for 1992: database development and analysis. NASA Append. D.

Boeing, 2013. Current Market Outlook 2013-2032. Market Analysis, Boeing Commercial Airplanes, Seattle.

Curran, R., 2006. Correction to Engine Emission Data Resulting from Engine Deterioration. QinetiQ Ltd.

EEA, 2014. Transport and environment reporting mechanism 2014.

EEA/EMEP, 2009. Emission Inventory Guidebook: 2009.

Elbir, T., 2008. Estimation of engine emissions from commercial aircraft at a midsized Turkish airport. J. Environ. Eng. 134, 210–215.

Fan, W., Sun, Y., Zhu, T., Wen, Y., 2012. Emissions of HC, CO, NOx, CO2, and SO2 from civil aviation in China in 2010. Atmos. Environ. 56, 52–57.

Fuglestvedt, J.S., Shine, K.P., Berntsen, T., Cook, J., Lee, D., Stenke, A., Skeie, R.B., Velders, G., Waitz, I., 2010. Transport impacts on atmosphere and climate: Metrics. Atmos. Environ. 44, 4648–4677.

Grampella, M., Martini, G., Scotti, D., Tassan, F., Zambon, G., 2017. Determinants of airports' environmental effects. Transp. Res. Part Transp. Environ. 50, 327–344.

Herndon, S.C., Jayne, J.T., Lobo, P., Onasch, T.B., Fleming, G., Hagen, D.E., Whitefield, P.D., Miake-Lye, R.C., 2008. Commercial aircraft engine

emissions characterization of in-use aircraft at Hartsfield-Jackson Atlanta International Airport. Environ. Sci. Technol. 42, 1877–1883.

Herndon, S.C., Wood, E.C., Northway, M.J., Miake-Lye, R., Thornhill, L., Beyersdorf, A., Anderson, B.E., Dowlin, R., Dodds, W., Knighton, W.B., 2009. Aircraft hydrocarbon emissions at Oakland international airport. Environ. Sci. Technol. 43, 1730–1736.

Hileman, J.I., Donohoo, P.E., Stratton, R.W., 2010. Energy content and alternative jet fuel viability. J. Propuls. Power 26, 1184–1196.

Hooper, P., 2005. The environment for Southeast Asia's new and evolving airlines. J. Air Transp. Manag. 11, 335–347. https://doi.org/10.1016/j.jairtraman.2005.07.004

ICAO, 2018. ICAO Engine Exhaust Emission Databank.

ICAO, 1993. International Standards and Recommended Practices, Environmental Protection Annex 16. Volume II Aircraft Engine Emissions. second ed.

ICAO (International Civil Aviation Organization), 2011. Airport Air Quality Manual, first ed.

IPCC, 2007. Climate Change 2007: Synthesis Report, p11.

IPCC, 1999. Aviation and the Global Atmosphere. Summary for Policymakers. IPCC Working Groups I and III, p. 23.

Kalivoda, M.T., Kudrna, M., 1997. Methodologies for estimating emissions from air traffic. Oct MEET Proj. Contract No ST-96-SC204.

Kim, B.Y., Fleming, G.G., Lee, J.J., Waitz, I.A., Clarke, J.-P., Balasubramanian, S., Malwitz, A., Klima, K., Locke, M., Holsclaw, C.A., Maurice, L.Q., Gupta, M.L., 2007. System for assessing Aviation's Global Emissions (SAGE), Part 1: Model description and inventory results. Transp. Res. Part Transp. Environ. 12, 325–346. https://doi.org/10.1016/j.trd.2007.03.007

Knighton, W., Herndon, S., Miake-Lye, R., 2009. Aircraft engine speciated organic gases: Speciation of unburned organic gases in aircraft exhaust. Environ. Prot. Agency Off. Transp. Air Qual.

Koudis, G.S., Hu, S.J., North, R.J., Majumdar, A., Stettler, M.E., 2017. The impact of aircraft takeoff thrust setting on NOX emissions. J. Air Transp. Manag. 65, 191–197.

Krzyzanowski, M., Cohen, A., 2008. Update of WHO air quality guidelines. Air Qual. Atmosphere Health 1, 7–13.

Kurniawan, J.S., Khardi, S., 2011. Comparison of methodologies estimating emissions of aircraft pollutants, environmental impact assessment around airports. Environ. Impact Assess. Rev. 31, 240–252. https://doi.org/10.1016/j.eiar.2010.09.001

Le Quéré, C., Raupach, M.R., Canadell, J.G., Marland, G., Bopp, L., Ciais, P., Conway, T.J., Doney, S.C., Feely, R.A., Foster, P., Friedlingstein, P., Gurney, K., Houghton, R.A., House, J.I., Huntingford, C., Levy, P.E., Lomas, M.R., Majkut, J., Metzl, N., Ometto, J.P., Peters, G.P., Prentice, I.C., Randerson, J.T., Running, S.W., Sarmiento, J.L., Schuster, U., Sitch, S., Takahashi, T., Viovy, N., van der Werf, G.R., Woodward, F.I., 2009. Trends in the sources and sinks of carbon dioxide. Nat. Geosci. 2, 831.

Lee, D., Pitari, G., Grewe, V., Gierens, K., Penner, J., Petzold, A., Prather, M., Schumann, U., Bais, A., Berntsen, T., 2010. Transport impacts on atmosphere and climate: Aviation. Atmos. Environ. 44, 4678–4734.

Lewis, J.S., Niedzwiecki, R.W., Bahr, D., Bullock, S., Cumpsty, N., Dodds, W., DuBois, D., Epstein, A., Ferguson, W., Fiorentino, A., 1999. Aircraft technology and its relation to emissions. Aviat. Glob. Atmosphere 291–70.

Liu, H., Tian, H., Hao, Y., Liu, S., Liu, X., Zhu, C., Wu, Y., Liu, W., Bai, X., Wu, B., 2019. Atmospheric emission inventory of multiple pollutants from civil aviation in China: Temporal trend, spatial distribution characteristics and emission features analysis. Sci. Total Environ. 648, 871–879.

Lukachko, S.P., Waitz, I.A., 1997. Effects of engine aging on aircraft NOx emissions. Presented at the ASME 1997 International Gas Turbine and Aeroengine Congress and Exhibition, American Society of Mechanical Engineers, p. V001T01A011-V001T01A011.

Macintosh, A., Wallace, L., 2009. International aviation emissions to 2025: Can emissions be stabilised without restricting demand? Energy Policy 37, 264–273. https://doi.org/10.1016/j.enpol.2008.08.029

Masiol, M., Harrison, R.M., 2014. Aircraft engine exhaust emissions and other airport-related contributions to ambient air pollution: A review. Atmos. Environ. 95, 409–455. https://doi.org/10.1016/j.atmosenv.2014.05.070

Ministry of Transportation, 2016. Transportation Information Book 2016, Transportation Statistics Book I 2015.

Mochamad, S., 2016. Analysis of Aircraft Growth Impact on Carbon Emission Load towards Juanda International Airport (Civil Engineering Final Project). Institut Teknologi Sepuluh Nopember, Surabaya.

Ofrial, S.A.M.P., Ahyudanari, E., Syafei, A.D., 2016. Estimation on the increasing value of CO based on the vehicle growth in Surabaya. Procedia-Soc. Behav. Sci. 227, 410–416.

Olsthoorn, X., 2001. Carbon dioxide emissions from international aviation: 1950–2050. J. Air Transp. Manag. 7, 87–93.

Patterson, J., Noel, G.J., Senzig, D.A., Roof, C.J., Fleming, G.G., 2009. Analysis of departure and arrival profiles using real-time aircraft data. J. Aircr. 46, 1094–1103.

Peters, G.P., Marland, G., Le Quéré, C., Boden, T., Canadell, J.G., Raupach, M.R., 2012. Rapid growth in CO 2 emissions after the 2008–2009 global financial crisis. Nat. Clim. Change 2, 2.

Presto, A.A., Nguyen, N.T., Ranjan, M., Reeder, A.J., Lipsky, E.M., Hennigan, C.J., Miracolo, M.A., Riemer, D.D., Robinson, A.L., 2011. Fine particle and organic vapor emissions from staged tests of an in-use aircraft engine. Atmos. Environ. 45, 3603–3612. https://doi.org/10.1016/j.atmosenv.2011.03.061

Ratliff, G., Sequeira, C., Waitz, I., Ohsfeldt, M., Thrasher, T., Graham, Michael, Thompson, Terence, Graham, M, Thompson, T, 2009. Aircraft impacts on local and regional air quality in the United States. Partn. Rep. Rep. No Partn.-COE-2009-002.

Richard de Neufville, Amedeo R. Odoni, Peter Belobaba, Tom Reynolds, 2013. Airport systems: planning, design, and management, Second edition. ed. McGraw-Hill Education LLC.

Robert Horonjeff, Francis X. McKelvey, William J. Sproule, Seth B. Young, 2010. Planning and Design of Airports, Fith edition. ed. McGraw-Hill Education LLC.

Romano, D., Gaudioso, D., De Lauretis, R., 1999. Aircraft emissions: a comparison of methodologies based on different data availability. Environ. Monit. Assess. 56, 51–74.

Schürmann, G., Schäfer, K., Jahn, C., Hoffmann, H., Bauerfeind, M., Fleuti, E., Rappenglück, B., 2007. The impact of NOx, CO and VOC emissions on the air quality of Zurich airport. Atmos. Environ. 41, 103–118.

Stettler, M.E.J., Eastham, S., Barrett, S.R.H., 2011. Air quality and public health impacts of UK airports. Part I: Emissions. Atmos. Environ. 45, 5415–5424. https://doi.org/10.1016/j.atmosenv.2011.07.012

Sunyer, J., Atkinson, R., Ballester, F., Le Tertre, A., Ayres, J.G., Forastiere, F., Forsberg, B., Vonk, J., Bisanti, L., Anderson, R., 2003a. Respiratory effects of sulphur dioxide: a hierarchical multicity analysis in the APHEA 2 study. Occup. Environ. Med. 60, e2–e2.

Sunyer, J., Ballester, F., Tertre, A.L., Atkinson, R., Ayres, J.G., Forastiere, F., Forsberg, B., Vonk, J.M., Bisanti, L., Tenías, J.M., 2003b. The association of daily sulfur dioxide air pollution levels with hospital admissions for cardiovascular diseases in Europe (The Aphea-II study). Eur. Heart J. 24, 752–760.

Sutkus Jr, D.J., Baughcum, S.L., DuBois, D.P., 2001. Scheduled civil aircraft emission inventories for 1999: database development and analysis.

Timko, M.T., Herndon, S.C., Wood, E.C., Onasch, T.B., Northway, M.J., Jayne, J.T., Canagaratna, M.R., Miake-Lye, R.C., Knighton, W.B., 2010. Gas turbine engine emissions—part I: volatile organic compounds and nitrogen oxides. J. Eng. Gas Turbines Power 132, 061504.

Turgut, E.T., Usanmaz, O., 2017. An assessment of cruise NOx emissions of short-haul commercial flights. Atmos. Environ. 171, 191–204.

UNEP, 2009. A Climate in Peril.

Vujović, D., Todorović, N., 2017. An assessment of pollutant emissions due to air traffic at Nikola Tesla International Airport, Belgrade, and the link between

local air quality and weather types. Transp. Res. Part Transp. Environ. 56, 85–94.

Watterson, J., Walker, C., Eggleston, S., 2004. Revision to the method of estimating emissions from aircraft in the UK greenhouse gas inventory. Rep. Glob. Atmosphere Div. UK Defra Rep. Number ED47052.

Wey, CC, Anderson, B., Hudgins, C., Wey, C, Li-Jones, X., Winstead, E., Thornhill, L., Lobo, P., Hagen, D., Whitefield, P., 2006. Aircraft Particle Emissions Experiment (APEX). NASA/TM-2006–214382, ARL-TR-3903. Natl. Aeronaut. Space Adm.

Wood, E.C., Herndon, S.C., Timko, M.T., Yelvington, P.E., Miake-Lye, R.C., 2008. Speciation and chemical evolution of nitrogen oxides in aircraft exhaust near airports. Environ. Sci. Technol. 42, 1884–1891.

Yang, X., Cheng, S., Lang, J., Xu, R., Lv, Z., 2018. Characterization of aircraft emissions and air quality impacts of an international airport. J. Environ. Sci. 72, 198–207. https://doi.org/10.1016/j.jes.2018.01.007

Yılmaz, İ., 2017. Emissions from passenger aircraft at Kayseri Airport, Turkey. J. Air Transp. Manag. 58, 176–182. https://doi.org/10.1016/j.jairtraman.2016.11.001

Zaporozhets, O., Synylo, K., 2017. Improvements on aircraft engine emission and emission inventory asesessment inside the airport area. Adv. Energy Technol. Aviat. 140, 1350–1357. https://doi.org/10.1016/j.energy.2017.07.178

https://www.climatefinance-developmenteffectiveness.org/CPEIR-Database

https://contentzone.eurocontrol.int/aircraftperformance/default.aspx?

https://www.geaviation.com/sites/default/files/datasheet-CF34-8C.pdf
https://www.easa.europa.eu/sites/default/files/dfu/EASA%20TCDS%20IM%20E%20053%20issue%2002%2016%20March%202017_0.1.pdf
https://www.easa.europa.eu/sites/default/files/dfu/EASA-TCDS-E.066_CFM_International_S.A._--_CFM56--2-----3_series_engines-01-28112008.pdf

https://www.easa.europa.eu/sites/default/files/dfu/EASA%20E%20110%20TCDS%20Issue%202%20LEAP-1A_1C_20161103_1.0.pdf

https://www.easa.europa.eu/sites/default/files/dfu/EASA-TCDS-E.007_(IM)_General_Electric_CF6--80E1_Series_engines-02-25102011.pdf

https://www.easa.europa.eu/sites/default/files/dfu/TCDS%20E.003%20issue%2004_20170928.pdf

https://www.boeing.com/resources/boeingdotcom/commercial/airports/acaps/737.pdf

https://aimindonesia.dephub.go.id/index.php?page=product-aip-electronik-vol123.html&id_aip=132

"This page is intentionally left blank"

ATTACHMENTS

ATTACHMENT 1: Emission Index Sheet

ATTACHMENT 2: Departure and Arrival Schedule

ATTACHEMNT 3; Temperature, density and Pressure

A 320									Airbus 320

category includes: Airbus 320
engine category: turbofan
standard engine types: CFM56-5
engine of category: engine mix
European traffic: 6,22% (share in European air traffic movements 1995)
max cruising speed: 487 mph | 903 km/h
av. cruising speed: 454 mph | 847 km/h (used here)

weights	from	to	(depending on exact type)
operational empty:	41.583	41.870	kg
max take off:	73.500	77.000	kg
cruise altitude	short	long	range (defaults if no actual data is available)
	370	390	FL (=100ft)

Equations for usage coefficients:
Variable x means CRALT

$$Y = b_0 + b_1 \cdot x + b_2 \cdot x^2 + b_3 \cdot x^3$$

$$Y = a_0 + a_1 \cdot \frac{1}{x}$$

$$Y = c_0 + c_1 \cdot \ln(x)$$

A 320	Airbus 320								

			duration of OS	distance of OS	Fuel consumption total [1]	specific	EI-NOx	EI-HC	EI-CO
operational state (OS)	Index [-]	coefficient [-]	DUR [s]	D [km]	FC [kg]	SFC	SE_{NOx} [g/kg]	SE_{HC} [g/kg]	SE_{CO} [g/kg]
OS 1 engine start	es								
OS 2 taxi out	txo		480		117,12 [kg/s]: 0,24400		5,1310	0,871	12,884
OS 3 take off	tff		45		105,93 [kg/s]: 2,35400		32,5780	0,160	0,689
OS 4 climb	cl	b0		-9,233E+00	-6,428E+01		3,288E+01	a0: 1,701E-01	a0: 7,104E-01
		b1		4,474E-03	6,045E-02		-1,033E-03	a1: -8,950E-02	a1: -3,973E-01
		b2		-9,910E-08	-9,614E-07		3,559E-08		
		b3		4,917E-12	1,921E-11		-5,197E-13		
OS 5 cruise	cr	b0			[kg/km]: 3,694E+00		3,556E+01	0,172	0,661
		b1			[kg/km]: 1,008E-02		-1,225E-01		
		b2			[kg/km]: -2,916E-05		1,260E-04		
OS 6 descent	dsc	b0		5,027E-01	5,745E+00		6,326E+00	c0: -6,055E-01	c0: -1,292E+01
		b1		5,394E-03	3,541E-03		-5,690E-04	c1: 1,411E-01	c1: 2,460E+00
		b2		-4,600E-08	-7,306E-08		2,860E-08		
		b3		9,871E-13	3,493E-12		-4,279E-13		
OS 7 landing	ld		15		35,31 [kg/s]: 2,35400		32,5690	0,170	0,680
OS 8 taxi in	txi		360		87,84 [kg/s]: 0,24400		5,1340	0,877	12,876
OS 9 ground operations	go								

$EI\text{-}CO_2$	3150	[g/kg]
$EI\text{-}SO_2$	1,00	[g/kg]
$EI\text{-}H_2O$	1240	[g/kg]

[1] total fuel that is burned during DUR [s] of operational state: FC = SFC * DUR

ATTACHMENT 1: Emission Index Sheet

B 737	Boeing 737

category includes: **Boeing 737-100, -200, -300, -400, -500, -600, -700, -800**
engine category: **turbofan**
standard engine types: **CFM56-3B-2, P&W JT8D**
engine of category: **engine mix**
European traffic: **20,04%** (share in European air traffic movements 1995)

max cruising speed: **509** mph / **943** km/h
av. cruising speed: **411** mph / **761** km/h (used here)

weights — from / to (depending on exact type)
operational empty: **25.878** / **34.270** kg
max take off: **49.940** / **76.430** kg

cruise altitude: short / long — range (defaults if no actual data is available)
330 / **350** FL (=100ft)

Equations for usage coefficients:
Variable x means CRALT

$$Y = b_0 + b_1 \cdot x + b_2 \cdot x^2 + b_3 \cdot x^3$$
$$Y = a_0 + a_1 \cdot \frac{1}{x}$$
$$Y = c_0 + c_1 \cdot \ln(x)$$

B 737	Boeing 737

operational state (OS)	Index	coefficient	duration of OS [s] DUR	distance of OS [km] D	Fuel consumption total[1] [kg] FC	specific SFC	EI-NOx [g/kg] SE_{NOx}	EI-HC [g/kg] SE_{HC}	EI-CO [g/kg] SE_{CO}
OS 1 engine start	es								
OS 2 taxi out	txo		480		141,41	[kg/s]: 0,29460	3,1470	10,600	33,300
OS 3 take off	tff		45		109,03	[kg/s]: 2,42289	19,1510	0,468	0,725
OS 4 climb	cl	b0		-1,926E+01	-9,020E+01		1,938E+01	a0: 5,235E-01	a0: 1,006E+00
		b1		8,645E-03	8,386E-02		-6,940E-04	a1: -1,115E+00	a1: -5,412E+00
		b2		-4,317E-07	-1,929E-06		2,511E-08		
		b3		1,398E-11	4,656E-11		-3,831E-13		
OS 5 cruise	cr	b0				[kg/km]: 1,943E+00	1,960E+01	0,520	1,000
		b1				[kg/km]: 2,345E-02	-6,625E-02		
		b2				[kg/km]: -5,318E-05	6,648E-05		
OS 6 descent	dsc	b0		-1,321E-01	4,061E+00		3,702E+00	c0: -8,772E+00	c0: -2,874E+01
		b1		5,479E-03	4,426E-04		-3,710E-04	c1: 1,881E+00	c1: 6,026E+00
		b2		-5,835E-08	-9,164E-08		2,071E-08		
		b3		1,346E-12	5,344E-12		-3,388E-13		
OS 7 landing	ld		15		36,34	[kg/s]: 2,42267	19,1520	0,468	0,715
OS 8 taxi in	txi		360		106,06	[kg/s]: 0,29461	3,1490	10,598	33,302
OS 9 ground operations	go								

EI-CO$_2$	3150	[g/kg]
EI-SO$_2$	1,00	[g/kg]
EI-H$_2$O	1240	[g/kg]

[1] total fuel that is burned during DUR [s] of operational state: FC = SFC * DUR

ATTACHMENT 2

Departure schedule 21/09/2018

TIME	FLIGHT	TO	AIRLINE	AIRCRAFT
5:00 AM	ID6150	Sorong (SOQ)	Batik Air	A320 (PK-LAV)
5:00 AM	SJ257	Jakarta (CGK)	Sriwijaya Air	B738 (PK-CLQ)
5:05 AM	QG171	Jakarta (HLP)	Citilink	A320 (PK-GQI)
5:05 AM	XT320	Kuala Lumpur (KUL)	AirAsia X	A320 (PK-AXF)
5:05 AM	XT7681	Jakarta (CGK)	AirAsia X	A320 (PK-AXG)
5:15 AM	XT384	Penang (PEN)	AirAsia X	A320 (PK-AXH)
5:15 AM	GA631	Makassar (UPG)	Garuda Indonesia	CRJX (PK-GRK)
5:25 AM	JT1708	Makassar (UPG)	Lion Airlines	739
5:25 AM	GA303	Jakarta (CGK)	Garuda Indonesia	B738 (PK-GFE)
5:25 AM	JT708	Makassar (UPG)	Lion Air	B738 (PK-LJW)
5:25 AM	QG820	Bandung (BDO)	Citilink	A320 (PK-GQJ)
5:30 AM	ID6401	Jakarta (CGK)	Batik Air	A320 (PK-LZH)
5:30 AM	ID6896	Jakarta (CGK)	Batik Air	32A
5:35 AM	QG416	Pontianak (PNK)	Citilink	A320 (PK-GLI)
5:45 AM	JT310	Banjarmasin (BDJ)	Lion Air	B739 (PK-LHQ)
5:45 AM	JT804	Denpasar (DPS)	Lion Air	B739 (PK-LJL)
5:45 AM	QG711	Jakarta (CGK)	Citilink Garuda Indonesia	A320 (PK-GQT)
5:55 AM	GA7302	Blimbingsari (BWX)	Garuda Indonesia	AT76 (PK-GAE)
6:00 AM	IW1804	Sampit Airport (SMQ)	Wings Air	AT75 (PK-WFP)
6:00 AM	IW1914	Surakarta (SOC)	Wings Air	AT76 (PK-WHF)
6:00 AM	JT571	Jakarta (CGK)	Lion Air	B738 (PK-LKH)
6:00 AM	JT979	Medan (KNO)	Lion Air	B739 (PK-LHH)
6:00 AM	SJ566	Makassar (UPG)	Sriwijaya Air	B738 (PK-CRF)
6:05 AM	CI752	Singapore (SIN)	China Airlines	A333 (B-18353)

6:05 AM	JT360	Balikpapan (BPN)	Lion Air	B739 (PK-LFK)
6:10 AM	BI796	Brunei (BWN)	Royal Brunei Airlines	A320 (V8-RBW)
6:10 AM	IL712	Pangkalan Bun (PKN)	Trigana Air	734
6:10 AM	QG430	Balikpapan (BPN)	Citilink	A320 (PK-GLP)
6:10 AM	QG484	Banjarmasin (BDJ)	Citilink	A320 (PK-GLX)
6:15 AM	GA305	Jakarta (CGK)	Garuda Indonesia	B738 (PK-GMG)
6:15 AM	ID6597	Jakarta (CGK)	Batik Air	A320 (PK-LZI)
6:15 AM	ID6852	Jakarta (CGK)	Batik Air	A320 (PK-LZI)
6:20 AM	QG946	Batam (BTH)	Citilink	A320 (PK-GQO)
6:20 AM	SJ236	Sampit Airport (SMQ)	Sriwijaya Air	735
6:25 AM	QG600	Kupang (KOE)	Citilink	A320 (PK-GQP)
6:35 AM	QG450	Palangkaraya (PKY)	Citilink	A320 (PK-GQK)
6:55 AM	JT262	Balikpapan (BPN)	Lion Air (50th 737-900ER Livery)	B739 (PK-LHY)
6:55 AM	JT690	Kupang (KOE)	Lion Air	B739 (PK-LFW)
6:55 AM	JT962	Lombok (LOP)	Lion Air	B739 (PK-LJG)
7:10 AM	QG346	Makassar (UPG)	Citilink	A320 (PK-GLE)
7:20 AM	JT806	Makassar (UPG)	Lion Air	B739 (PK-LHV)
7:25 AM	ID7510	Jakarta (HLP)	Batik Air	B738 (PK-LBZ)
7:30 AM	GA368	Semarang (SRG)	Garuda Indonesia	CRJX (PK-GRN)
7:30 AM	IW1843	Yogyakarta (JOG)	Wings Air	AT76 (PK-WHI)
7:30 AM	SJ268	Jayapura (DJJ)	Sriwijaya Air	733
7:35 AM	ID6174	Ambon (AMQ)	Batik Air	A320 (PK-LUQ)
7:35 AM	ID6596	Ambon (AMQ)	Batik Air	738
7:35 AM	IW1839	Semarang (SRG)	Wings Air	AT76 (PK-WGJ)
7:35 AM	QZ7689	Jakarta (CGK)	AirAsia	A320 (PK-AXR)
7:40 AM	GA854	Singapore (SIN)	Garuda Indonesia	B738 (PK-GFD)
7:45 AM	IN276	Denpasar (DPS)	Nam Air	735
7:45 AM	IN377	Denpasar (DPS)	NAM Air	B735 (PK-NAU)

7:50 AM	GA307	Jakarta (CGK)	Garuda Indonesia	B738 (PK-GFO)
7:55 AM	QG694	Denpasar (DPS)	Citilink	A320 (PK-GLA)
8:00 AM	JT856	Palembang (PLM)	Lion Air	B738 (PK-LOG)
8:05 AM	IN9276	Denpasar (DPS)	Nam Air	735
8:05 AM	JT911	Bandung (BDO)	Lion Air	B738 (PK-LPR)
8:05 AM	JT971	Batam (BTH)	Lion Air	B739 (PK-LFS)
8:10 AM	JT748	Manado (MDC)	Lion Air	B38M (PK-LQP)
8:10 AM	JT929	Manado (MDC)	Lion Airlines	739
8:20 AM	GA449	Jakarta (CGK)	Garuda Indonesia	B738 (PK-GFC)
8:20 AM	ID6391	Jakarta (CGK)	Batik Air	A320 (PK-LUL)
8:25 AM	CX780	Hong Kong (HKG)	Cathay Pacific	A333 (B-LAR)
8:30 AM	JT264	Balikpapan (BPN)	Lion Air	B739 (PK-LHS)
8:35 AM	JT836	Pontianak (PNK)	Lion Air	B738 (PK-LPJ)
8:35 AM	XT695	Jakarta (CGK)	AirAsia X	A320 (PK-AXI)
8:45 AM	XT8297	Kuala Lumpur (KUL)	AirAsia X	A320 (PK-AXJ)
8:50 AM	GA309	Jakarta (CGK)	Garuda Indonesia	A332 (PK-GPQ)
8:50 AM	GA7306	Jember (JBB)	Garuda Indonesia	AT76 (PK-GAE)
9:00 AM	JT786	Makassar (UPG)	Lion Air	B739 (PK-LGW)
9:00 AM	JT852	Makassar (UPG)	Lion Air	B739 (PK-LJH)
9:00 AM	JT992	Makassar (UPG)	Lion Airlines	738
9:05 AM	JT573	Jakarta (CGK)	Lion Air	B738 (PK-LJY)
9:20 AM	JT226	Banjarmasin (BDJ)	Lion Air	B738 (PK-LPT)
9:25 AM	JT951	Bandung (BDO)	Lion Air (90th 737NG Livery)	B738 (PK-LKV)
9:25 AM	QG670	Lombok (LOP)	Citilink	A320 (PK-GQJ)
9:30 AM	JT646	Lombok (LOP)	Lion Air	B739 (PK-LHL)
9:30 AM	QG800	Semarang (SRG)	Citilink	A320 (PK-GLX)
9:30 AM	QG432	Balikpapan (BPN)	Citilink	320
9:35 AM	IN3771	Denpasar (DPS)	Nam Air	735

9:45 AM	QG713	Jakarta (CGK)	Citilink Garuda Indonesia	A320 (PK-GQT)
9:50 AM	JT680	Palangkaraya (PKY)	Lion Air	B739 (PK-LHQ)
9:55 AM	SJ269	Jakarta (CGK)	Sriwijaya Air	735
10:00 AM	MH870	Kuala Lumpur (KUL)	Malaysia Airlines	B738 (9M-MXB)
10:00 AM	JT169	Kuala Lumpur (KUL)	Lion Air	B738 (PK-LPL)
10:05 AM	GA311	Jakarta (CGK)	Garuda Indonesia (SkyTeam Livery)	B738 (PK-GMH)
10:10 AM	IW1872	Jember (JBB)	Wings Air	AT75 (PK-WFP)
10:10 AM	SQ931	Singapore (SIN)	Singapore Airlines	A333 (9V-STZ)
10:15 AM	JT922	Denpasar (DPS)	Lion Air	B739 (PK-LJG)
10:15 AM	TR265	Singapore (SIN)	Scoot	A320 (9V-TRN)
10:25 AM	JT362	Balikpapan (BPN)	Lion Air	B739 (PK-LFK)
10:30 AM	IW1835	Semarang (SRG)	Wings Air	AT75 (PK-WFP)
10:30 AM	JT312	Banjarmasin (BDJ)	Lion Air	B739 (PK-LHW)
10:35 AM	ID6573	Jakarta (CGK)	Batik Air	A320 (PK-LAK)
10:40 AM	SJ225	Semarang (SRG)	Sriwijaya Air	B738 (PK-CMN)
10:40 AM	QG715	Jakarta (CGK)	Citilink	A320 (PK-GLP)
10:40 AM	SJ564	Makassar (UPG)	Sriwijaya Air	733
10:45 AM	IW1811	Yogyakarta (JOG)	Wings Air	AT76 (PK-WGQ)
10:50 AM	GA364	Lombok (LOP)	Garuda Indonesia	CRJX (PK-GRN)
11:00 AM	GA342	Denpasar (DPS)	Garuda Indonesia	B738 (PK-GMC)
11:00 AM	SJ254	Kupang (KOE)	Sriwijaya Air	738
11:00 AM	QG486	Banjarmasin (BDJ)	Citilink	A320 (PK-GLA)
11:00 AM	SJ252	Balikpapan (BPN)	Sriwijaya Air	735
11:10 AM	GA313	Jakarta (CGK)	Garuda Indonesia	B738 (PK-GMW)
11:10 AM	ID6130	Labuan Bajo (LBJ)	Batik Air	A320 (PK-LUP)
11:10 AM	XT324	Kuala Lumpur (KUL)	AirAsia X	A320 (PK-AXF)
11:20 AM	JT692	Kupang (KOE)	Lion Air	B739 (PK-LGZ)
11:30 AM	QG930	Pekanbaru (PKU)	Citilink	320

11:35 AM	ID6230	Makassar (UPG)	Batik Air	738
11:35 AM	ID6284	Makassar (UPG)	Batik Air	A320 (PK-LUT)
11:35 AM	JT222	Banjarmasin (BDJ)	Lion Air	B38M (PK-LQG)
11:35 AM	QG434	Balikpapan (BPN)	Citilink	320
11:45 AM	GA7304	Blimbingsari (BWX)	Garuda Indonesia	AT76 (PK-GAE)
11:50 AM	ID7083	Jakarta (HLP)	Batik Air	32A
11:50 AM	ID7512	Jakarta (HLP)	Batik Air	B738 (PK-LBZ)
11:50 AM	JT973	Batam (BTH)	Lion Air	B739 (PK-LFV)
11:50 AM	QG717	Jakarta (CGK)	Citilink	A320 (PK-GQK)
11:50 AM	QG948	Batam (BTH)	Citilink	A20N (PK-GTF)
12:00 PM	IN116	Batu Licin (BTW)	Nam Air	ATR
12:00 PM	IW1880	Blimbingsari (BWX)	Wings Air	AT76 (PK-WHF)
12:05 PM	JT260	Balikpapan (BPN)	Lion Air (50th 737-900ER Livery)	B739 (PK-LHY)
12:10 PM	JT591	Jakarta (CGK)	Lion Air	B739 (PK-LHI)
12:10 PM	JT916	Bandung (BDO)	Lion Air	B738 (PK-LKT)
12:25 PM	XT322	Kuala Lumpur (KUL)	AirAsia X	A320 (PK-AXH)
12:30 PM	GA315	Jakarta (CGK)	Garuda Indonesia	B738 (PK-GFO)
12:35 PM	QG834	Majalengka (KJT)	Citilink	A320 (PK-GQP)
12:40 PM	ID6575	Jakarta (CGK)	Batik Air	B739 (PK-LBH)
12:40 PM	SJ334	Bandar Lampung (TKG)	Sriwijaya Air	738
12:45 PM	IW1808	Sumenep-Madura Island (SUP)	Wings Air	AT76 (PK-WHI)
12:45 PM	QG986	Palembang (PLM)	Citilink	A320 (PK-GQJ)
12:50 PM	JT706	Makassar (UPG)	Lion Air	B739 (PK-LFW)
12:55 PM	QG436	Balikpapan (BPN)	Citilink	320
12:55 PM	QG696	Denpasar (DPS)	Citilink	A320 (PK-GQO)
1:00 PM	JT178	Lombok (LOP)	Lion Air	B739 (PK-LHL)
1:05 PM	JT266	Balikpapan (BPN)	Lion Air	B738 (PK-LPT)
1:20 PM	QG692	Denpasar (DPS)	Citilink	A320 (PK-GLY)

1:20 PM	3K248	Singapore (SIN)	Jetstar Airways	A320 (9V-JSR)
1:30 PM	GA317	Jakarta (CGK)	Garuda Indonesia	B738 (PK-GFX)
1:30 PM	JT736	Manado (MDC)	Lion Air	B739 (PK-LHV)
1:30 PM	ID6412	Denpasar (DPS)	Batik Air	A320 (PK-LAR)
1:30 PM	IN192	Pangkalan Bun (PKN)	Nam Air	735
1:30 PM	IW1845	Yogyakarta (JOG)	Wings Air	AT76 (PK-WGJ)
1:30 PM	IW1873	Denpasar (DPS)	Wings Air	AT7
1:30 PM	JT910	Denpasar (DPS)	Lion Air	B739 (PK-LJG)
1:40 PM	JT694	Kupang (KOE)	Lion Air	B738 (PK-LJY)
1:40 PM	QG307	Makassar (UPG)	Citilink	A320 (PK-GLX)
1:50 PM	JT577	Jakarta (CGK)	Lion Air	B738 (PK-LOG)
1:50 PM	JT695	Jakarta (CGK)	Lion Airlines	738
1:50 PM	QG173	Jakarta (HLP)	Citilink	A20N (PK-GTI)
2:00 PM	JT949	Batam (BTH)	Lion Air	B738 (PK-LPJ)
2:10 PM	JT316	Banjarmasin (BDJ)	Lion Air	B739 (PK-LHW)
2:20 PM	QG824	Bandung (BDO)	Citilink Garuda Indonesia	A320 (PK-GQT)
2:30 PM	IW1897	Semarang (SRG)	Wings Air	AT76 (PK-WHF)
2:35 PM	JT749	Jakarta (CGK)	Lion Air	B38M (PK-LQP)
2:40 PM	GA365	Semarang (SRG)	Garuda Indonesia	CRJX (PK-GRN)
2:40 PM	IW1890	Pangkalan Bun (PKN)	Wings Air	AT76 (PK-WHI)
2:40 PM	SJ238	Sampit Airport (SMQ)	Sriwijaya Air	735
2:45 PM	GA7308	Yogyakarta (JOG)	Garuda Indonesia	AT76 (PK-GAE)
2:45 PM	JT366	Balikpapan (BPN)	Lion Air	B739 (PK-LFK)
2:45 PM	QG438	Balikpapan (BPN)	Citilink	A320 (PK-GLA)
3:00 PM	JT864	Lombok (LOP)	Lion Air	B739 (PK-LHQ)
3:00 PM	QG175	Jakarta (HLP)	Citilink	A320 (PK-GLE)
3:05 PM	ID7502	Jakarta (HLP)	Batik Air	A320 (PK-LAP)
3:10 PM	SJ232	Balikpapan (BPN)	Sriwijaya Air	B735 (PK-CLK)

Time	Flight	Destination	Airline	Aircraft
3:10 PM	XT326	Kuala Lumpur (KUL)	AirAsia X	A320 (PK-AXI)
3:15 PM	IW1809	Banjarmasin (BDJ)	Wings Air	AT7
3:15 PM	JT220	Banjarmasin (BDJ)	Lion Air	B738 (PK-LPQ)
3:15 PM	JT268	Tarakan (TRK)	Lion Air	B38M (PK-LQG)
3:30 PM	GA319	Jakarta (CGK)	Garuda Indonesia	B738 (PK-GMF)
3:35 PM	ID7508	Jakarta (HLP)	Batik Air	A320 (PK-LAK)
3:35 PM	QG672	Lombok (LOP)	Citilink	A320 (PK-GQK)
3:40 PM	JT581	Jakarta (CGK)	Lion Air	B739 (PK-LGT)
3:50 PM	GA321	Jakarta (CGK)	Garuda Indonesia	B738 (PK-GMC)
4:00 PM	JT318	Banjarmasin (BDJ)	Lion Air	B739 (PK-LHP)
4:15 PM	JT838	Pontianak (PNK)	Lion Air	B738 (PK-LKR)
4:15 PM	JT822	Lombok (LOP)	Lion Air	B738 (PK-LKT)
4:15 PM	JT982	Pekanbaru (PKU)	Lion Air (50th 737-900ER Livery)	B739 (PK-LHY)
4:20 PM	SJ235	Yogyakarta (JOG)	Sriwijaya Air	B739 (PK-CMP)
4:20 PM	ID7107	Jakarta (HLP)	Batik Air	738
4:20 PM	ID7514	Jakarta (HLP)	Batik Air	B738 (PK-LBZ)
4:20 PM	XT330	Kuala Lumpur (KUL)	AirAsia X	A320 (PK-AXJ)
4:25 PM	GA344	Denpasar (DPS)	Garuda Indonesia	B738 (PK-GFI)
4:30 PM	JT722	Kendari (KDI)	Lion Air	B739 (PK-LGV)
4:30 PM	MI223	Singapore (SIN)	SilkAir	A320 (9V-SLG)
4:30 PM	JT599	Jakarta (CGK)	Lion Airlines	739
4:35 PM	SJ255	Jakarta (CGK)	Sriwijaya Air	B738 (PK-CRF)
4:35 PM	IW1816	Yogyakarta (JOG)	Wings Air	AT76 (PK-WGJ)
4:50 PM	JT693	Jakarta (CGK)	Lion Air	B739 (PK-LHT)
5:00 PM	JT165	Kuala Lumpur (KUL)	Lion Airlines	738
5:00 PM	QG488	Banjarmasin (BDJ)	Citilink	A320 (PK-GLY)
5:10 PM	GA338	Denpasar (DPS)	Garuda Indonesia	CRJX (PK-GRE)
5:20 PM	QG348	Makassar (UPG)	Citilink	A320 (PK-GLL)

5:25 PM	ID7579	Jakarta (CGK)	Batik Air	A320 (PK-LUK)
5:30 PM	QG719	Jakarta (CGK)	Citilink	A320 (PK-GQP)
5:40 PM	JT2661	Haikou (HAK)	Lion Air	B739 (PK-LHL)
5:45 PM	GA373	Bandung (BDO)	Garuda Indonesia	B738 (PK-GMK)
5:45 PM	XT7693	Jakarta (CGK)	AirAsia X	A320 (PK-AXF)
5:50 PM	IN376	Bandung (BDO)	Nam Air	735
5:50 PM	JT780	Makassar (UPG)	Lion Air	B739 (PK-LHQ)
5:55 PM	IN9376	Bandung (BDO)	Nam Air	735
6:00 PM	GA323	Jakarta (CGK)	Garuda Indonesia	A333 (PK-GPX)
6:00 PM	GA367	Makassar (UPG)	Garuda Indonesia	CRJX (PK-GRN)
6:00 PM	JT642	Lombok (LOP)	Lion Airlines	739
6:00 PM	QG418	Pontianak (PNK)	Citilink	A20N (PK-GTF)
6:05 PM	JT858	Balikpapan (BPN)	Lion Air	B738 (PK-LPU)
6:10 PM	QG698	Denpasar (DPS)	Citilink	A20N (PK-GTI)
6:15 PM	JT149	Bandar Lampung (TKG)	Lion Air (90th 737NG Livery)	B738 (PK-LKV)
6:20 PM	GA448	Kupang (KOE)	Garuda Indonesia (Retro 1969 Livery)	B738 (PK-GFN)
6:20 PM	JT704	Makassar (UPG)	Lion Air	B738 (PK-LKJ)
6:25 PM	ID6581	Jakarta (CGK)	Batik Air	A320 (PK-LAV)
6:25 PM	SJ259	Jakarta (CGK)	Sriwijaya Air	733
6:30 PM	QG177	Jakarta (HLP)	Citilink	A320 (PK-GQE)
6:40 PM	GA325	Jakarta (CGK)	Garuda Indonesia	B738 (PK-GFK)
6:40 PM	MI225	Singapore (SIN)	SilkAir	A320 (9V-SLP)
6:40 PM	JT682	Palangkaraya (PKY)	Lion Air	B739 (PK-LGW)
6:40 PM	JT730	Balikpapan (BPN)	Lion Air	B738 (PK-LPQ)
6:45 PM	ID7516	Jakarta (HLP)	Garuda Indonesia	CRJX (PK-GRC)
6:45 PM	XT7624	Denpasar (DPS)	AirAsia X	A320 (PK-AXH)
6:50 PM	SJ227	Semarang (SRG)	Sriwijaya Air	735
6:50 PM	SJ264	Denpasar (DPS)	Sriwijaya Air	B738 (PK-CRH)

6:55 PM	QG806	Semarang (SRG)	Citilink	A320 (PK-GLA)
7:00 PM	JT696	Kupang (KOE)	Lion Air (Dreamliner Livery)	B739 (PK-LFG)
7:10 PM	QG721	Jakarta (CGK)	Citilink	A320 (PK-GQK)
7:15 PM	JT697	Jakarta (CGK)	Lion Air	B738 (PK-LJY)
7:30 PM	IW1813	Yogyakarta (JOG)	Wings Air	AT76 (PK-WHI)
7:30 PM	SJ267	Jakarta (CGK)	Sriwijaya Air	B738 (PK-CMW)
7:35 PM	GA327	Jakarta (CGK)	Garuda Indonesia	B738 (PK-GMJ)
7:40 PM	IW1801	Semarang (SRG)	Wings Air (50th ATR to Lion Group Livery)	AT76 (PK-WHG)
7:40 PM	QG179	Jakarta (HLP)	Citilink	A320 (PK-GQD)
7:40 PM	QG440	Balikpapan (BPN)	Citilink	A320 (PK-GQJ)
7:45 PM	JT990	Denpasar (DPS)	Lion Air	B739 (PK-LKO)
7:45 PM	JT585	Jakarta (CGK)	Lion Airlines	739
7:55 PM	ID6175	Jakarta (CGK)	Batik Air	32A
7:55 PM	ID7520	Jakarta (CGK)	Batik Air	A320 (PK-LAK)
8:00 PM	QG723	Jakarta (CGK)	Citilink	A320 (PK-GLN)
8:30 PM	GA329	Jakarta (CGK)	Garuda Indonesia	B738 (PK-GNE)
8:30 PM	QG725	Jakarta (CGK)	Citilink	A320 (PK-GQN)
8:50 PM	IW1847	Yogyakarta (JOG)	Wings Air	AT75 (PK-WFW)
8:55 PM	GA331	Jakarta (CGK)	Garuda Indonesia	B738 (PK-GMC)
8:55 PM	ID7518	Jakarta (HLP)	Batik Air	B738 (PK-LBZ)
9:10 PM	ID6309	Jakarta (CGK)	Batik Air	A320 (PK-LAU)
9:15 PM	QG727	Jakarta (CGK)	Citilink	A320 (PK-GLG)
9:15 PM	SJ570	Makassar (UPG)	Sriwijaya Air	735
9:25 PM	SJ562	Makassar (UPG)	Sriwijaya Air	B738 (PK-CMK)
9:30 PM	JT595	Jakarta (CGK)	Lion Air	B739 (PK-LHP)
9:45 PM	ID6583	Jakarta (CGK)	Batik Air	A320 (PK-LUK)
10:00 PM	ID6136	Makassar (UPG)	Batik Air	A320 (PK-LUP)
10:00 PM	ID8196	Makassar (UPG)	Batik Air	32A

10:25 PM	JT800	Makassar (UPG)	Lion Air	B739 (PK-LFU)
10:25 PM	JT880	Makassar (UPG)	Lion Airlines	739
10:25 PM	JT1798	Makassar (UPG)	Lion Airlines	739
10:35 PM	JT821	Jakarta (CGK)	Lion Air	B739 (PK-LHJ)

ATTACHMENT 2

Arrival Schedule 21/09/2018

TIME	FLIGHT	FROM	AIRLINE	AIRCRAFT
12:35 AM	SV5410	Medina (MED)	Saudia	B744 (TF-AAJ)
5:40 AM	QG710	Jakarta (CGK)	Citilink	A320 (PK-GQP)
6:00 AM	ID6596	Jakarta (CGK)	Batik Air	A320 (PK-LUQ)
6:20 AM	JT311	Banjarmasin (BDJ)	Lion Air (50th 737-900ER Livery)	B739 (PK-LHY)
6:20 AM	QG7261	Jakarta (CGK)	Citilink	320
6:30 AM	JT690	Jakarta (CGK)	Lion Air	B739 (PK-LFW)
6:45 AM	ID7511	Jakarta (HLP)	Batik Air	B738 (PK-LBZ)
6:45 AM	SJ268	Jakarta (CGK)	Sriwijaya Air	733
6:50 AM	GA368	Makassar (UPG)	Garuda Indonesia	CRJX (PK-GRN)
6:50 AM	JT929	Denpasar (DPS)	Lion Air	B739 (PK-LHV)
7:01 AM	JT823	Lombok (LOP)	Lion Air	B738 (PK-LPJ)
7:05 AM	GA302	Jakarta (CGK)	Garuda Indonesia	B738 (PK-GFO)
7:05 AM	JT691	Kupang (KOE)	Lion Air	B739 (PK-LGW)
7:05 AM	QZ7688	Jakarta (CGK)	AirAsia	A320 (PK-AXR)
7:10 AM	IW1800	Semarang (SRG)	Wings Air	AT76 (PK-WGJ)
7:10 AM	IW1814	Yogyakarta (JOG)	Wings Air	AT76 (PK-WHI)
7:10 AM	JT801	Makassar (UPG)	Lion Air	B738 (PK-LOG)
7:15 AM	IN377	Bandung (BDO)	NAM Air	B735 (PK-NAU)
7:20 AM	JT367	Balikpapan (BPN)	Lion Air	B739 (PK-LFS)
7:25 AM	IN9377	Bandung (BDO)	Nam Air	735
7:25 AM	JT918	Bandung (BDO)	Lion Air	B738 (PK-LPR)
7:25 AM	QG712	Jakarta (CGK)	Citilink	A320 (PK-GLA)
7:30 AM	ID6370	Jakarta (CGK)	Batik Air	A320 (PK-LUL)
7:30 AM	JT748	Jakarta (CGK)	Lion Air	B38M (PK-LQP)

7:35 AM	GA449	Kupang (KOE)	Garuda Indonesia	B738 (PK-GFC)
7:50 AM	GA304	Jakarta (CGK)	Garuda Indonesia	A332 (PK-GPQ)
7:50 AM	JT683	Palangkaraya (PKY)	Lion Air	B739 (PK-LHS)
8:15 AM	JT861	Palu (PLW)	Lion Air	B738 (PK-LJY)
8:20 AM	GA7303	Blimbingsari (BWX)	Garuda Indonesia	AT76 (PK-GAE)
8:20 AM	XT7680	Jakarta (CGK)	AirAsia X	A320 (PK-AXJ)
8:30 AM	JT805	Denpasar (DPS)	Lion Air	B739 (PK-LHL)
8:35 AM	JT645	Lombok (LOP)	Lion Air	B738 (PK-LPT)
8:45 AM	JT731	Balikpapan (BPN)	Lion Air (90th 737NG Livery)	B738 (PK-LKV)
8:45 AM	JT859	Balikpapan (BPN)	Lion Airlines	738
8:55 AM	QG821	Bandung (BDO)	Citilink	A320 (PK-GQJ)
8:55 AM	IN3770	Denpasar (DPS)	Nam Air	735
9:00 AM	GA306	Jakarta (CGK)	Garuda Indonesia (SkyTeam Livery)	B738 (PK-GMH)
9:00 AM	QG485	Banjarmasin (BDJ)	Citilink	A320 (PK-GLX)
9:05 AM	SQ930	Singapore (SIN)	Singapore Airlines	A333 (9V-STZ)
9:10 AM	MH871	Kuala Lumpur (KUL)	Malaysia Airlines	B738 (9M-MXB)
9:10 AM	IW1872	Banjarmasin (BDJ)	Wings Air	AT7
9:10 AM	JT315	Banjarmasin (BDJ)	Lion Air	B739 (PK-LHQ)
9:10 AM	SJ237	Sampit Airport (SMQ)	Sriwijaya Air	735
9:15 AM	JT168	Kuala Lumpur (KUL)	Lion Air	B738 (PK-LPL)
9:15 AM	QG714	Jakarta (CGK)	Citilink Garuda Indonesia	A320 (PK-GQT)
9:30 AM	SJ224	Semarang (SRG)	Sriwijaya Air	B738 (PK-CMN)
9:35 AM	JT865	Lombok (LOP)	Lion Air	B739 (PK-LJG)
9:35 AM	TR264	Singapore (SIN)	Scoot	A320 (9V-TRN)
9:45 AM	ID6572	Jakarta (CGK)	Batik Air	A320 (PK-LAK)
9:45 AM	IW1805	Sampit Airport (SMQ)	Wings Air	AT75 (PK-WFP)
9:45 AM	JT361	Balikpapan (BPN)	Lion Air	B739 (PK-LFK)
9:50 AM	SJ233	Balikpapan (BPN)	Sriwijaya Air	733

9:55 AM	SJ565	Makassar (UPG)	Sriwijaya Air	B738 (PK-CRF)
10:00 AM	JT791	Makassar (UPG)	Lion Air	B739 (PK-LHW)
10:00 AM	JT1781	Makassar (UPG)	Lion Airlines	739
10:00 AM	QG431	Balikpapan (BPN)	Citilink	A320 (PK-GLP)
10:05 AM	QG695	Denpasar (DPS)	Citilink	A320 (PK-GLA)
10:10 AM	GA341	Denpasar (DPS)	Garuda Indonesia	B738 (PK-GMC)
10:10 AM	GA364	Semarang (SRG)	Garuda Indonesia	CRJX (PK-GRN)
10:10 AM	IW1844	Yogyakarta (JOG)	Wings Air	AT76 (PK-WHI)
10:20 AM	IW1838	Semarang (SRG)	Wings Air	AT76 (PK-WGQ)
10:25 AM	GA308	Jakarta (CGK)	Garuda Indonesia	B738 (PK-GMW)
10:30 AM	ID6137	Makassar (UPG)	Batik Air	A320 (PK-LUP)
10:35 AM	QG451	Palangkaraya (PKY)	Citilink	A320 (PK-GQK)
10:40 AM	JT692	Jakarta (CGK)	Lion Air	B739 (PK-LGZ)
10:45 AM	XT321	Kuala Lumpur (KUL)	AirAsia X	A320 (PK-AXF)
10:50 AM	ID6197	Makassar (UPG)	Batik Air	A320 (PK-LUT)
10:50 AM	JT267	Tarakan (TRK)	Lion Air	B38M (PK-LQG)
10:55 AM	QG601	Kupang (KOE)	Citilink	A320 (PK-GQP)
11:00 AM	JT983	Pekanbaru (PKU)	Lion Air	B738 (PK-LKT)
11:05 AM	ID7513	Jakarta (HLP)	Batik Air	B738 (PK-LBZ)
11:10 AM	JT970	Batam (BTH)	Lion Air	B739 (PK-LFV)
11:15 AM	GA7307	Jember (JBB)	Garuda Indonesia	AT76 (PK-GAE)
11:15 AM	QG417	Pontianak (PNK)	Citilink	A20N (PK-GTF)
11:20 AM	QG947	Batam (BTH)	Citilink	A320 (PK-GQO)
11:30 AM	IN117	Batu Licin (BTW)	NAM Air	AT76 (PK-NYT)
11:30 AM	JT588	Jakarta (CGK)	Lion Air	B739 (PK-LHI)
11:35 AM	IW1808	Balikpapan (BPN)	Wings Air	AT7
11:35 AM	IW1917	Surakarta (SOC)	Wings Air	AT76 (PK-WHF)
11:35 AM	JT365	Balikpapan (BPN)	Lion Air (50th 737-900ER Livery)	B739 (PK-LHY)

11:45 AM	GA310	Jakarta (CGK)	Garuda Indonesia	B738 (PK-GFO)
11:50 AM	XT385	Penang (PEN)	AirAsia X	A320 (PK-AXH)
11:55 AM	SV5412	Medina (MED)	Saudia	B744 (TF-AAC)
11:55 AM	QG801	Semarang (SRG)	Citilink	A320 (PK-GLX)
11:55 AM	SJ335	Bandar Lampung (TKG)	Sriwijaya Air	738
12:00 PM	ID6576	Jakarta (CGK)	Batik Air	B739 (PK-LBH)
12:00 PM	JT807	Makassar (UPG)	Lion Air	B739 (PK-LHV)
12:10 PM	JT177	Lombok (LOP)	Lion Air	B739 (PK-LHL)
12:10 PM	JT695	Kupang (KOE)	Lion Air	B739 (PK-LFW)
12:15 PM	IW1873	Jember (JBB)	Wings Air	AT75 (PK-WFP)
12:15 PM	QG437	Balikpapan (BPN)	Citilink	320
12:15 PM	QG671	Lombok (LOP)	Citilink	A320 (PK-GQJ)
12:15 PM	QG697	Denpasar (DPS)	Citilink	A320 (PK-GLY)
12:20 PM	JT227	Banjarmasin (BDJ)	Lion Air	B738 (PK-LPT)
12:30 PM	3K247	Singapore (SIN)	Jetstar Airways	A320 (9V-JSP)
12:35 PM	ID6413	Denpasar (DPS)	Batik Air	A320 (PK-LAR)
12:35 PM	JT857	Palembang (PLM)	Lion Air	B738 (PK-LOG)
12:35 PM	QG306	Makassar (UPG)	Citilink	A20N (PK-GTI)
12:40 PM	JT736	Denpasar (DPS)	Lion Airlines	739
12:40 PM	JT923	Denpasar (DPS)	Lion Air	B739 (PK-LJG)
12:45 PM	GA312	Jakarta (CGK)	Garuda Indonesia	B738 (PK-GFX)
12:45 PM	IN193	Pangkalan Bun (PKN)	Nam Air	735
12:45 PM	JT837	Pontianak (PNK)	Lion Air	B738 (PK-LPJ)
12:50 PM	JT681	Palangkaraya (PKY)	Lion Air	B739 (PK-LHQ)
12:50 PM	JT694	Jakarta (CGK)	Lion Air	B738 (PK-LJY)
12:55 PM	QG433	Balikpapan (BPN)	Citilink	320
1:10 PM	IW1834	Semarang (SRG)	Wings Air	AT76 (PK-WGJ)
1:25 PM	QG716	Jakarta (CGK)	Citilink Garuda Indonesia	A320 (PK-GQT)

1:30 PM	JT313	Banjarmasin (BDJ)	Lion Air	B739 (PK-LHW)
1:45 PM	SJ571	Makassar (UPG)	Sriwijaya Air	735
1:55 PM	JT749	Manado (MDC)	Lion Air	B38M (PK-LQP)
1:55 PM	XT696	Jakarta (CGK)	AirAsia X	A320 (PK-AXI)
2:00 PM	GA365	Lombok (LOP)	Garuda Indonesia	CRJX (PK-GRN)
2:00 PM	QG347	Makassar (UPG)	Citilink	A320 (PK-GLE)
2:00 PM	QG487	Banjarmasin (BDJ)	Citilink	A320 (PK-GLA)
2:05 PM	IW1881	Blimbingsari (BWX)	Wings Air	AT76 (PK-WHF)
2:05 PM	JT363	Balikpapan (BPN)	Lion Air	B739 (PK-LFK)
2:15 PM	GA7305	Blimbingsari (BWX)	Garuda Indonesia	AT76 (PK-GAE)
2:20 PM	GA347	Denpasar (DPS)	Garuda Indonesia	B738 (PK-GMC)
2:20 PM	ID7042	Jakarta (HLP)	Batik Air	32A
2:20 PM	ID7501	Jakarta (HLP)	Batik Air	A320 (PK-LAP)
2:20 PM	IW1809	Sumenep-Madura Island (SUP)	Wings Air	AT76 (PK-WHI)
2:25 PM	ID6406	Jakarta (CGK)	Batik Air	A320 (PK-LAK)
2:25 PM	SJ266	Jakarta (CGK)	Sriwijaya Air	B735 (PK-CLK)
2:25 PM	XT327	Kuala Lumpur (KUL)	AirAsia X	A320 (PK-AXJ)
2:30 PM	GA314	Jakarta (CGK)	Garuda Indonesia	B738 (PK-GMF)
2:35 PM	JT223	Banjarmasin (BDJ)	Lion Air	B38M (PK-LQG)
2:35 PM	JT709	Makassar (UPG)	Lion Air	B738 (PK-LPQ)
2:35 PM	JT1709	Makassar (UPG)	Lion Airlines	738
2:35 PM	JT1797	Makassar (UPG)	Lion Airlines	738
2:55 PM	ID6131	Labuan Bajo (LBJ)	Batik Air	A320 (PK-LUP)
3:00 PM	SJ563	Makassar (UPG)	Sriwijaya Air	B739 (PK-CMP)
3:05 PM	GA316	Jakarta (CGK)	Garuda Indonesia	B738 (PK-GFI)
3:05 PM	JT582	Jakarta (CGK)	Lion Air	B739 (PK-LGT)
3:10 PM	QG718	Jakarta (CGK)	Citilink	A320 (PK-GQK)
3:15 PM	JT917	Bandung (BDO)	Lion Air	B738 (PK-LKT)

3:30 PM	JT649	Lombok (LOP)	Lion Air	B739 (PK-LHL)
3:35 PM	SJ255	Kupang (KOE)	Sriwijaya Air	738
3:35 PM	ID7515	Jakarta (HLP)	Batik Air	B738 (PK-LBZ)
3:35 PM	QG435	Balikpapan (BPN)	Citilink	320
3:40 PM	MI224	Singapore (SIN)	SilkAir	A320 (9V-SLG)
3:45 PM	JT839	Pontianak (PNK)	Lion Air	B738 (PK-LKR)
3:45 PM	ID6155	Sorong (SOQ)	Batik Air	A320 (PK-LAV)
3:45 PM	IW1356	Balikpapan (BPN)	Wings Air	739
3:45 PM	JT261	Balikpapan (BPN)	Lion Air (50th 737-900ER Livery)	B739 (PK-LHY)
3:50 PM	JT707	Makassar (UPG)	Lion Air	B739 (PK-LGV)
3:50 PM	JT598	Jakarta (CGK)	Lion Airlines	739
4:00 PM	GA630	Makassar (UPG)	Garuda Indonesia	CRK
4:05 PM	QG699	Denpasar (DPS)	Citilink	A320 (PK-GLY)
4:10 PM	IL711	Pangkalan Bun (PKN)	Trigana Air	734
4:10 PM	IW1846	Yogyakarta (JOG)	Wings Air	AT76 (PK-WGJ)
4:10 PM	JT693	Kupang (KOE)	Lion Air	B739 (PK-LHT)
4:20 PM	JT164	Kuala Lumpur (KUL)	Lion Air	B738 (PK-LPL)
4:40 PM	QG835	Majalengka (KJT)	Citilink	A320 (PK-GQP)
4:45 PM	QG693	Denpasar (DPS)	Citilink	A320 (PK-GLL)
4:45 PM	QG949	Batam (BTH)	Citilink	A20N (PK-GTF)
4:50 PM	GA372	Bandung (BDO)	Garuda Indonesia	B738 (PK-GMK)
4:50 PM	ID6578	Jakarta (CGK)	Batik Air	A320 (PK-LUK)
4:50 PM	IN277	Denpasar (DPS)	Nam Air	735
5:00 PM	GA318	Jakarta (CGK)	Garuda Indonesia	A333 (PK-GPX)
5:00 PM	JT265	Balikpapan (BPN)	Lion Air	B739 (PK-LKO)
5:05 PM	IN376	Denpasar (DPS)	Nam Air	735
5:05 PM	JT972	Batam (BTH)	Lion Air	B739 (PK-LHP)
5:05 PM	XT325	Kuala Lumpur (KUL)	AirAsia X	A320 (PK-AXF)

5:10 PM	IN9277	Denpasar (DPS)	Nam Air	735
5:10 PM	SJ259	Jayapura (DJJ)	Sriwijaya Air	733
5:15 PM	ID7517	Jakarta (HLP)	Garuda Indonesia	CRJX (PK-GRC)
5:15 PM	IW1812	Yogyakarta (JOG)	Wings Air (50th ATR to Lion Group Livery)	AT76 (PK-WHG)
5:15 PM	QG931	Pekanbaru (PKU)	Citilink	320
5:20 PM	GA367	Semarang (SRG)	Garuda Indonesia	CRJX (PK-GRN)
5:20 PM	QG170	Jakarta (HLP)	Citilink	A20N (PK-GTI)
5:25 PM	GA448	Jakarta (CGK)	Garuda Indonesia (Retro 1969 Livery)	B738 (PK-GFN)
5:25 PM	JT950	Bandung (BDO)	Lion Air (90th 737NG Livery)	B738 (PK-LKV)
5:30 PM	JT965	Lombok (LOP)	Lion Air	B739 (PK-LHQ)
5:30 PM	QG720	Jakarta (CGK)	Citilink	A320 (PK-GQE)
5:30 PM	SJ239	Sampit Airport (SMQ)	Sriwijaya Air	735
5:40 PM	JT596	Jakarta (CGK)	Lion Air	B738 (PK-LKJ)
5:50 PM	CX779	Hong Kong (HKG)	Cathay Pacific	A333 (B-LAQ)
5:50 PM	GA320	Jakarta (CGK)	Garuda Indonesia	B738 (PK-GFK)
5:50 PM	MI226	Singapore (SIN)	SilkAir	A320 (9V-SLP)
6:00 PM	GA7309	Yogyakarta (JOG)	Garuda Indonesia	AT76 (PK-GAE)
6:00 PM	JT855	Makassar (UPG)	Lion Airlines	739
6:00 PM	SJ253	Balikpapan (BPN)	Sriwijaya Air	735
6:05 PM	SJ254	Jakarta (CGK)	Sriwijaya Air	B738 (PK-CRH)
6:05 PM	JT787	Makassar (UPG)	Lion Air	B739 (PK-LGW)
6:05 PM	JT1777	Makassar (UPG)	Lion Airlines	738
6:05 PM	SJ567	Makassar (UPG)	Sriwijaya Air	B738 (PK-CMW)
6:10 PM	JT225	Banjarmasin (BDJ)	Lion Air	B738 (PK-LPQ)
6:20 PM	IW1891	Pangkalan Bun (PKN)	Wings Air	AT76 (PK-WHI)
6:20 PM	JT696	Jakarta (CGK)	Lion Air (Dreamliner Livery)	B739 (PK-LFG)
6:20 PM	QG673	Lombok (LOP)	Citilink	A320 (PK-GQK)
6:20 PM	XT323	Kuala Lumpur (KUL)	AirAsia X	A320 (PK-AXH)

6:30 PM	JT697	Kupang (KOE)	Lion Air	B738 (PK-LJY)
6:30 PM	QG439	Balikpapan (BPN)	Citilink	A320 (PK-GLA)
6:40 PM	QG722	Jakarta (CGK)	Citilink	A320 (PK-GLN)
6:50 PM	GA322	Jakarta (CGK)	Garuda Indonesia	B738 (PK-GMJ)
6:50 PM	ID6175	Ambon (AMQ)	Batik Air	A320 (PK-LUQ)
6:50 PM	ID6582	Jakarta (CGK)	Batik Air	A320 (PK-LUF)
6:50 PM	QG172	Jakarta (HLP)	Citilink	A320 (PK-GLE)
7:00 PM	JT319	Banjarmasin (BDJ)	Lion Air	B739 (PK-LHP)
7:00 PM	QG174	Jakarta (HLP)	Citilink	A320 (PK-GQD)
7:10 PM	JT737	Manado (MDC)	Lion Air	B739 (PK-LKF)
7:10 PM	QG419	Pontianak (PNK)	Citilink	A320 (PK-GLI)
7:10 PM	QG441	Balikpapan (BPN)	Citilink	A320 (PK-GQN)
7:10 PM	JT592	Jakarta (CGK)	Lion Airlines	739
7:15 PM	ID7509	Jakarta (HLP)	Batik Air	A320 (PK-LAK)
7:20 PM	IW1817	Yogyakarta (JOG)	Wings Air	AT76 (PK-WGJ)
7:20 PM	QG825	Bandung (BDO)	Citilink	A320 (PK-GQJ)
7:45 PM	SJ234	Yogyakarta (JOG)	Sriwijaya Air	B738 (PK-CML)
7:45 PM	QG489	Banjarmasin (BDJ)	Citilink	A320 (PK-GLY)
7:50 PM	GA324	Jakarta (CGK)	Garuda Indonesia	B738 (PK-GNE)
7:50 PM	SJ256	Jakarta (CGK)	Sriwijaya Air	B738 (PK-CMK)
8:00 PM	JT919	Denpasar (DPS)	Lion Air	B739 (PK-LFU)
8:00 PM	QG176	Jakarta (HLP)	Citilink	A320 (PK-GQC)
8:05 PM	GA330	Jakarta (CGK)	Garuda Indonesia	B738 (PK-GMC)
8:05 PM	ID7519	Jakarta (HLP)	Batik Air	B738 (PK-LBZ)
8:20 PM	GA349	Denpasar (DPS)	Garuda Indonesia	CRJX (PK-GRE)
8:20 PM	ID6308	Jakarta (CGK)	Batik Air	A320 (PK-LAU)
8:20 PM	QG724	Jakarta (CGK)	Citilink	A320 (PK-GLZ)
8:25 PM	IW1896	Semarang (SRG)	Wings Air	AT76 (PK-WHF)

8:30 PM	JT948	Batam (BTH)	Lion Air	B739 (PK-LHJ)
8:30 PM	SJ258	Jakarta (CGK)	Sriwijaya Air	733
8:40 PM	JT727	Kendari (KDI)	Lion Air	B739 (PK-LGV)
8:45 PM	QG349	Makassar (UPG)	Citilink	A320 (PK-GLG)
8:55 PM	GA855	Singapore (SIN)	Garuda Indonesia	B738 (PK-GFD)
8:55 PM	XT8298	Kuala Lumpur (KUL)	AirAsia X	A320 (PK-AXI)
9:00 PM	ID8580	Jakarta (CGK)	Batik Air	A320 (PK-LUK)
9:00 PM	QG987	Palembang (PLM)	Citilink	A320 (PK-GLS)
9:05 PM	GA326	Jakarta (CGK)	Garuda Indonesia	B738 (PK-GMS)
9:05 PM	QG726	Jakarta (CGK)	Citilink	A320 (PK-GQP)
9:10 PM	JT975	Lombok (LOP)	Lion Airlines	738
9:10 PM	SJ226	Semarang (SRG)	Sriwijaya Air	735
9:15 PM	ID7058	Jakarta (HLP)	Batik Air	32A
9:15 PM	ID7082	Jakarta (HLP)	Batik Air	32A
9:15 PM	ID7521	Jakarta (HLP)	Batik Air	A320 (PK-LUZ)
9:20 PM	XT7625	Denpasar (DPS)	AirAsia X	A320 (PK-AXH)
9:20 PM	XT7692	Jakarta (CGK)	AirAsia X	A320 (PK-AXF)
9:25 PM	JT369	Balikpapan (BPN)	Lion Air	B739 (PK-LKL)
9:30 PM	QG807	Semarang (SRG)	Citilink	A320 (PK-GLA)
9:35 PM	QG178	Jakarta (HLP)	Citilink	A320 (PK-GQE)
9:45 PM	CI751	Singapore (SIN)	China Airlines	A333 (B-18356)
9:45 PM	GA328	Jakarta (CGK)	Garuda Indonesia	B738 (PK-GFO)
9:50 PM	SJ265	Denpasar (DPS)	Sriwijaya Air	B738 (PK-CRH)
10:00 PM	XT331	Kuala Lumpur (KUL)	AirAsia X	A320 (PK-AXJ)
10:15 PM	IW1842	Yogyakarta (JOG)	Wings Air	AT76 (PK-WHI)
10:15 PM	JT590	Jakarta (CGK)	Lion Air (Dreamliner Livery)	B739 (PK-LFF)
10:25 PM	BI795	Brunei (BWN)	Royal Brunei Airlines	A320 (V8-RBX)
10:25 PM	JT148	Bandar Lampung (TKG)	Lion Air (90th 737NG Livery)	B738 (PK-LKV)

| 10:25 PM | SV5510 | Medina (MED) | Saudia | B744 (TF-AAD) |
| 10:30 PM | JT978 | Medan (KNO) | Lion Air | B738 (PK-LPJ) |

"This page intentionally left blank"

ATTACHEMENT 3

TEMPERATURE, DENSITY AND PRESSURE

Temperature above mean sea level and below tropopause is given by (Airbus, 2002)

$$T = 15 - 1.98 \times \left(\frac{Alt}{1000}\right) \dots\dots\dots\dots\dots\dots\dots\dots\dots\dots\dots\dots\dots\dots\dots\dots (2.1)$$

Where Alt = Altitude in feet

Temperature T above tropopause is given by

T = -56.5°C = 216.65 K

Pressure.

Pressure also decreasing with the increasing of the altitude. To calculate pressure at given altitude we assumed temperature is standard versus altitude and air is a perfect gas. According to Airbus, (2002) pressure variation can be calculated as follow

$$dP = \rho g dh \dots\dots\dots\dots\dots\dots\dots\dots\dots\dots\dots\dots\dots\dots\dots\dots\dots\dots\dots\dots\dots\dots (2.2)$$

Where;

p   = air density at an altitude h

g   = acceleration due to gravity (9.806665 m/s2)

dh   = height of the volume unit

dP   = pressure variation on dh

With universal gas constant (R) equal to 287.053 J/kg/K and perfect gas equation we get;

$$\frac{P}{\rho} = RT \dots\dots\dots\dots\dots\dots\dots\dots\dots\dots\dots\dots\dots\dots\dots\dots\dots\dots\dots\dots\dots\dots\dots (2.3)$$

Therefore

Pressure at mean sea level (P$_o$) is given by

P₀   = 1013.25 hPa

Pressure above mean sea level and below tropopause (36089 ft is given by;

$$P = P_o \left(1 - \frac{\alpha}{T_o} h\right)^{\frac{go}{\alpha R}} \dots \dots \dots \dots \dots \dots \dots \dots \dots \dots \dots \dots \dots \dots \dots \dots \dots \dots (2.4)$$

where

P₀   = 1013.25 hPa (standard pressure at sea level)

T₀   = 288.15 K (Standard temperature at sea level)

h   = altitude (in metre)

go   = 9.80665m/s²

α   = 0.0065 °C/m

Pressure above tropopause (36089 ft) is given by

$$P = P_1 e^{\frac{-go(h-h_1)}{RT_1}} \dots \dots \dots \dots \dots \dots \dots \dots \dots \dots \dots \dots \dots \dots \dots \dots \dots \dots \dots (2.5)$$

Where;

P₁   = 226.32 hPa (Standard pressure at 11000m)

T₁   = 216.65 K (Standard temperature at 11000m)

go   = 9.80665 m/s²

h   = Altitude in metre

R   = 287.053 J/Kg/K

The altitude (PA) is the altitude found from the measurement of the pressure. The variations of pressure with altitudes can be seen on diagram 2.1.
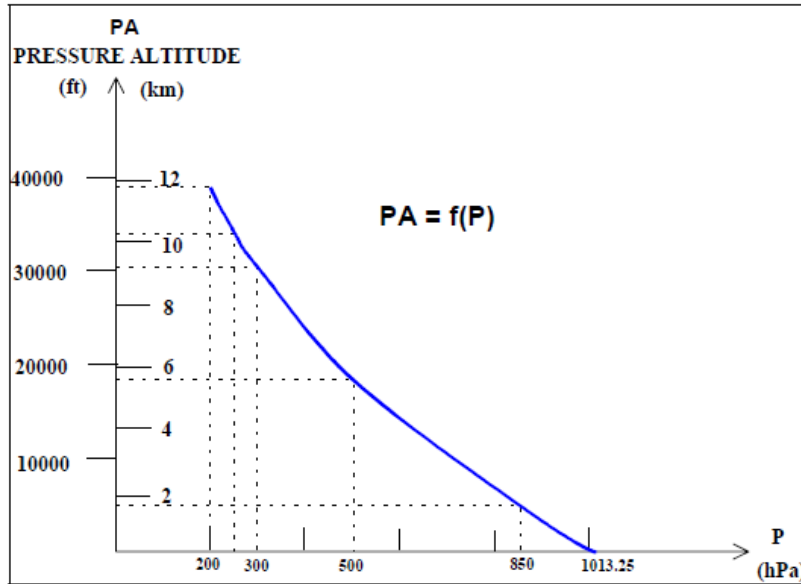
Figure 2.1 Pressure altitude function of pressure (source Airbus, 2002*)*

Example of calculation of altitude pressure can be seen on the following table;

Table 2.1 Pressure altitude values

Pressure (hPa)	Pressure altitude (PA)		FL= P/100
	(feet)	(meters)	
200	386661	11784	390
250	34000	10363	340
300	30066	9164	300
500	18287	5574	180
850	4813	1467	50
1013	0	0	0

Source Airbus, 2002

Density

At a given altitude the standard density can be calculated by assuming the air is a perfect gas. The following equation can be used to calculate density at a given altitude.

$$\rho = \frac{P}{RT} \dots\dots\dots\dots\dots\dots\dots\dots\dots\dots\dots\dots\dots\dots\dots\dots\dots\dots\dots (2.5)$$

Where

p   = density in kg/m^3

P   = pressure in pascal

R   = universal gas constant

T   = temperature in Kelvin

BIOGRAPHY

Freddy David Chilongola is Master student in Transportation Engineering and Management at Civil Engineering Department, Institut Teknologi Sepuluh Nopember (ITS), Since August 2017.

Freddy was born in the city of Dar es Salaam in Tanzania, on 31 August 1984. He received his BSc. With Education degree from University of Dar es Salaam in 2009. Immediately after graduation, he become entrepreneurs by self-employed and start business of selling electronic products. In 2012 He acquired a scholarship from Tanzania Civil Aviation Authority (TCAA) as Aeronautical Information officer Trainee for one year at Civil Aviation Training Centre (CATC) in Dar es salaam, Tanzania and East Africa School of Aviation (EASA) Nairobi, Kenya. After competition of the course in 2013 he was employed as Aeronautical Information Management Officer by Tanzania Civil Aviation Authority (TCAA) and was allocated at Kilimanjaro International Airport (KIA). After three years work experience as Aeronautical Information management officer, Freddy got scholarship for his master degree program from Indonesian Government (KNB Scholarship) in August 2016. Under this scholarship scheme, he took basic Bahasa Indonesia class for eight months learning culture and Indonesia language. After completing Bahasa Indonesia class, he started his master degree study in Transportation Engineering and Management in Civil Engineering department on August 2017. Parallel to his study, Freddy has been engaged in various academics and non-academic activities hosted by civil engineering department and ITS International office (IO).